

# Natural Products as Non-Covalent and Covalent Modulators of the KEAP1/NRF2 Pathway Exerting Antioxidant Effects

Giulia Culetta <sup>1</sup>, Brigitta Buttari <sup>2</sup>, Marzia Arese <sup>3</sup>, Simone Brogi <sup>4,5,\*</sup>, Anna Maria Almerico <sup>1</sup>, Luciano Saso <sup>6</sup> and Marco Tutone <sup>1,\*</sup>

<sup>1</sup>Dipartimento di Scienze e Tecnologie Biologiche Chimiche e Farmaceutiche (STEBICEF), Università degli Studi di Palermo, Via Archirafi 32, 90123 Palermo, Italy;

<sup>2</sup>Department of Cardiovascular, Endocrine-metabolic Diseases, and Aging, Italian National Institute of Health, 00161 Rome, Italy;

<sup>3</sup>Department of Biochemical Sciences "A. Rossi Fanelli", Sapienza University of Rome, 00185 Rome, Italy;

<sup>4</sup>Department of Pharmacy, University of Pisa, Via Bonanno 6, 56126, Pisa, Italy;

<sup>5</sup>Bioinformatics Research Center, School of Pharmacy and Pharmaceutical Sciences, Isfahan University of Medical Sciences, Isfahan 81746-73461, Iran;

<sup>6</sup>Department of Physiology and Pharmacology "Vittorio Erspamer", Sapienza University of Rome, P.Le Aldo Moro 5, 00185, Rome, Italy;

\* Correspondence: [simone.brogi@unipi.it](mailto:simone.brogi@unipi.it) (S.B.); [marco.tutone@unipa.it](mailto:marco.tutone@unipa.it) (M.T.)

**Abstract:** By controlling several antioxidant and detoxifying genes at the transcriptional level, the KEAP1/NRF2 pathway plays a crucial role in the oxidative stress response. Accordingly, the discovery of modulators of this pathway, activating cellular signaling through NRF2, and targeting the antioxidant response element (ARE) gene is pivotal for the development of effective antioxidant agents. In this context, natural products could represent promising drug candidates for supplementation to provide antioxidant capacity to human cells. In the last decades, by coupling in silico and experimental methods, several natural products have been characterized to exert antioxidant effects by targeting the KEAP1/NRF2 pathway. In this review article, we analyze several natural products that were investigated experimentally and in silico for their ability to modulate KEAP1/NRF2 by non-covalent and covalent mechanisms. These latter represent the two main sections of this article. For each class of inhibitors, we have reviewed their antioxidant effects possible therapeutic applications, and the main computational techniques used for the most promising identified compounds, providing an updated view on the development of natural products as antioxidant agents.

**Keywords:** Oxidative stress; reactive oxygen species; KEAP1/NRF2 pathway, natural products

## Introduction

Oxidative stress is a result of the alteration of the balance between reactive oxygen species (ROS) production and the detoxification enzyme system, leading to the modulation of various signaling pathways and multiple biological processes. The fact that oxidative stress is one of the most significant pathways in the development, progression, and consequences of chronic degenerative illnesses suggests that it might be added to the list of potential drug targets. As a result of protein modifications, DNA lesions, and lipid peroxidation, persistent oxidative stress may promote the activation of cell responses, such as inflammation, apoptosis, and endoplasmic reticulum stress, and impair biological processes such as mitochondrial function/metabolism and the deregulation of autophagy, leading to a dysfunctional immune response and acceleration of all mechanisms involved in the pathological progression and exacerbation of symptoms. Although there has been clear progress in recent years, combating diseases caused by oxidative stress remains challenging [1].

Drugs that target oxidative stress-related pathways could be an effective pharmacological approach for the prevention of several disorders. The potential modulation of oxidative stress by supplementation/pharmacological therapy has generated considerable interest; however, the achievement of debatable results has reduced these expectations, following antioxidant interventions. A wide range of ROS concentrations can be associated with different essential signaling and metabolic functions. Instead, the recent focus of medical research has been on finding and selectively modifying ROS enzymatic sources that, in a certain configuration, cause the disorder while leaving ROS physiologic signaling and metabolic activities unaffected. This new pharmacological approach is based on the positive modulation of the endogenous redox homeostatic system through the activation of the nuclear factor erythroid 2-related factor 2 (NRF2). This protein is a component of the Kelch-like ECH-associated protein 1 (KEAP1)/NRF2 signaling pathway. Thus, through the transcriptional control of more than 250 genes involved in the regulation of redox metabolism, inflammation, and proteostasis balance, NRF2 plays a crucial role in the oxidative stress response. [2, 3]. Under homeostatic conditions, KEAP1, the key inhibitor of NRF2 activity, unceasingly targets NRF2 for ubiquitination and proteasomal degradation. In contrast, electrophiles decrease KEAP1 activity and boost NRF2 nuclear translocation. This event leads to the consequent binding to the antioxidant response element (ARE) in the promoter regions of genes involved in the production of cellular antioxidants and detoxifying proteins when exposed to stress-inducing endogenous or exogenous stimuli [4]. NRF2 was isolated via cloning experiments in 1994 [5], and during the last decades, substantial progress has been made in comprehending the impact of NRF2 activation and its role in activating ARE genes, in regulating antioxidant and cytoprotective genes, and its role in homeostatic response, thus providing the basis for drug development considering KEAP1/NRF2 as a pharmacological target [6-9]. Furthermore, a non-canonical role for NRF2 has also been described related to the maintenance of mitochondrial health to control oxidative stress [10].

Moreover, the NRF2 signaling pathway is also at the center of the sophisticated regulatory network of the human body and is essential for many biological processes, including metabolism, autophagy, inflammation, immunological response, and proteostasis [4, 11]. Although the KEAP1/NRF2 system is protective in maintaining overall redox homeostasis and other cellular functions, NRF2 overactivation may have negative consequences due to the so-called reductive stress event, which is harmful in muscle diseases and other cardiomyopathies [12, 13]. When it is active in tumor cells, it can result in drug resistance, and its overactivation can be adverse, as in cancer and resistance to chemotherapy [14]. Therefore, it is debatable whether pharmacologic inactivation of KEAP1 or NRF2 activation, or inhibition of the NRF2 system can be effectively used in preventing or treating cancer or other disorders in which the KEAP1/NRF2 system is frequently dysregulated. Given the consequences of NRF2 activation and depletion on critical biological processes, the NRF2 signaling pathway has emerged as a key pharmacological target for medical research [15]. To this end, natural products play a crucial role in inhibiting the KEAP1/NRF2 complex formation, activating NRF2 that can exert its antioxidant role, being fundamental for the transcription of ARE genes. This type of NRF2 activation mechanism could be pursued in two different ways, considering the two diverse regions of KEAP1. KEAP1's C-terminal Kelch domain binds a high-affinity ETGE motif and a low-affinity DLG motif in NRF2's NRF2-ECH homology 2 (Neh2) domain. Three arginine residues (Arg380, Arg415, and Arg483) that interact with glutamic and aspartic acid residues in the two NRF2 motifs that are necessary for high-affinity binding may be found in the huge (550 - 780 Å) buried surface area of KEAP1's Neh2-binding pocket. The side chains of Glu79 and Glu82 in the ETGE motif of NRF2 interact with these three arginine moieties to produce a complex network of salt bridges and hydrogen bonds. Accordingly, the NRF2 binding site has been identified as a drug target to disrupt KEAP1/NRF2 complex formation, and many natural products could exert their antioxidant profile through non-covalent interactions within the mentioned binding site on KEAP1. In contrast, the second domain that is important in KEAP1/NRF2 complex formation is the BTB domain of KEAP1. In fact, KEAP1 contains many cysteine residues that function as regulatory amino acids and are sensitive to redox variation and electrophilic agents. The most relevant cysteines are located in the BTB domain, with Cys151 being the most susceptible to this mechanism. Several natural compounds may contain functional groups that can form covalent adducts. In this case, KEAP1 will not be able to play a physiological role in forming the complex with NRF2, which is free in the cytosol, where it could be phosphorylated and can translocate in the nucleus to act as a transcription factor for the ARE genes. Finally, few natural compounds were found to bind to the BTB domain by non-covalent interactions, and few others were found to interact directly with NRF2. In all these cases, the NRF2 antioxidant pathway was activated, protecting the cell from oxidant stimuli.

In this paper, the physiological modulation of NRF2 in the context of the KEAP1/NRF2 pathway will be reviewed, and the mechanism of different natural products that can act as possible antioxidant and anti-inflammatory agents, and the limitations of their effectiveness will be highlighted.

## **KEAP1/NRF2 signaling pathway**

### *Domain structures of NRF2*

NRF2 is a member of the Cap n' Collar family. It behaves as a transcription factor containing a basic leucine zipper (bZIP) structure and seven domains (Neh1-Neh7), and it is composed of 589 amino acid residues. NRF2 has a well-developed adaptive mechanism to counteract the deleterious effects of oxidative stress in the cellular environment [5]. The Neh1 domain has a bZIP region that regulates DNA binding by enabling NRF2 dimerization with small Maf proteins (sMafs) [16] as well as a nuclear localization signal (NLS) that governs nuclear protein localization [17]. Neh2 and Neh6 domains include degradation signals that allow NRF2 to target proteasomal degradation by KEAP1 and  $\beta$ -transducin repeats-containing proteins ( $\beta$ -TrCP) [18]. The N-terminal regulatory domain of Neh2 has seven lysine residues and two peptide-binding motifs (DLG and ETGE) that control interaction with various proteins/enzymes involved in the ubiquitination and proteasomal degradation of the NRF2 protein under normal physiological conditions [19]. The transactivation domains Neh3, Neh4, and Neh5 modulate the binding of NRF2 to other coactivator proteins [20, 21], whereas the Neh5 domain regulates the cytoplasmic localization of NRF2 [22]. Neh6 acts as a negative regulatory domain and binds with  $\beta$ -TrCP for NRF2 ubiquitination [23]. The Neh7 domain interacts with the retinoic X receptor  $\alpha$  (RXR $\alpha$ ), thus contributing to the inhibition of the NRF2/ARE signaling pathway [24].

### *Physiological regulation of NRF2 and the KEAP1/NRF2/ARE pathway*

NRF2 and its main negative regulatory protein, the E3 ligase adaptor KEAP1, have significant implications in numerous biological processes, including antioxidant metabolism, prevention of xenobiotic and endobiotic-related oxidative damage [19], metabolism of carbohydrates [25], lipids and iron [26], redox signaling, protection against triptolide-induced oxidative stress [27], and inflammatory conditions [28]. NRF2 expression is tightly regulated, its mRNA is constitutively expressed under normal homeostatic conditions [29], and the protein is sequestered in the cytoplasm by its regulatory protein KEAP1. KEAP1 is a cysteine-rich protein that is an adaptor constituent of the Cullin3 (Cul-3)-based ubiquitin E3 ligase complex, which leads to its ubiquitylation and proteasomal degradation. KEAP1 is structured in five domains, an N-terminal region (NTR), a tramtrack-bric-à-brac (BTB) domain, a central intervening region (IVR) with nuclear export signal (NES) regulating its cytoplasmic localization, six Kelch repeats, and a C-terminal domain (CTD) [30]. NRF2 is constitutively ubiquitinated by KEAP1, and the rate of NRF2 ubiquitination and

degradation in non-stressed cells is mostly cell-type dependent because of the variability in KEAP1 protein concentrations [31]. In addition, p97, an ATP-dependent segregase, was recently discovered to be a classical negative regulator of NRF2. Indeed, p97 negatively regulates NRF2 by extracting ubiquitinated NRF2 from the KEAP1/Cul-3/E3 complex, for efficient proteasomal degradation [32]. In pathological/oxidative stress conditions, autophagy impairment may interfere with the clearance capacity of cells in the elimination of damaged organelles, thus causing accumulation of long-lived and misfolded proteins [33]. Under these circumstances, the autophagy chaperone p62/sequestosome-1 accumulates and competitively binds to KEAP1, increasing the free NRF2 concentration and activating NRF2-related signaling [34-36].

Under stress-inducing conditions [37-39], cells activate the KEAP1/NRF2/ARE signaling pathway, alter the KEAP1/NRF2 complex conformation, and inhibit NRF2 ubiquitylation. In this manner, free KEAP1 is not regenerated, and the de novo synthesized NRF2 translocates into the nucleus, after its phosphorylation, where it heterodimerizes with sMaf before binding to the promoter of ARE genes. Once in the nucleus, NRF2 promotes the expression of antioxidant and detoxifying genes and down-modulates the production of pro-inflammatory mediators [11, 40]. ARE sequences (5'-RTGACnnnGC-3') exists in the promoter of diverse genes, including NAD(P)H quinone oxidoreductase 1 (NQO1), multidrug resistance-associated proteins (MRPs), UDP-glucuronosyltransferase (UGT), glutamate-cysteine ligase catalytic (GCLC) and modifier (GCLM) subunits, glutathione S-transferase (GST), sulfiredoxin1 (SRXN1), and heme-oxygenase-1 (HMOX1). The existence of ARE in the promoter of the HMOX1 gene indicates NRF2-mediated synthesis of the heme oxygenase protein (HO-1), an enzyme that catalyzes the first and rate-limiting step in heme degradation [41].

To elucidate the regulation of NRF2 stability, two models have been reported in the literature. The first theory, commonly known as the "hinge and latch model," states that KEAP1's contact with NRF2's ETGE domain serves as a hinge, whereas a weaker interaction with Neh2's DLGex motif serves as a latch [42]. Interestingly, latch disruption precludes NRF2 ubiquitination [43]. The finding that somatic mutations in the DLGex and ETGE motifs of NRF2 occur extremely often in a variety of cancer cells [44, 45] suggests a two-site binding mode. These mutations affect the two-site binding of KEAP1/NRF2 and cause constitutive accumulation of NRF2, which supports cancer cell growth [46]. Horie and colleagues used competitive inhibition NMR tests to show that the hinge-latch mechanism is actively used in KEAP1/NRF2 protein-protein interaction (PPI) inhibitors (PRL295 and NG262) but not in electrophilic NRF2 activators in the activation of NRF2 [47]. Furthermore, in addition to the hinge-latch, it has been hypothesized that there are additional NRF2 activation mechanisms. Moreover, they found that the phosphorylated p62/sequestosome-1 peptide negatively influenced the binding of the DLGex motif with the Neh2 domain to KEAP1, thus opening the latch

site and suppressing the effective ubiquitination and rapid degradation of NRF2 [47]. The second hypothesis, often referred to as KEAP1-independent regulation, proposes that under normal circumstances, the Neh6 domain binds to the DSGIS and DSAPGS motifs of the  $\beta$ -TrCP, which in turn serves as a substrate receptor for the Skp1-Cul1-Rbx1/Roc1 ubiquitin ligase complex that catalyzes NRF2 ubiquitination. The Neh6 domain of NRF2 is phosphorylated by glycogen synthase kinase-3 beta (GSK-3 $\beta$ ), which controls how  $\beta$ -TrCP26 recognizes it. According to both models, the novel produced NRF2 translocates into the nucleus [43, 48].

#### *Regulation of NRF2 at the nuclear level*

The accumulation of activated NRF2 in the nucleus allows it to interact with other transcription factors and cofactors and control the transcription of its target genes. Its abundance in the nucleus is finely regulated. After NRF2-mediated induction of defensive gene expression, NRF2 is phosphorylated at tyrosine residue 568 by Fyn, a member of the Src kinase family, which leads to chromosomal region maintenance-1 (Crm-1) mediated nuclear export and degradation [49]. In addition, NRF2 is negatively regulated by GSK-3 $\beta$ , a kinase that sensitizes cells to death. In fact, NRF2 nuclear exclusion is facilitated by GSK-3 phosphorylation, which prevents ARE binding and activation [50].

The BTB and CNC homology 1 (BACH1) transcription factor is a negative NRF2 competitor because of its binding sites on DNA [51]. BACH1 is a molecular sensor of intracellular heme and a MAF-related transcriptional repressor; it establishes heterodimers with sMaf (MafK and MafG) proteins on DNA, leading to the repression of ARE-mediated gene induction and expression [52], in a highly conserved regulatory pathway that is ubiquitously expressed in tissues [53, 54]. In the presence of an antioxidant, BACH1 becomes phosphorylated at Tyr486, is exported to the cytosol, and is degraded, thus allowing NRF2 access to the ARE [55]. Antioxidants also lead to increased synthesis of BACH1, which is imported into the nucleus to achieve normal levels of BACH1 and repress antioxidant gene expression. Under oxidative stress conditions, heme is released from hemoproteins, leading to increased oxidative stress. As a heme-sensor, BACH1 binds heme and induces not only its nuclear export but also its polyubiquitination and degradation [56], becoming not able to act as a repressor. Figure 1 illustrates the mechanism of KEAP1/NRF2 pathway activation.

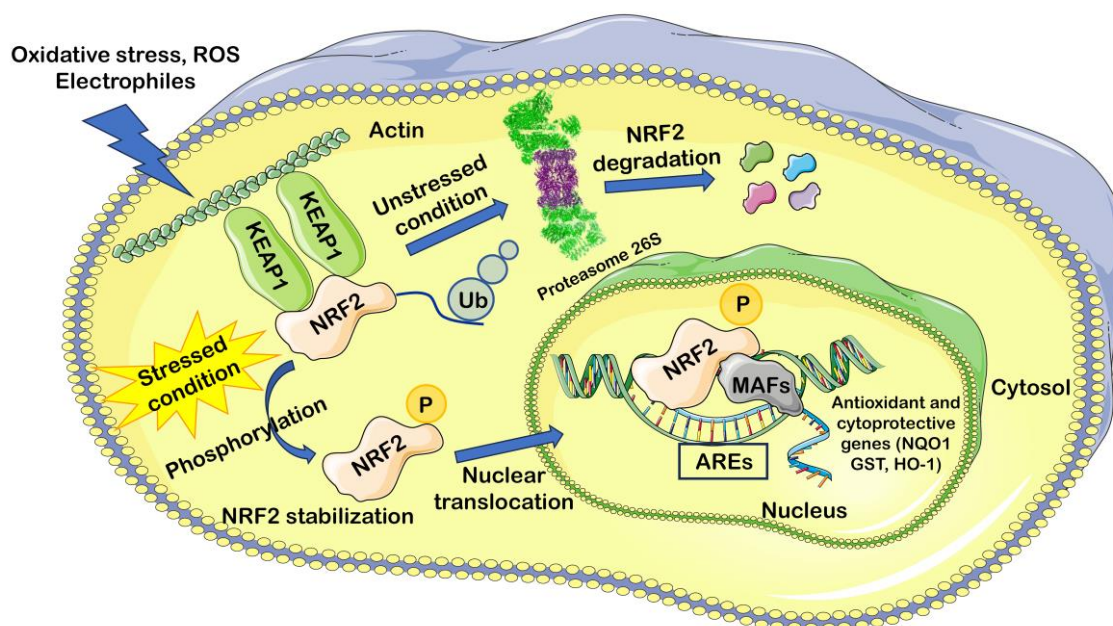
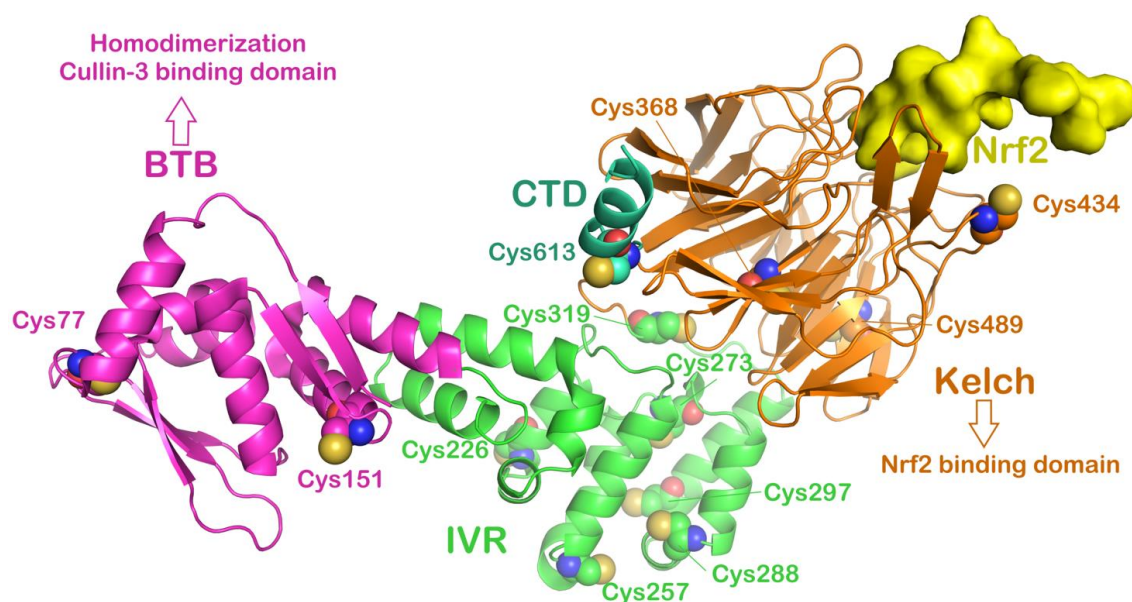


**Figure 1.** Illustration of the mechanism by which the KEAP1/NRF2 complex transcriptionally regulates oxidative responses. The picture was prepared by using Smart SERVIER MEDICAL ART provided under Creative Commons Attribution 3.0 Unported License.

### Natural products as modulators of the KEAP1/NRF2 pathway

*Natural products covalently bind to KEAP1, thereby improving the expression of antioxidant genes*

In addition to the direct targeting of KEAP1/NRF2 to preclude the recognition of NRF2, a valuable strategy for negatively modulating its interaction with NRF2 has been described. In particular, considering that the KEAP1 protein is a cysteine-rich enzyme enclosing 27 cysteine residues showing different degrees of reactivity [57, 58], it has been reported that some of the cysteine residues are crucial in the regulation of KEAP1 functions, including the recognition of NRF2 and the subsequent activation of the mentioned protein as well as the negative modulation of client proteins such as Cul-3. In fact, this protein, along with RBX1, can form a complex with Cul-3/RBX1, which is necessary for the ubiquitination process performed by E3 ligase after the interaction of NRF2 with KEAP1. Thus, NRF2 can be degraded by proteasome 26S. The lack of formation of the Cul-3/RBX1 complex mediated by KEAP1 results in the absence of NRF2 degradation that can be activated by the phosphorylation process to enter the nucleus and participate in the transcription of antioxidant genes [59-61]. Accordingly, at least eight cysteine residues, namely Cys77, Cys151, Cys257, Cys273, Cys288, Cys297, Cys434, and Cys613, are directly involved in redox sensing and NRF2 activation (Figure 2) [40, 57, 62, 63].

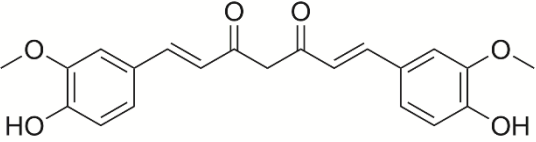
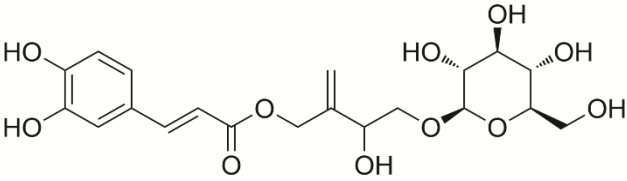
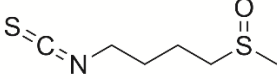
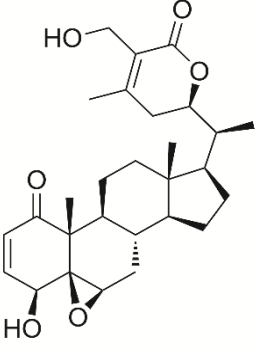
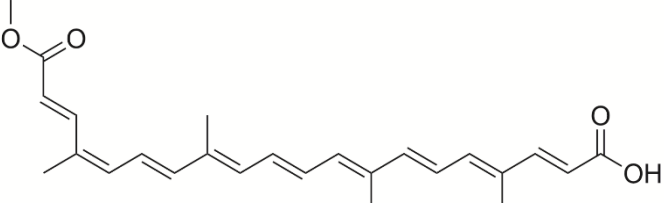
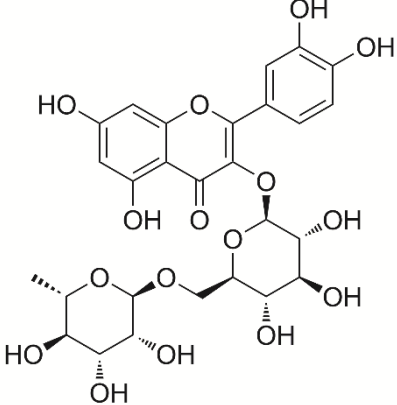
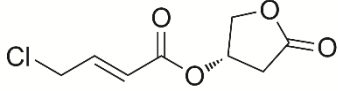
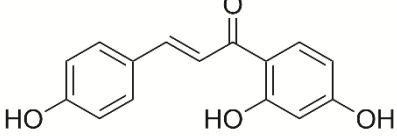
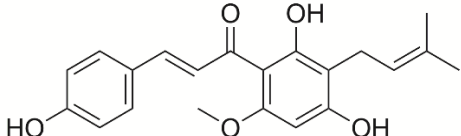


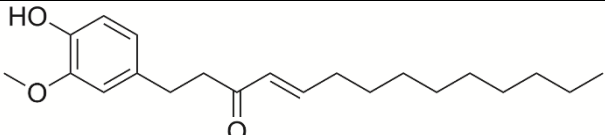
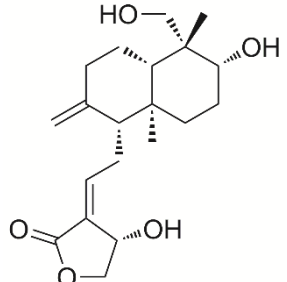
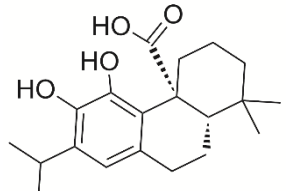
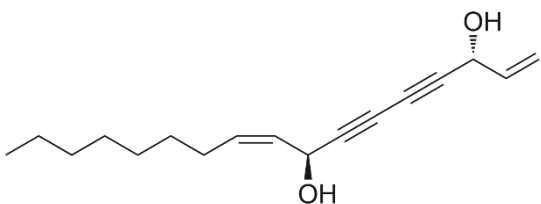
**Figure 2.** Full-length KEAP1 protein modeled according to the alpha-fold output (AF-Q14145-F1; <https://alphafold.ebi.ac.uk/entry/Q14145>, accessed on 04 August 2023) and the following crystal structures 6WCQ and 2FLU, with highlighted domains and cysteine residues more susceptible to modifications by reacting with electrophile agents and the NRF2-interacting region (yellow surface). Picture was generated by PyMOL (the PyMOL Molecular Graphics System, v1.8; Schrödinger, LLC, New York, NY, USA, 2015). Abbreviations: Broad-complex, tramtrack and bric-à-brac (BTB) domain (magenta); intervening region (IVR) (green), Kelch domain (orange), and C-terminal domain (CTD) (dark green). The BTB domain is associated with Cul-3-E3-ligase binding and KEAP1 homodimerization. IVR contains several important cysteine residues that modulate KEAP1/NRF2 activity. The Kelch domain is associated with NRF2 and P62. Information was extracted from UniProtKB (<https://www.uniprot.org/uniprotkb/Q14145/entry>, accessed on 04 August 2023).

In this context, several synthetic small-molecules have been investigated [64-67], including approved drugs (i.e., dimethyl fumarate approved drug for treating relapsing multiple sclerosis) [68], for their ability to form covalent adducts with regulatory cysteine residues. More interesting is the investigation of natural products acting as covalent KEAP1 binders. Because of their reduced toxicity and undesired effects, natural products can be administered as food supplements and/or included in the dietary regimen. Some interesting examples of this class of compounds capable of modifying cysteine residues on KEAP1 have been reported in the literature [69, 70]. In this review article, we also report the recent discoveries on NRF2 activation by cysteine residue modification of KEAP1 that could be useful for a comprehensive point of view. Table 1 reports a series of natural products involved in the formation of covalent adducts with different cysteine residues located in different KEAP1 domains (Figure 2).

**Table 1.** Some natural products able to covalently bind KEAP1.

Compound	Chemical structure	Cysteine residues targeted
----------	--------------------	----------------------------

Curcumin		Cys151 Cys257 Cys273 Cys288 Cys297 Cys613
Pubescenoside A		Cys77 Cys434
Sulforaphane		Cys38 Cys151 Cys368 Cys489
Withaferin A		Cys151 Cys319 Cys434 Cys489 Cys613
Bixin		Cys151
Rutin		Cys151
Honaucin A		To be determined
Isoliquiritigenin		Cys151
Xanthohumol		Cys151

10-Shogaol		Cys151
Andrographolide		Cys77 Cys151 Cys273 Cys368
Carnosic acid		Cys151
Falcarindiol		Cys151

One of the most studied compounds that can form covalent adducts with KEAP1 by exploiting its antioxidant effects is curcumin (Table 1). This molecule can target different cysteine residues located in the regulatory domains of KEAP1, thereby interfering with the interaction with NRF2. In particular, this yellow pigment belonging to *Curcuma longa* possesses a plethora of significant pharmacological properties, including antioxidant, antimicrobial, anti-inflammatory, anticancer, neuroprotective, and anti-ischemic effects [71-73]. Regarding the antioxidant profile, several studies have highlighted that curcumin exerts this effect by acting on the regulatory cysteine residues of KEAP1. The chemical structure of curcumin showed two Michael acceptor functions belonging to the  $\alpha,\beta$ -unsaturated 1,3-diketone moiety. These reactive groups were able to target cysteine residues considering the reaction that can occur between the nucleophilic moiety of cysteine (-SH group) and the unsaturated ketone function. As previously mentioned, several cysteine residues of KEAP1 are susceptible to the formation of covalent adducts. Regarding curcumin, Shin and coworkers investigated the preferred cysteine binding of curcumin to establish its possible mechanism of action. Their findings clearly indicated that Cys151 is required for NRF2 transcriptional activity in response to curcumin treatment [74]. Furthermore, the authors investigated the role of two other cysteine residues (Cys273 and Cys288) that could be considered important in activating NRF2-mediated antioxidant gene transcription [40]. By combining *in silico*, mass spectral analysis (LC-ESI-MS/MS), and mutagenesis studies, they observed that different mutations on the selected cysteine residues (KEAP1-Cys151Ser,

KEAP1-Cys273Ser, and KEAP1-Cys288Ser) influenced NRF2 activation. In fact, when Cys151 was mutated, NRF2 activation dramatically decreased. In contrast, NRF2-induced activation of targeted genes was marginally affected when cells were transfected with KEAP1 containing mutated Cys273 and Cys288 residues. Accordingly, based on this work, curcumin showed a preferred binding site on KEAP1 located at the BTB domain, in which Cys151 is present [74]. In another interesting study, Jo and collaborators analyzed the possibility of curcumin covalently modifying other cysteine residues. In particular, in addition to the previously discussed covalent binding, computer-aided methods were used to explore whether curcumin could interact with Cys257, Cys297, and Cys613. After the positive results obtained by *in silico* studies, they experimentally confirmed direct binding to these residues. Notably, this study highlighted the role of curcumin supplementation in the potential treatment of chronic obstructive pulmonary disease (COPD). Their investigation encompassed a randomized controlled trial and acrolein-induced pneumonitis in a preclinical animal model. Interestingly, by the mentioned mechanism of action, curcumin was able to reduce pro-inflammatory cytokines increased in pneumonitis as well as to increase the level of anti-inflammatory cytokines. Furthermore, preclinical studies demonstrated that curcumin suppressed pneumonitis complications by suppressing extrinsic and intrinsic apoptotic pathways, enhancing redox sensing, and improving GSH synthesis and restoration. Accordingly, curcumin has been proven to be a safe and effective anti-inflammatory drug against air pollution-induced respiratory disorders, such as pneumonitis and COPD, in both animal studies and human trials [75].

Another interesting natural product with a relevant pharmacological profile is pubescenoside A (Table 1). This compound is a bioactive metabolite of *Ilex pubescens* and has anti-inflammatory and antioxidant effects. In a recent study, Cheng and coworkers investigated the possible role of pubescenoside A in myocardial I/R injury, clarifying the possible mechanism of action of this compound in this type of disease. Using an animal model of myocardial I/R injury, they evaluated the cardioprotective effect of pubescenoside A. In particular, the model of myocardial I/R injury was induced by left anterior descending artery ligation, and the mechanism of action was investigated by employing several experiments that combined *in vitro*, *in vivo*, and *in silico* methods. They demonstrated that pubescenoside A could play a pivotal role in protecting cardiomyocytes, suppressing NLRP3 inflammation activation, and inducing the NRF2 signaling pathway. Regarding the mechanism of action, they found that pubescenoside A can directly target conserved cysteine residues of KEAP1 by selectively covalently binding Cys77 located in the BTB domain and Cys434 located in the Kelch domain. They demonstrated that this occurrence was pivotal for inhibiting NRF2 ubiquitination and consequently promoting its translocation into the nucleus, activating antioxidant enzymes via the NRF2 pathway. Furthermore, they explored the influence of pubescenoside A on other reactive cysteine residues of KEAP1. Interestingly, different activation degrees induced by

pubescenoside A were observed. In particular, the susceptibility of the cysteine residues of KEAP1 to pubescenoside A can be summarized as follows: Cys77 > Cys434 > Cys23 > Cys38 > Cys226 > Cys273. Accordingly, pubescenoside A was found to be an NRF2 activator that was able to covalently bind cysteine residues in two different domains of KEAP1 (BTB and Kelch). In particular, the binding to Cys77 and Cys434 was shown to be necessary for the positive regulation of NRF2 signaling. By this mechanism, pubescenoside A showed relevant cardioprotective activities against myocardial I/R injury [76].

Another attractive NRF2 activator is sulforaphane (Table 1). It is a natural product of the *Brassicaceae* family and a well-described nutraceutical agent with several significant pharmacological effects. It has been demonstrated that sulforaphane can act as a neuroprotective, cardioprotective, and cytoprotective agent with an interesting anticancer profile. In this context, most pathways activated by sulforaphane are strictly linked to NRF2 activation. Numerous studies have reported that the action of sulforaphane on the KEAP1/NRF2 signaling pathway is ascribable to its capability to form covalent adducts with reactive cysteines located in different KEAP1 domains. In particular, in one of the first studies aimed at elucidating the mechanism of action of sulforaphane, Hu and colleagues identified several cysteine residues that could react with sulforaphane with different degrees of reactivity. Mass spectrometry-based studies showed that the most susceptible cysteine residues were Cys38 in the N-terminal domain, Cys151 in the BTB domain, and Cys368 and Cys489 in the Kelch domain. The five cysteines that did not react with sulforaphane were Cys13 and Cys14 in the N-terminal domain and Cys249, Cys257, and Cys297 in the central linker domain. Cys406 is the third most readily modified cysteine residue. Interestingly, free cysteine KEAP1 abolished sulforaphane activity. Accordingly, this strong activity against KEAP1 could be one of the mechanisms by which sulforaphane showed relevant pharmacological effects; thus, sulforaphane can be used in a variety of preclinical investigations aimed at determining the potential benefits of activating this pathway in treating a variety of diseases, as demonstrated by the over 20 ongoing clinical trials in which sulforaphane is currently employed [77-79].

Withaferin A (Table 1), a natural steroidal lactone in *Withania somnifera*, is another important compound with an antioxidant profile targeting the KEAP1/NRF2 pathway. In particular, several studies on this molecule have highlighted the mechanism of action for exerting its effects. Heyninck and coworkers used this compound to assess its role in the expression of antioxidant genes and cytoprotective Phase II detoxifying enzymes. The scientists treated primary human umbilical vein endothelial cells (HUVECs) and an endothelial cell line (EA.hy926) with withaferin A. Assessment of the RNA microarray of withaferin A on treated HUVEC cells clearly showed an increase in the expression of the antioxidant gene HO-1. To provide information on the mechanism of action of the direct targeting of KEAP1 by withaferin A, the KEAP1 recombinant protein was incubated with the

molecule after digestion of KEAP1 with trypsin, and the obtained fragments were examined using MALDI-TOF. The results showed that Cys151, Cys319, Cys434, Cys489, and Cys613 were more susceptible to form adducts with withaferin A according to the mechanism of action. Furthermore, in silico studies supported the possible Michael addition reactions of withaferin A with cysteine residues located in different KEAP1 domains, with the lowest energy obtained for Cys319 [80]. Palliyaguru and collaborators investigated the potential role of withaferin A as a cytoprotective agent, being able to activate the NRF2 antioxidant pathway, conducting diverse experiments including in vivo studies. They determined that withaferin A protected mice from acetaminophen-induced hepatotoxicity via an NRF2-dependent mechanism [81].

In addition, other natural products were found to be able to covalently target KEAP1, inducing an antioxidant response via NRF2 activation. An apocarotenoid bixin (Table 1) found in the seeds of achiotte trees from the species *Bixa orellana*, commonly used as a cooking spice, activated the NRF2 pathway by targeting KEAP1. Tao and colleagues investigated the role of bixin as an antioxidant and cytoprotective agent under different injury conditions. In the first study, they demonstrated the significant role of this natural product in protecting mice from UV-induced skin damage when topically administered to the skin. Skin photoprotection was observed in SKH-1 mice, providing evidence that cytoprotection occurred by the activation of NRF2. In fact, to demonstrate NRF2-dependent effects, NRF2<sup>+/+</sup> versus NRF2<sup>-/-</sup> SKH-1 mice were treated with the apocarotenoid, and the authors reported that the protection was detectable only in NRF2<sup>+/+</sup> mice, demonstrating the involvement of this pathway in the pharmacological effect of bixin in preventing cutaneous photodamage arising from exposure to solar UV. Although the exact nature of the adduct formed by bixin with KEAP1 has not yet been fully elucidated, the authors found that one of the modified cysteine residues was Cys151 [82]. Furthermore, the same research group investigated the protective effects of bixin on ventilation-induced lung injury (VILI) in vivo. Intraperitoneal administration of this compound resulted in remarkable restoration of lung cell morphology, attenuation of inflammatory processes, and oxidative DNA damage after mechanical ventilation. To demonstrate the involvement of the NRF2 pathway in this beneficial effect, the researchers employed NRF2<sup>+/+</sup> and NRF2<sup>-/-</sup> mice. As expected, they observed protective effects only on NRF2<sup>+/+</sup> mice, confirming that the mechanism of action of bixin implicated the activation of NRF2. Notably, this study provided the first proof-of-principle in which NRF2 activators could be used in clinical settings to prevent lung damage following mechanical ventilation therapy [83]. Moreover, bixin was investigated by Xu and coworkers in cardiac damage caused by diabetes. High-fat diet mice were used in the abovementioned study to establish the progression of cardiac injury. Bixin improved cardiac function by inhibiting ROS formation, reducing cardiac fibrosis (reduction of collagen deposition), and inflammation (downregulation of pro-inflammatory cytokines secretion via TLR4/NF-κB pathway). The same

results were obtained in vitro by inducing the overexpression of pro-inflammatory cytokines using LPS against cardiac cells. Bixin, by targeting the TLR4/NF- $\kappa$ B pathway, reduced the production of pro-inflammatory cytokines and inflammatory signals [84]. Interestingly, this compound was evaluated in vivo as a potent protective agent against lung injury caused by fine particulate matter, indicating the potential application of bixin as a prophylaxis for individuals who live in urban areas characterized by heavy air pollution [85, 86].

Continuing the dissertation about the natural products able to covalently bind KEAP1, activating the NRF2 pathway, the flavonoid rutin (Table 1), abundantly present in the fruit of the genus *Citrus*, deserves attention. Sthijns and collaborators demonstrated the antioxidant effect of rutin in HUVECs. They found that the compound underwent an oxidative process to form a quinone derivative, and the HUVECs treated with rutin quinone showed strong protection against oxidative stress, being able to activate the NRF2 pathway and inducing an inhibition of the enzyme thioredoxin reductase 1, and a stimulation of glutamate cysteine ligase, which represent the first step of the synthesis of the detoxifying molecule glutathione. Moreover, the authors found that in addition to the observed effects mentioned above, the activation of HIF and NF- $\kappa$ B was dramatically reduced by treating the cells with rutin, and finally that it can protect human chorionic plate placental vessels after hydrogen peroxide treatment, preserving endothelial function. Furthermore, experiments were conducted to investigate the mechanism of action of rutin in activating the NRF2 pathway. In particular, LC-MS/MS studies highlighted that rutin quinone was able to form a covalent adduct with one of the most important regulatory cysteine residues of KEAP1. In fact, this compound can undoubtedly modify the residue Cys151 to promote its beneficial effects [87, 88].

Mascuch and colleagues described the activation of the NRF2 pathway by the natural product honaucin A (Table 1), a compound isolated from the marine cyanobacterium *Leptolyngbya crossbyana* [89]. This molecule showed anti-inflammatory properties, and the authors investigated its possible mechanism of action by targeting the KEAP1/NRF2 pathway. Honaucin A activated this pathway in cultured human MCF7, as highlighted by the NRF2 luciferase reporter assay. The researchers performed in vitro studies to determine whether the activation can be ascribed to the formation of adducts on KEAP1 because of the presence of the molecule, which has a Michael acceptor function. High-resolution mass spectrometry studies confirmed the possibility that the molecule could interact with the sulfhydryl groups on KEAP1, although the exact cysteine residues targeted by this molecule were not determined. Furthermore, via this mechanism, honaucin A plays a critical role in reducing the expression of pro-inflammatory chemokines and cytokines. The authors also reported that honaucin A was not able to interact with other sulfhydryl group-containing molecules such as glutathione, thereby precluding possible toxic effects [89].

Attempts to characterize natural products as potential NRF2 activators by covalently targeting KEAP1 were conducted by Luo and colleagues. They preliminarily characterized three Michael acceptors containing compounds, xanthohumol (*Humulus lupulus*), isoliquiritigenin (*Glycyrrhiza glabra*), and 10-shogaol (*Zingiber officinale*) (Table 1), using liquid chromatographic–tandem mass spectrometry (LC-MS/MS) with a cylindrical ion trap mass spectrometer and a hybrid linear ion trap FT ICR mass spectrometer. This allowed a more inclusive analysis concerning the coverage of the peptide sequence, enabling the identification of a larger number of modified cysteine residues by forming covalent adducts. The studied compounds were found to activate the NRF2 pathway by targeting the KEAP1 BTB domain through a covalent interaction with Cys151, which has been established as a more reactive residue against the three natural products [90]. Xanthohumol was further investigated for its potential neuroprotective effect against oxidative stress-induced neuronal cell injury using the neuron-like rat pheochromocytoma cell line PC12. Results indicated that xanthohumol showed a moderate free-radical scavenging profile, while it is a potent antioxidant at submicromolar concentrations, being able to target KEAP1 forming covalent adducts by the  $\alpha,\beta$ -unsaturated ketone moiety, increasing NRF2 levels, which upregulated several protective/antioxidant genes culminating in an overproduction of several proteins including HO-1, thioredoxin and thioredoxin reductase, quinone reductase. Based on these results, xanthohumol can be considered for further studies to prevent neurodegeneration [91]. Subsequently, another component of *Zingiber officinale*, 6-shogaol, was found to act as an NRF2 inducer, forming a covalent adduct with the KEAP1 protein, showing significant antioxidant effects [92]. Accordingly, xanthohumol, isoliquiritigenin, and shogaol derivatives require further biological characterization as chemopreventive agents.

Andrographolide (Table 1), the main constituent of *Andrographis paniculate* that is commonly utilized as a medicinal herb and health food in China, India, and East Asia, was investigated for its antioxidant effects via the KEAP1/NRF2 pathway by Yuan and colleagues [93]. Using the LC-MS/MS technique, the researchers found that the compound reacted with different cysteine residues on KEAP1 (Cys77, Cys151, Cys273 and Cys368), inducing quinone reductase expression via the NRF2 pathway. Further characterization of the mechanism of action was conducted by Wong and collaborators. In this study, the HEK293T cell line was treated with andrographolide for 4 h. The results showed that andrographolide induced a significant time-dependent expression of NRF2. According to previous results, researchers investigated whether the compound could also increase NRF2 levels by inhibiting KEAP1 targeting cysteine residues. Transfected cells with mutant KEAP1 (Cys151Ser) and wild-type KEAP1 were used. Increasing NRF2 levels were only observed in wild-type KEAP1 cells, whereas a dramatic decrease in NRF2 levels was detected in mutant cells, demonstrating a biological effect of andrographolide Cys151-dependent, similar to that found for

sulforaphane. Interestingly, the authors described a fascinating concentration-dependent effect of andrographolide. In fact, at low concentrations, it was able to decrease the binding between KEAP1 and Cul-3, stabilizing NRF2 in a Cys151-dependent manner, while increasing concentrations of andrographolide (until 100  $\mu$ M) resulting in an increase in the expression of NRF2 and of the binding of KEAP1 with Cul-3 in a Cys151-dependent manner, as already observed for other compounds with similar behavior (e.g., arsenite, monomethylarsonous). The correct physiological role of the increase in KEAP1/Cul-3 binding is not fully understood. Further studies are necessary to better characterize the significance of this increasing association for improving knowledge about KEAP1 functions, enabling the rational design of innovative chemopreventive agents [94]. Very recently, andrographolide and some semisynthetic derivatives were investigated in the SARS-CoV-2 drug discovery campaign. Interestingly, andrographolide was found to inhibit viral replication in the low micromolar range in Vero-E6-infected cells. The authors speculated that this activity can be mediated by the activation of NRF2, which is consequent to the covalent binding of andrographolide to KEAP1. In effect, NRF2 plays a pivotal role in the viral replication defense of SARS-CoV-2, being able to directly and indirectly modulate several host proteins involved in the viral life cycle. In particular, andrographolide via NRF2 is involved in the expression of angiotensin-converting enzyme 2 (ACE-2), HO-1, and interferon regulatory factor 3 (IRF-3). Considering these aspects, NRF2 can downregulate the production of interferon, attenuating inflammation-induced cell injury. Notably, NRF2 expression was drastically reduced in COVID-19 patients; therefore, activating this pathway with drug molecules is an interesting option for developing antiviral agents that can limit the inflammatory host response. Moreover, the activation of ARE genes for producing endogenous antioxidants could mitigate the symptoms caused by the cytokine storm after the entry of the virus [95].

Satoh and collaborators investigated the natural product carnosic acid (Table 1), a component of rosemary (*Rosmarinus officinalis*) and common sage (*Salvia officinalis*). The performed studies allowed the scientists to identify the KEAP1 regions necessary for the binding of carnosic acid. The results highlighted that the preferred binding site is located in the BTB domain, and the involvement of Cys151 is highly probable. Carnosic acid was demonstrated to activate the NRF2 pathway and act as a neuroprotective agent in vitro and in vivo. They found that the protection exerted by carnosic acid interested neuronal and non-neuronal cells, but because of the accumulation of compound in the brain, carnosic acid is a good candidate for the potential treatment of neurodegenerative disorders. In fact, in PC12h cells, carnosic acid activated the NRF2 pathway, whereas in immature cortical neurons in primary culture from an oxidative glutamate insult and in neuronal/glia cortical cell cultures (E17, DIV21), significant neuroprotection was clearly detectable. Furthermore, in an animal model with

MCAO/reperfusion injury, carnosic acid protects the brain by decreasing the volume of cerebral infarcts through a mechanism in which NRF2 is involved [96].

Finally, the compound falcarindiol (Table 1), one of the components of carrot roots (*Daucus carota*), was investigated by Ohnuma and collaborators for its possible effects on the KEAP1/NRF2 pathway [97, 98]. They reported that falcarindiol was able to induce the expression of enzymes with antioxidant capacity and phase II drug-metabolizing proteins via the NRF2 pathway, protecting cells from rat liver (Clone9) from menadione-induced cell death. In another report, the authors elucidated the mechanism of action of falcarindiol in the activation of NRF2. Using the NMR technique, they demonstrated that falcarindiol was able to interact with KEAP1, forming covalent adducts with cysteine residues by the conjugated diacetylene carbon atoms, which act as electrophilic functional groups. Moreover, by employing matrix-assisted laser desorption/ionization time-of-flight mass spectrometry and circular dichroism spectroscopy, the authors reported that falcarindiol produced an S-alkylation against cysteine residues located in KEAP1, altering its secondary structure. Additional experiments conducted on transfected cells confirmed the ability of falcarindiol to activate NRF2. ARE-luciferase activity was inhibited by the entire KEAP1 protein according to transfection studies using the pure KEAP1 protein, a luciferase reporter construct, and an NRF2-expressing plasmid. Notably, the falcarindiol-alkylated KEAP1 protein did not inhibit this activity. Furthermore, in HEK293 cells treated with falcarindiol, overexpressing KEAP1, the authors observed a KEAP1 form with high molecular weight due to the adduct formation by falcarindiol on Cys151, which can be considered the only residue necessary for the formation of high molecular weight KEAP1 and for increasing ARE-luciferase activity.

#### *Natural products as non-covalent modulators of KEAP1/NRF2 pathway, improving the expression of antioxidant genes*

In these paragraphs, we have reported the natural compounds that showed antioxidant effects by improving NRF2 activity, characterized by non-covalent binding with KEAP1. In most cases, the interaction of the natural compounds with KEAP1 was analyzed using computational methods. Computational methods are of fundamental importance in the discovery of the mechanisms of action of drugs obtained using synthetic procedures or natural products. In many papers reviewed, there is evidence of upregulation of NRF2, but there is no unequivocally direct evidence of the interaction between the natural compound and KEAP1. Demonstrating a direct binding event requires a cell-free assay with isolated proteins. A cell-based assay is harder to interpret alone because changes in NRF2 activity may be mediated by other indirect responses to the small molecule in cells, e.g. oxidative stress - such effects are difficult to rule out. We are aware that juxtaposing cell-based data with molecular modeling predictions that imply specific direct interactions with KEAP1 without any

caveats could be misleading, but we have limited our review to what was reported in the original manuscripts. Moreover, although not supported by direct experimental evidence, the computational studies reported in these paragraphs deserve to be cited with the aim of designing more potent and selective antioxidant agents. For the reasons mentioned above, we have dedicated separate sections to molecular dynamics (MD) simulations, pharmacophore modeling, in silico analysis of mutations, data mining, and fragment-based approaches.

## Coumarins

Umbelliferone (UMB) (Figure 3A), a 7-hydroxycoumarin (or chemically a benzopyrone derivative), isolated from *Angelica decursiva*, is present in various parts of plants, such as leaf, roots, and fruits of the Umbelliferae family, and has a plethora of biological activities, including anticancer and antiapoptotic effects. In vivo studies and successive immunohistochemistry assays showed that UMB treatment significantly alleviated allergic symptoms and attenuated the oxidative stress by improving the expression of NRF2 and iNOS. Based on docking analysis of UMB within the Kelch domain of KEAP1 (PDB ID: 2FLU), it was predicted that UMB formed stable interactions with key residues of the active site (Ala366, Gly367, Val606) with three H-bonds [99].

Osthole (Figure 3B), a derivative of benzopyran-2-one related to coumarins, isolated from *Cnidium monnieri* (L.) Cuss., activated NRF2, showing agonistic activity, thus inhibiting the KEAP1/NRF2 interaction. Docking studies (PDB ID: 3VNG) demonstrated that this compound could bind KEAP1 to activate NRF2 transcription. The derivative O15 (Figure 3C) exhibited higher inhibitory activity against KEAP1, as demonstrated by the cellular thermal shift assay (CETSA). Docking studies (PDB ID: 3VNG) demonstrated that osthole binds to KEAP1 to activate NRF2 transcription. Modified derivatives, such as the most active one, O15 (Figure 3C), were able to form a stable H-bond interaction with the residue Try251, whereas they interacted with the protonated nitrogen in Arg94 to form cation- $\pi$ , besides further H-bond interactions with the oxygen atoms of the six-member ring. Furthermore, the additional benzene ring present in O15 formed stable  $\pi$ - $\pi$  interactions with Phe256 [100]. **Moreover, in terms of SAR, the cyclization of the aliphatic chain in the dihydropyran ring seems to improve the activity, as well as the bromine atom in the coumarine ring.**

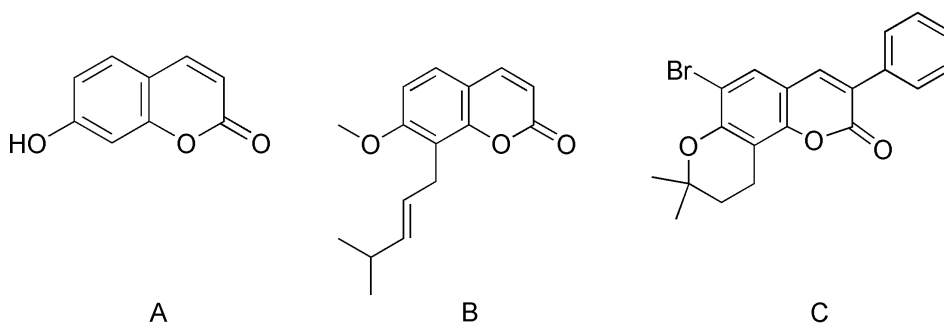


**Figure 3.** Structure of umbrelliferone (A), osthole (B), and its analog O15 (C).

Scopoletin (6-methoxy-7-hydroxycoumarin) (Figure 4A) is the most abundant bioactive coumarin isolated from diverse plant species, such as *Erycibe obtusifolia* Benth and *Foeniculum vulgare*. In vivo tests demonstrated that scopoletin efficiently reduced oxidative stress biomarkers and inflammatory mediators. Moreover, histological and immunohistochemical examination showed the downregulation of KEAP1 levels and upregulation of the NRF2 pathway. It presents an aromatic ring and diverse polar groups, and in docking analysis with KEAP1 (PDB ID: 4L7B), it exhibited a strong H-bond network with several residues (Ser363, Asn382, Asn414 from chain A, and Tyr334 and Asn382 from chain B) at the dimeric interface of the protein. Further  $\pi$ - $\pi$  interactions with the aromatic ring of Tyr334 have been reported [101].

Against the same KEAP1 structure (PDB ID: 4L7B), a docking analysis with visnagin (VIS; 4-methoxy-7-methyl-5*H*-furo[3,2-*g*][1]-benzopyran-5-one, Figure 4B) was performed. This natural compound has been found in *Ammi visnaga* fruits and has several pharmacological activities, including anti-inflammatory and antioxidant effects. In vivo tests have shown that VIS upregulates NRF2 expression, thereby preventing isoproterenol-induced myocardial injury [102]. The complex VIS/KEAP1 is stabilized by two H-bonds with residues Ser363 and Ser602. Furthermore, hydrophobic interactions in the cavity formed by the following amino acids were observed: Tyr334, Gly364, Asn382, Ala556, Phe577, and Gly603.

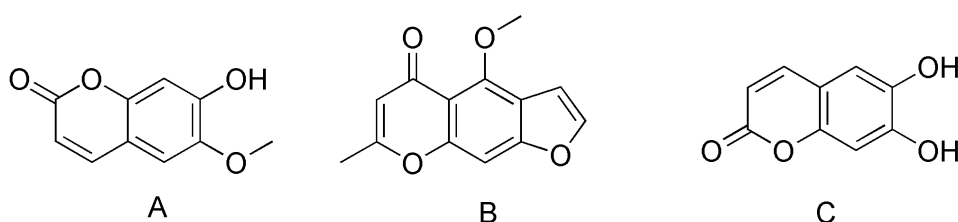


**Figure 4.** Structure of scopoletin (A), visnagin (B), and esculetin (C).

The effect of esculetin (Figure 4C), a 6,7-dihydroxy-coumarin NRF2, on the gene expression of the antioxidant response element pathway was monitored by quantitative real-time PCR (qRT-PCR). The interaction between NRF2 and KEAP1 was lost following esculetin treatment in PANC-1 and MIA Paca-2 cells. Moreover, esculetin was docked in the KEAP1 structure [103]. This coumarin derivative was found to interact specifically with the P1 and P3 sub-pockets of the target via a  $\pi$ - $\pi$  interaction through the two aromatic rings with residues Arg415 and Tyr525. Furthermore, these rings were observed to interact via a  $\pi$ -cationic interaction with the same arginine residue. Esculetin was also involved in the formation of H-bonds with the sidechains of Arg483 and Ala556, and several hydrophobic interactions were found with Ser508, Ser555, Gln530, Gly462, and Ile461 residues. Similarly, alanine scanning was applied to the same complex. **In terms of SAR, the activity of**

scopoletin and esculetin could not be influenced by hydroxyl or methoxyl group, as well as in visnagin where the dihydrofuran ring could be establish both hydrophobic and H-bond interactions

Some coumarin derivatives isolated from *Wikstroemai indica* can be used for the treatment of diabetic nephropathy. Cell-based assays have indicated that the coumarin derivative, shown in Figure 5, as an NRF2 activator attenuated oxidative stress and fibrosis induced by high glucose concentration in mesangial cells by disrupting the interaction between KEAP1 and NRF2. Molecular docking was employed to screen these compounds using the KEAP1 Kelch domain (PDB ID: 4IQK), the NRF2-binding site, and to explore the five sub-pockets in which it is divided. From structural analysis, polar amino acid residues were found in P1 and P2, which can be involved in electrostatic interactions, whereas hydrophobic interactions could be formed by nonpolar parts in P4 and P5. The best ligand, the coumarin derivative shown in Figure 5, was able to occupy some sub-pockets in the domain, forming several H-bonds with key residues in P2 (Arg380, Asn414), P3 (Ser602), and P4 (Gln530) together with Asn382. Further,  $\pi$ - $\pi$  stacking with Tyr525 in P4 and hydrophobic interactions with Tyr525 in P4 and Ala556 in P3 stabilized the complex [104]. In terms of SAR, it is fundamental the presence of the glucose moiety with respect the other derivatives useful to establish a higher net of H-bonds with the subpockets.

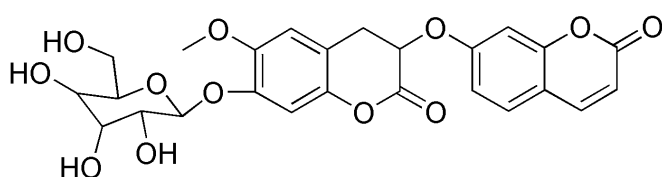


**Figure 5.** Structure of the coumarin derivative.

Polypodiside (Figure 6) is a heterodimer of coumaric acid glucosides, identified from the Chinese fern *Polypodium hastatum*, which can attenuate oxidative stress and help treat some severe microvascular complications of diabetes mellitus. The effect of the polypodiside on the KEAP1/NRF2 complex was evaluated by immunofluorescence assay, dual luciferase reported assay, Western blot analysis, and co-immunoprecipitation assay. Moreover, molecular docking analysis with the KEAP1 Kelch domain (PDB ID: 4IQK) evidenced that this compound forms a complex with the target through H-bonds with key residues (Asn414, Arg415, Ile416, Gln530, and Tyr572), which is further stabilized by  $\pi$ - $\pi$  stacking, hydrophobic and electrostatic interactions, and van der Waals' force. These findings demonstrate how the polypodiside interacts with KEAP1 to interfere with the formation of the KEAP1/NRF2 biological assembly [104, 105]. In terms of SAR, of the glucose moiety seems to be fundamental as showed for the most active coumarine derivative isolated from *Wikstroemai indica*, as described above.

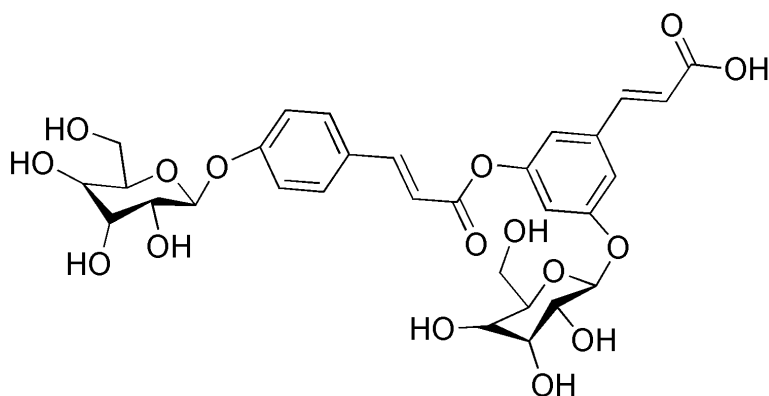


**Figure 6.** Structure of polypodiside.

### Flavones

Simple 3-OH and 7-OH flavone derivatives showed protective effects against NIC-induced cytotoxicity in cultured renal proximal tubule cells. The 7-OH flavone derivative elicited protective activity via the ERK/NRF2/HO-1 pathway. Simple 3-OH and 7-OH flavone derivatives, known for their antioxidant properties, were docked with protein KEAP1/NRF2 (PDB ID: 2DYH), and MD simulations were performed. The results showed that the two isomers interact with different binding modes, with a binding energy 15.7% higher in the case of the isomer substituted in position 7. The complex was stabilized by four H-bond interactions with key residues (Val418, Val606, and Gly367), whereas in the case of the 3-OH compounds, there were only two H-bonds, with Ala510, and Val512, clearly indicating the different influence of the hydroxy group in the interaction [106].

Morin (MRN) (Figure 7A), a known natural flavonol, has demonstrated shielding ability against ischemia/reperfusion (I/R) lesions in various organs. Morin actuates the NRF2/HO-1 trajectory to exert its protective effect, as demonstrated by *in vivo* tests on male Sprague Dawley rats, followed by Western blot analysis to evaluate the expression of NRF2. In the docking analysis of KEAP1 binding (PDB ID: 1X2R), where the NRF2 ETGE peptide ligand is co-crystallized, it was possible to evidence the formation of two H-bonds, with a water molecule and Ser555, through the hydroxyl and carbonyl groups; a H- $\pi$ -bond with Tyr525 was also found [107].

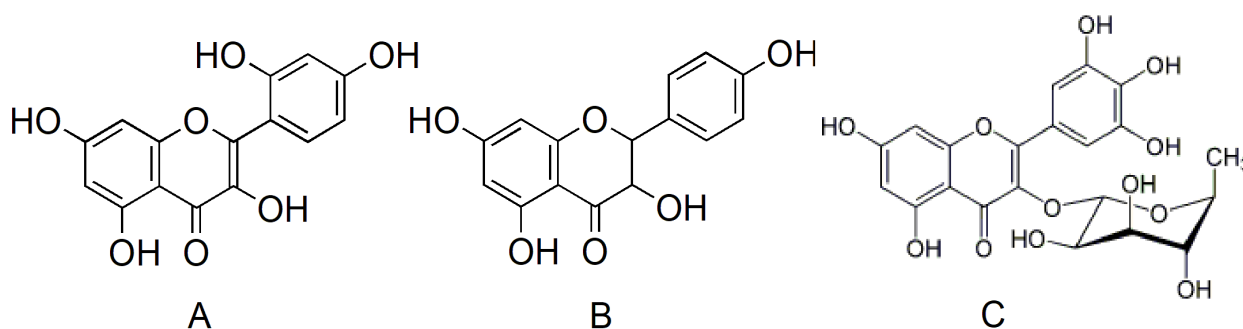


**Figure 7.** Structure of morin (A), dihydrokaempferol (B), and myricitrin (C).

Dihydrokaempferol (DHK) (Figure 7B), a natural flavonoid extracted from *Bauhinia championii*, showed interesting activity against severe acute pancreatitis (SAP), a nonbacterial inflammatory disease that causes a high mortality rate. In vivo studies have demonstrated that DHK improves pancreatic oxidative stress injury by regulating the KEAP1/NRF2 pathway. The molecular docking results were consistent with the activity from the in vivo and in vitro models [108]. DHK interacted with the active site of the KEAP1 N-terminal BTB domain and C-terminal Kelch region with a similar binding energy; thus, DHK showed distinct affinities to the binding sites acting as agonists of the KEAP1/NRF2 pathway. H-bonds with Arg415, Ser363, and Ile416 of the Kelch domain and with Ser146 and Tyr85 of the BTB domain were found. In terms of SAR, comparing the structures of morin and DHK, the presence of a hydroxyl in meta of phenyl ring of morin, as well as a double bond in the flavone moiety seems to be not relevant for the activity.

Myricitrin (Figure 7C), the main component of aqueous/alcoholic extracts from the leaves of *E. hygrophilus*, exhibited anti-influenza activity and neuroprotective effects. This derivative [a 3',4',5,5',7-pentahydroxy-3-( $\alpha$ -L-rhamnopyranosyloxy)flavone] and other analogs were docked into the BTB domain of KEAP1 (PDB ID: 4CXT) to explore if these compounds could interfere with the network of several cysteine residues, which are the critical amino acids in the BTB domain of KEAP1 (Cys151, Cys273, and Cys288). Among the reactive cysteine residues, Cys151 is a crucial amino acid to target for disrupting the KEAP1/NRF2 interaction. The authors limited their work to computational analysis, and no in vitro or in vivo tests were reported in the original manuscript [109]. Based on the in silico analysis, the complex was stabilized by several H-bonds (with Gln86, Gly127, and Cys151) and other types of interactions (van der Waals,  $\pi$ -alkyl). Because Cys151 plays a fundamental role in the KEAP1/NRF2 interaction, molecular docking was also performed between myricitrin and the KEAP1 mutant Cys151Trp (PDB ID: 4CXJ). As a result, it was possible to demonstrate that the non-covalent interactions (H-bonds and  $\pi$ -alkyl interactions) were diminished by mutation. In terms of SAR, comparing the structures of morin and DHK, the presence of a hydroxyl in meta of phenyl ring of morin, as well as a double bond in the flavone moiety seems to be not relevant for the activity. In terms of SAR, for this extract component, the rhamnose sugar moiety revealed to be useful to establish a H-bond network.

Flavanone liquiritigenin (LG) and its analog 4'-O-glucosideliquiritin (LQ) (Figure 8) were found in *Glycyrrhizae Radix et Rhizoma* (Gan-Cao), an herbal medicine commonly utilized for centuries in Asia for its good detoxification activity. LG and LQ attenuated MCT-induced HSOS, and MCT-induced liver oxidative injury in rats. Both compounds induced the activation of the NRF2 antioxidant pathway by binding to KEAP1. Both when docked in the human KEAP1 binding site (PDB ID: 4L7B) formed complexes stabilized by several H-bonds (some of them also through a water molecule) joint to H- $\pi$  interaction mainly with Arg415, but with additional binding with Arg415, Ala556, and Tyr572

in the case of LQ. In terms of SAR, in the presence of the hydrophilic glucide, the whole binding of this last resulted in greater stability [110].

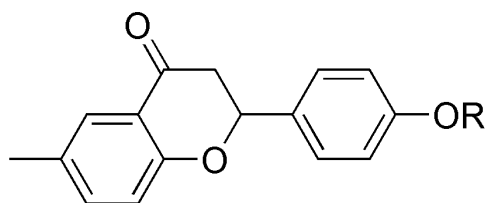


**Figure 8.** Structure of liquiritigenin (R=H) and liquiritin (R=4'-( $\beta$ -D-Glucopyranosyl)).

Apigenin (4',5,7-trihydroxyflavone, API) (Figure 9A), a naturally occurring plant flavone, can be found in many fruits, vegetables, herbs, and spices, and has shown protective effects against metabolic syndrome. In vivo tests showed that API improved insulin resistance, alleviated liver injury, and inhibited the alterations of lipid profile in high-fructose diet-fed mice via the modulation of the KEAP1/NRF2 pathway, thus leading to the accumulation of NRF2, as highlighted by Western blot analysis. Its behavior in the KEAP1 binding site (PDB ID: 4L7B) demonstrated that API can be positioned in the hydrophobic pocket of the protein, surrounded by the residues Tyr334, Tyr572, and Phe577, which form stable hydrophobic contacts [111]. A  $\pi$ - $\pi$  stacking interaction with the sidechain of Tyr572 occurred with the 4-OH group, whereas the flavone scaffold exhibited cation- $\pi$  interaction with Arg415, which was further stabilized by an H-bond with the residue Ser602.

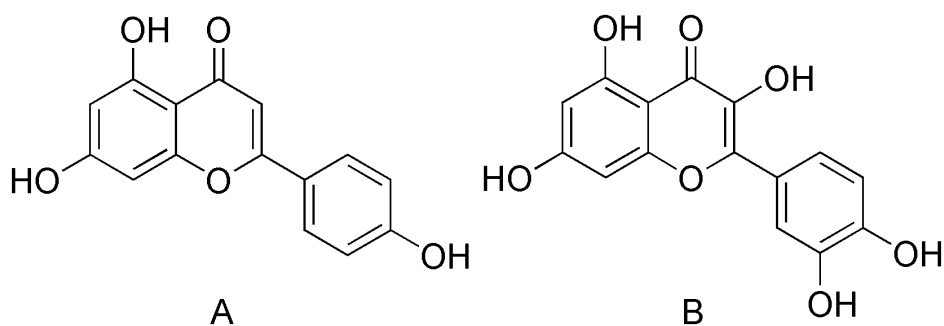


**Figure 9.** Structure of apigenin (A) and quercetin (B).

Quercetin (3,3',4',5,7-pentahydroxyflavone, QUE) (Figure 9B) is one of the most abundant dietary natural flavonoids and is found in various vegetables, tea, fruits, medicinal herbs, and red wine. It has been demonstrated to have protective functions against hepatotoxicity. Several in vitro tests were used to evaluate its protective role in activating the NRF2/ARE antioxidative signaling pathway. Moreover, it has also been extensively studied with in silico approaches, mainly molecular docking analysis. QUE could target the KEAP1/NRF2 complex (PDB ID: 4XMB) interacting with five residues located in the active sites (Ser363, Arg380, Arg415, Arg483, Ser508), forming van der Waals, salt bridge, alkyl, and H-bonds, and it could disrupt the KEAP1/NRF2 complex, driving the translocation of NRF2 into the nucleus [112]. QUE is also capable of interacting with the well-characterized binding

site of human KEAP1 inhibitors. In fact, docking results with KEAP1 (PDB ID: 4L7B) showed two possible H-benzene contacts between the residue Arg415 and the benzene rings of chromone, further stabilized with H-benzene interaction between the residue Tyr527 and hydrogen atom at the 5'-position, and H-bond with Gly364 with its carbonyl group. Notably, QUE is one of the approved senolytic agents, having curative effects against intervertebral disk degeneration (IDD), which is one of the main causes of low back pain [113]. In terms of SAR, API and QUE differ for a hydroxyl group in the chromone ring and a hydroxyl group in the phenyl ring, but both do not seem to influence the binding.

Taxifolin (TAX) is a pentahydroxyflavanone that is a 2,3-dihydro derivative of QUE and has a chemopreventive effect on colon carcinogenesis. TAX stimulated the expression of NRF2 by inhibiting Wnt signaling in DMH-induced mice. When docked against NRF2 (details about PDB ID used for the docking studies were missed in the original manuscript), it exhibited a wide network of interactions through H-bonds with Ala69, Phe70, Phe71, Ala72, Gln73, Gln75, and Leu84 [114].

Oxidized products (Figure 10A), which can be obtained by processes also enzymatically induced, can exhibit better antioxidant activity than QUE itself. Among them 2,5,7,3',4'-pentahydroxy-3,4-flavandione or its tautomer [2-(3,4-dihydroxybenzoyl)-2,4,6-trihydroxy-3(2H)-benzofuranone] (Figure 10B), when docked with KEAP1 (PDB ID: 4L7B), evidenced their capability to bind at the active site of the protein via a network of H-bonds, and several hydrophobic contacts. Computational assessment of numerous physicochemical properties (e.g., bond dissociation enthalpies, proton affinities, potential energy surface) was performed on QUE and its main oxidized species using density functional theory (DFT). This information was useful in investigating the antioxidant activity in these species, which is mainly due to the sequential proton loss electron transfer (SPLET) mechanism. Interestingly, the best KEAP1-metabolite interaction energy correlated well with these properties because the benzofuranone derivative was identified as the most thermodynamically stable oxidized isomer. Finally, QUE was identified as a better direct antioxidant than its oxidized analogs because of its kinetically favored SPLET reactions. The caveat of this interesting theoretical study is the lack of experimental evaluation [115].

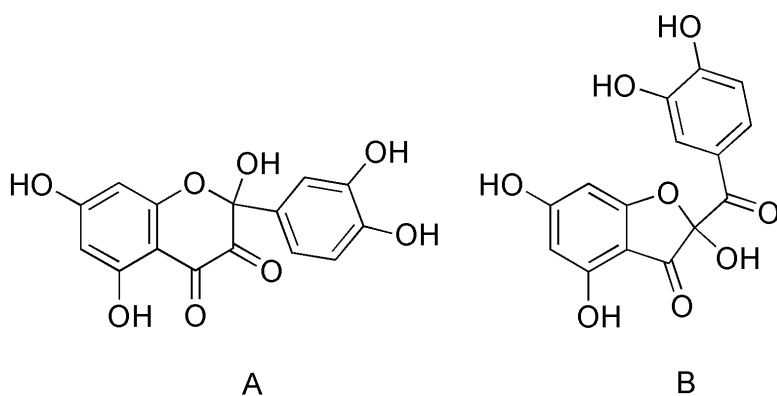


**Figure 10.** Structure of oxidized flavandione (A) and benzofuranone (B).

Tricetin (Figure 11), a rare type of aglycone flavonoid, has been isolated from different plants (*Ginkgo biloba L.*, *Carica papaya L.*, *Murraya exotica L.*) and has shown cytostatic properties and anti-metastatic activity against many solid cancers. In vitro assays showed that tricetin induced the protein expression of NRF2 and its transcriptional activation, resulting in the upregulated expression of HO-1, which conferred neuroprotection against 6-OHDA-induced oxidative damage. It has also been proposed as an anti-Parkinson drug. When docked in apo-KEAP1 (PDB ID: 4IFN), the derivative was found to be anchored to the binding site through several H-bonds with Val418, Val465, Ile416, Ala510, and Gly509, whereas the CO group interacted, again by means of H-bonds, with Val606 and Ile559 [116]. **In terms of SAR, we could make the same considerations as above for API and QUE.**

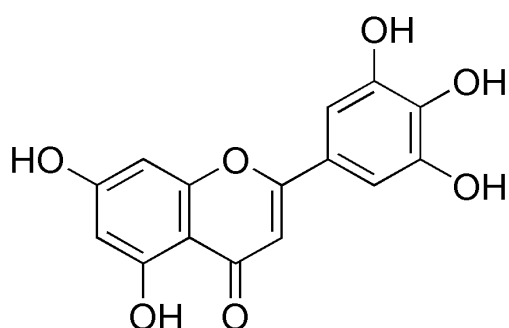


**Figure 11.** Structure of tricetin.

Rhoifolin (ROF) (Figure 12A), a glycosyloxyflavone (functionalized at 7-hydroxyl group with rhamnopyranosyl and glucopyranosyl moieties), showed a considerable anti-inflammatory profile. The role of ROF in the expression of senescence-associated secretory phenotype (SASP) factors was investigated using qRT-PCR, western blotting, and ELISA. SASP factors and cellular senescence were further assessed after transfection with NRF2 siRNA. ROF was docked against NRF2 (PDB ID: 2LZ1), showing a relevant energy score, and knock-down studies demonstrated that ROF might bind to NRF2 to suppress the NF- $\kappa$ B pathway. In vivo, ROF ameliorated the osteoarthritis (OA) in an anterior cruciate ligament transection ACLT rat model [117].

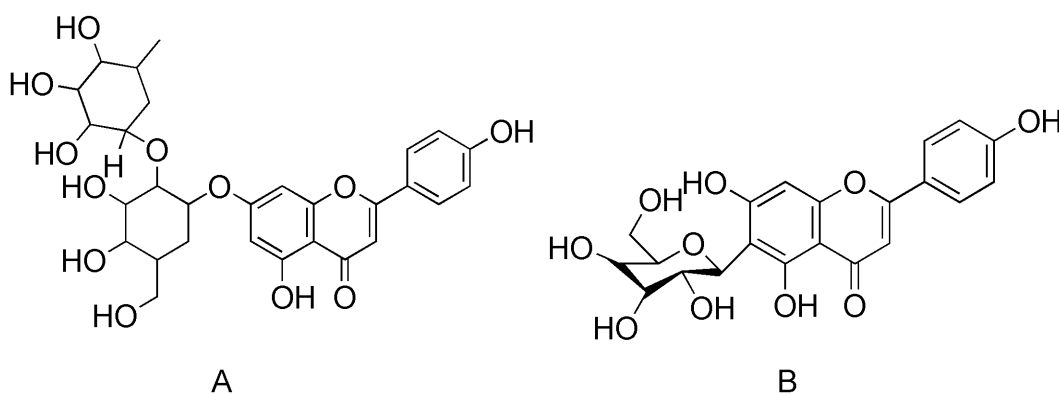


**Figure 12.** Structure of rhoifolin (A) and isovitexin (B).

Isovitexin (IVX) (Figure 12B) (a C-glycosyl-flavone with a 1,5-anhydro-D-glucitol moiety at position 6), found in passionflower, cannabis, and palm, is known for its anti-inflammatory properties. The role and underlying mechanism used by IVX in its regulation of OA development was investigated in vitro (CCK-8 assays, qPCR, Western blot, and ELISA), while docking studies of this compound with NRF2 binding site (PDB ID: 3WN7) showed binding via van der Waals, H-bonds (through Arg415, Ser602, Gly433, Arg380 residues) and  $\pi$ -alkyl interaction with the amino acid Ala556 [118]. **In terms of SAR, the presence of glycosil moieties could be an interesting starting point to design new derivatives with different glycosil ring or reach the conclusion that the flavone is the only responsible for the activity.**

Glyceollins (Figure 13), prenylated isoflavones derived from daidzein in soybean exposed to various types of fungi, showed several pharmacological activities, including anticancer and anti-estrogenic effects. Western blot analysis showed that the compounds increased the expression of some representative antioxidant enzymes, such as HO-1, gamma-glutamylcysteine synthase, and glutathione reductase, by promoting nuclear translocation of NRF2. Therefore, they were investigated for their ability to interfere with the release mechanism of NRF2 from KEAP1, by modeling the region that includes residues 77–287 of KEAP1 (PDB ID: 3I3N), and the role of KEAP1-Cys151 as a key residue in the BTB-BACK domains of human KLHL11. This is a shallow binding pocket, mostly positively charged all around, which surrounds Cys151. Thus, the binding of polar compounds is favored in contrast to the negatively charged area outside the Cys151 binding domain. The docking simulations strongly suggested that the isomers tightly bind into the binding pocket around Cys151, thus precluding KEAP1/NRF2 binding, although it was problematic to discriminate between the three isomers because they bind in a similar fashion around Cys151 [119]. **Data reported in the original manuscript did not help us to define the most active compound and try to highlight a SAR as well as the authors did.**

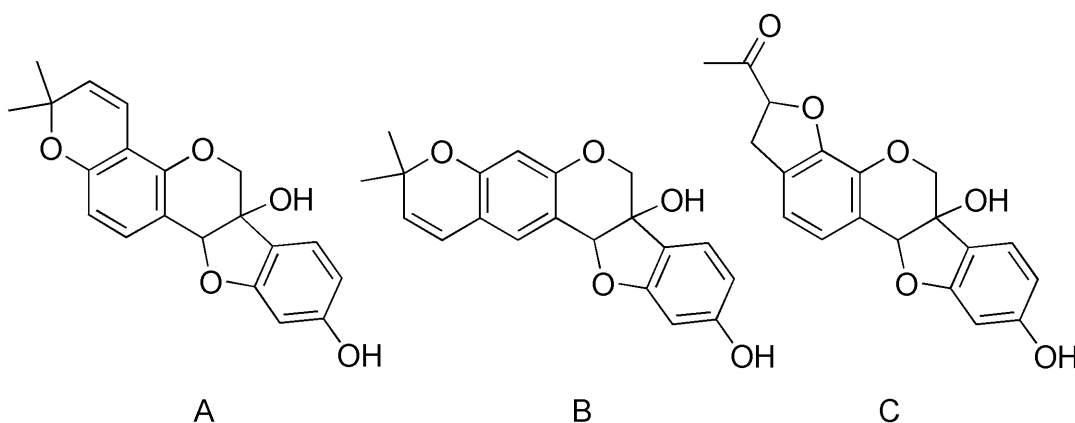


**Figure 13.** Structures of glyceollins.

Biochanin A (BCA) (Figure 14A), a 4'-O-methylated isoflavone, showed low direct antioxidant activity as an NRF2/ARE activator (Western blotting, EMSA, qRT-PCR). It was docked into KEAP1, in the NRF2 binding site (PDB ID: 4ZY3). BCA was able to interact with key residues of the protein (Arg415, Ser508, Asn414 and Asn382), which are known for their importance in modulating KEAP1/NRF2 PPI [120].

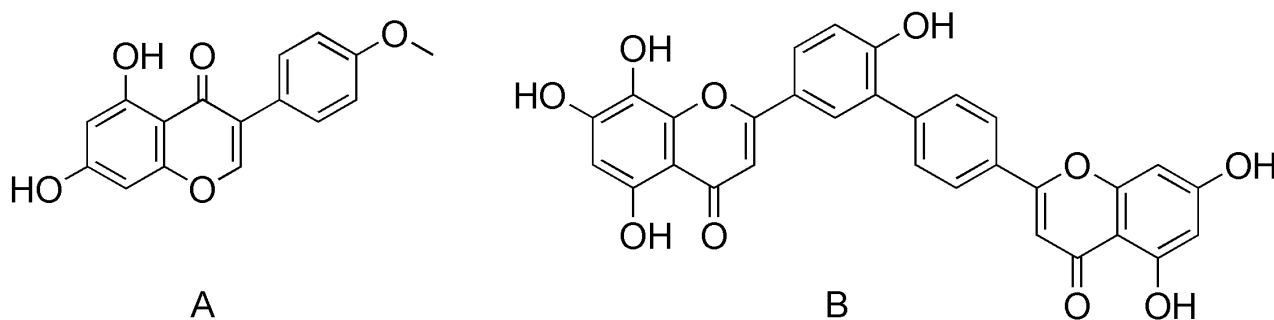


**Figure 14.** Structure of biochanin A (A) and japo flavone D (B).

Biflavonoids are substances with significant antioxidant properties, such as japo flavone D (JFD) (Figure 14B), isolated from *Lonicera japonica* flower buds. In vitro tests showed that JFD inhibited cell viability in all hepatoma cell lines examined, downregulating the KEAP1/NRF2/ARE signaling axis. Docking analysis to explore the binding mode of JFD in the NRF2 binding site of KEAP1 (PDB ID: 5WFV) showed that it can be well located in the hydrophobic pocket, surrounded by the residues Tyr525, Ala556 and Tyr572, forming stable bonding interactions. CH- $\pi$  and  $\pi$ - $\pi$  stacking interactions were formed between the two chromen-4-one groups and Tyr525 and Tyr334. In addition, cation- $\pi$  interactions with Arg380 and Arg415 and H-bonds with Arg380, Asn382, and Gln528 contributed to the stabilization of the complex, suggesting that JFD could act as a KEAP1 inhibitor [121]. **The chromen-4-one group showed its importance in these last two derivatives much more than the hydroxyl groups, confirming that the flavone ring is crucial for the binding with KEAP1**

#### Catechins

Catechins are a type of natural polyphenol widely present in teas, coffee beans, and various fruits. Among them, (-)-epicatechin (EPI) (Figure 15A), a natural flavanol, was investigated for the treatment of hepatic sinusoidal obstruction syndrome (HSOS), a rare liver disease with considerable morbidity and mortality. EPI enhanced the nuclear translocation of NRF2 and increased the expression of its downstream antioxidant genes in rats. Molecular docking results revealed the potential interaction of EPI with the NRF2 binding site in KEAP1 (PDB ID: 4L7B), observing a direct H-bond with Asn382 and a water-mediated H-bond with Ser508 [122]. In addition, (+)-catechin hydrate exerted the same type of protection. Thus, docking analysis on the same protein (PDB ID:

4L7B) evidenced the formation of an H-bond between Ser508 bridging by one water molecule and two other H-bonds with residues Asn382 and Ser602 [123].

Epigallocatechin gallate (EGCG) (Figure 15B) is one of the most abundant catechins in tea and is known for its antioxidant and anti-inflammatory potential. EGCG potentially reduces fluoride-induced lung oxidative stress, and inflammation via the KEAP1/NRF2 signaling pathway in rats. When docked with human KEAP1 (PDB ID: 1ZGK) protein, several H-bonds, hydrophobic and charged interactions were found anchoring the ligand to the key residues Gly343, Thr595, Leu578, and Asp579 [124]. SAR of these catechins do not differ from previous considerations made for coumarine and flavone derivatives.

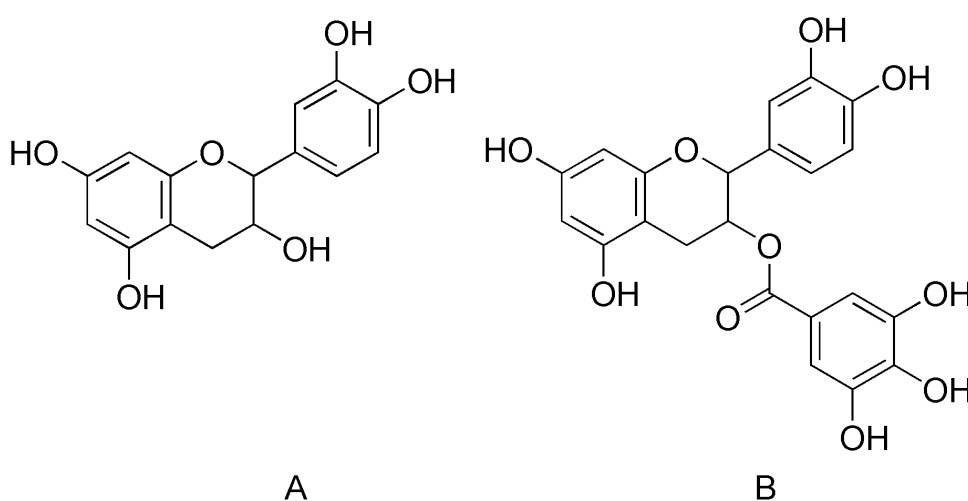


**Figure 15.** Structure of (-)-epicatechin (A) and epigallocatechin gallate (B).

### Polyphenols

Among polyphenols from natural sources and of biological importance, it is impossible not to briefly cite resveratrol (Figure 16A). It has been known for a long time and has broad applications for treating neurodegenerative disorders. It was demonstrated that resveratrol attenuates methamphetamine-induced memory impairment by inhibiting oxidative stress and apoptosis in mice. The expression of KEAP1 was significantly increased, whereas the translocation and activation of NRF2 into the nucleus and expression of its downstream proteins were greatly decreased in the hippocampus. The proposed mechanism is the interaction with KEAP1, as supported by docking into the protein structure of KEAP1 (PDB ID: 6LRZ) showing good affinity. The complex was stabilized by H-bonds with the key amino acids Leu365, Leu557, and Ile559 [125].

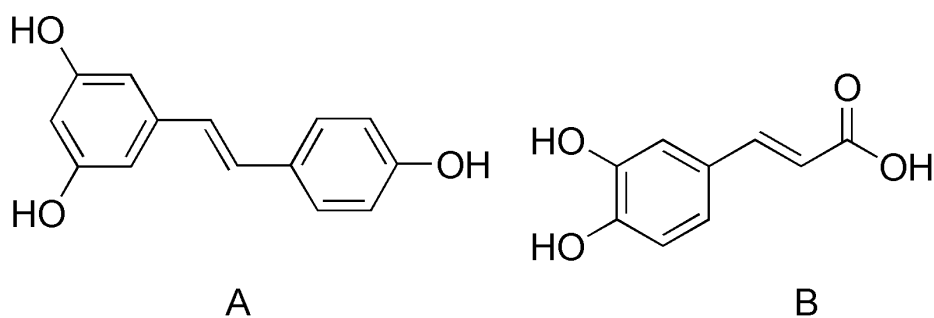


**Figure 16.** Structure of resveratrol (A) and caffeic acid (B).

Caffeic acid (Figure 16B), a well-known phenolic compound synthesized by all plant species and present in foods (tea, coffee, wine) has shown antioxidant, cardioprotective, and neuroprotective activity, and can also be used as a biological target for NRF2. In fact, co-exposure to caffeic acid reduced mortality and markedly attenuated the biochemical changes induced by paraquat, a widely used herbicide. In fact, docking analysis against the protein (PDB ID: 4IQK) evidenced that the acid can accommodate well in the active pocket of NRF2 and entered the bound region of the KEAP1 Kelch domain within NRF2; it also showed relevant interactions via four H-bonds, with six hydrophobic interactions with Arg415, Ile416, Val463, and Ala510, mainly with glycine residues (364, 462, 464, 509, 603) and Ala556 [126].

Chlorogenic acid (CGA) (Figure 17), a dietary polyphenol (found in coffee and black tea), that is the ester of caffeic acid and quinic acid, has potential antioxidant and chemopreventive activities and prevents APAP-induced liver injury and enhanced NRF2 activation in mice and hepatocytes in vitro. Molecular docking results indicated that it is capable of interacting with the NRF2 binding site in KEAP1, forming interactions with key residues (Arg415, Ala556, Tyr525) and two H-bonds with Arg415 and Gln530 [127].

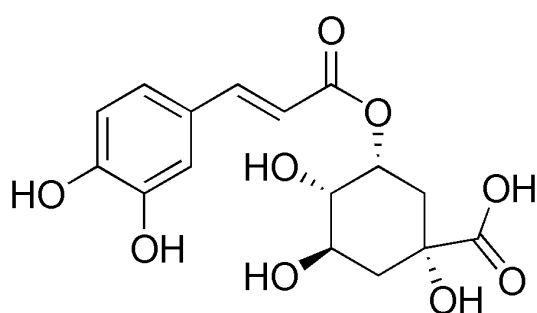


**Figure 17.** Structure of chlorogenic acid.

Phlorizin (Figure 18A), a natural product found in apples, has significant antioxidant capacity and is a powerful free radical scavenger. Phlorizin protects cells against oxidative stress-mediated injuries by downregulating dangerous free radicals. In vivo analysis on *Drosophila melanogaster* showed that phlorizin extended the life span and reduced age-related decline in locomotor function.

Computational studies based on molecular docking were performed to investigate the interaction between two molecules (phlorizin and curcumin (Figure 18)) and KEAP1 binding site (PDB ID: 2FLU). The output of the molecular docking calculations indicated that the two compounds were able to bind KEAP1 in the same fashion with a comparable binding mode. Based on the docking results, they established H-bonds, polar and van der Waals interactions with key residues such as Val369, Gly419, Val465, Ala466, Cys513, Leu557, Gly558, Ile559, Val561, and Val606 [128].

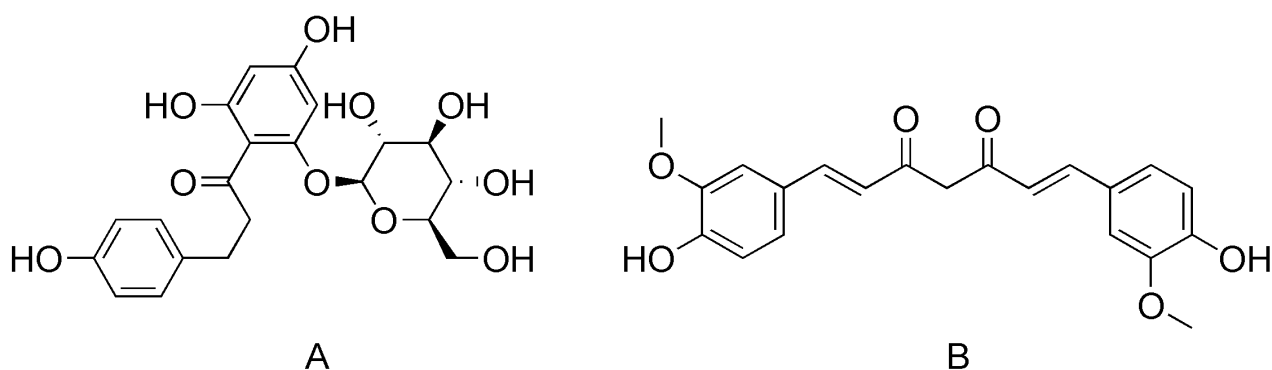


**Figure 18.** Structure of phlorizin (A) and curcumin (B).

The strong antioxidant astaxanthin (AST) (Figure 19), which is related to carotenoid and found in rich *H. pluvialis* species, due to its modulatory effect on the KEAP1/NRF2 pathway, slowed aging-related alterations in the liver by increasing endogenous antioxidant capacity. The molecular docking on NRF2 suggested that AST could bind to NRF2 with high affinity [129].

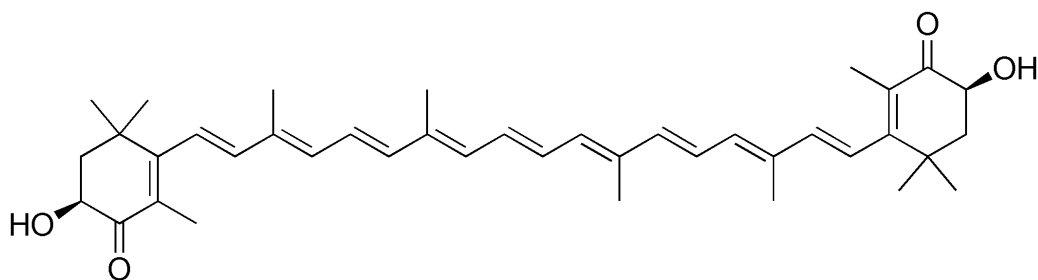


**Figure 19.** Structure of astaxanthin.

Gallic acid (GAL, Figure 20A), a natural polyphenol found in various functional foods and medicinal herbs, exhibited health-promoting effects. It protects against tert-butyl hydroperoxide-induced hepatotoxicity by activating the KEAP1/NRF2/ERK-mediated antioxidative response. Interestingly, the authors found that GAL could enhance the thermal stability of KEAP1, indicating a potential interaction between GAL and KEAP1. Molecular docking calculations of GAL within the NRF2 binding site on KEAP1 (PDB ID: 4L7B) indicated that it can compete with NRF2 for the binding to KEAP1. The complex was stabilized mainly by H-bonds with Asn414 [130].

A natural product related to GAL is ginnalin A (GA, 2,6-digalloyl-1,5-anhydro-D-glucitol) (Figure 20B), which is found in several *Acer* species in East Asia and North America. It has been demonstrated a possible role as a ROS scavenger or NRF2 activator in cancer cells. Fluorescence imaging indicated that upon GA pre-treatment, NRF2 dissociated from KEAP1 and translocated into the nucleus to activate the cellular antioxidant system. This event was also verified by qRT-PCR quantification and Western blot analysis. Molecular docking studies with KEAP1 (PDB ID: 4IQK) showed that GA occupied sub-pockets P1, P2, and P3, forming stable interactions with Arg415 in P1, Ser363 and Asn414 in P2, and Ala556 and Ser602 in P3, mainly through hydrogen bonding. Further hydrophobic interactions in the Kelch domain support the hypothesis that GA can preclude KEAP1/NRF2 recognition. Other interactions in the center of the cavity involving the glycosidic moiety were also observed. Compared with GAL, the interaction between KEAP1 and the GA complex was nearly 20% lower. Thus, the stability of the GA/KEAP1 complex is greater than that of the GAL/KEAP1 complex. **GA is equivalent to two GAL molecules in terms of structure** [131].

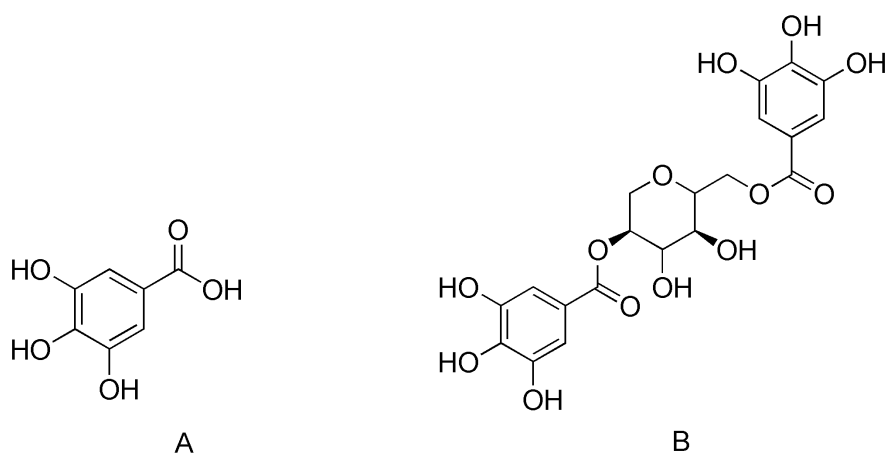


**Figure 20.** Structure of gallic acid (A) and ginnalin A (B).

Ellagic acid (ELL) (Figure 21A), a polyphenol isolated from many vegetables and fruits, is the dilactone of hexahydroxydiphenic acid. The chemical arrangement bears a resemblance to that of two GAL molecules assembled “head to tail” and bound together by a C–C bond (as in biphenyl) and two lactone links. Notably, ELL was identified in the crude extract of *Geranium shiedeanum*. Pre-treatment with the crude extract in a model of thioacetamide-induced hepatotoxicity in rats, decreased and delayed liver injury by 66% at 24 h because of the antioxidant properties of the hydrolysable tannins. In the docking analysis with the structure PDB ID: 1X2R, it was demonstrated that GAL and ELL can accommodate in a cavity connecting the Kelch and BDT domains, without altering its binding with NRF2, MD simulations also supported this finding [132, 133].

Urolithins (Figure 21B), a type of polyphenol, are naturally occurring metabolites originating from the gut microbiota after the intake of foods rich in ellagitannins and ELL. Among them, urolithin A

(UA) was shown to protect against acetaminophen-induced liver injury (AILI). Transcriptomics assay revealed that UA promotes mitophagy and activates NRF2/ARE signaling in the liver. Consistent with this, mitophagy and NRF2/ARE signaling were activated, with reduced oxidative stress in the UA-treated liver. Molecular docking and MD simulation studies showed that the binding mode between UA and KEAP1/NRF2 (PDB ID: 1X2R) was stabilized by a network of H-bonds, mainly among the oxygen atoms and residues Arg415, Ser508, and Ser602, which can trigger NRF2 nuclear translocation [134]. In terms of SAR, it is not to identify the spotlights that define the most active polyphenol due to the similar structural pathways of hydroxyls and phenyl rings for all the compounds described. As matter of fact, the hydroxyl network is fundamental for the binding as the previously described class of compounds. Moreover, docking simulation of Astaxanthin were performed on NRF2 unlike the other polyphenols that were docked against KEAP1.

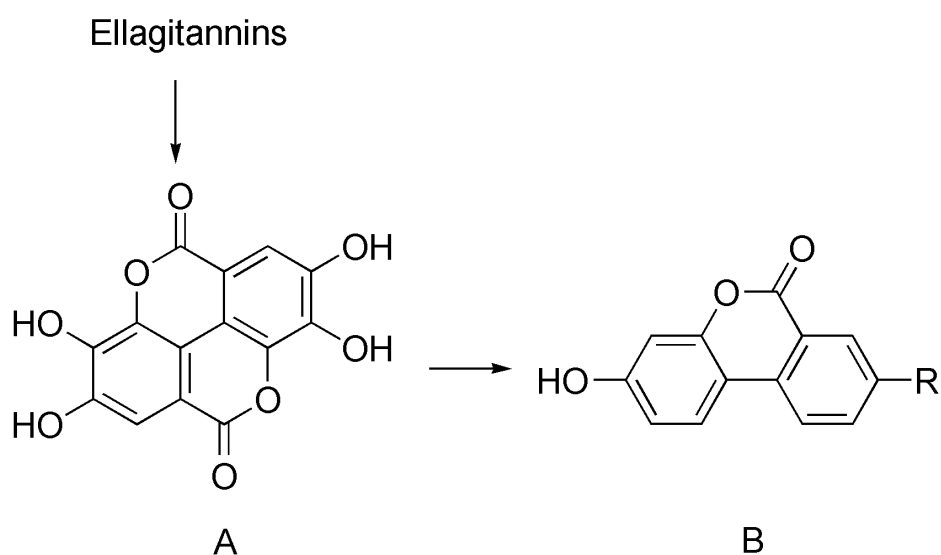


**Figure 21.** Structure of ellagic acid (A) and R=OH urolithin A, R=H urolithin B (B).

### Terpenes

An iridoid monoterpenoid glycoside, asperuloside (Figure 22), increased NRF2 nuclear accumulation in RAW 264.7 macrophages. It was docked against KEAP1 into the NRF2 binding site (PDB ID: 6QMC), showing binding through H-bonds with residues Ile416 and Val604 [135].

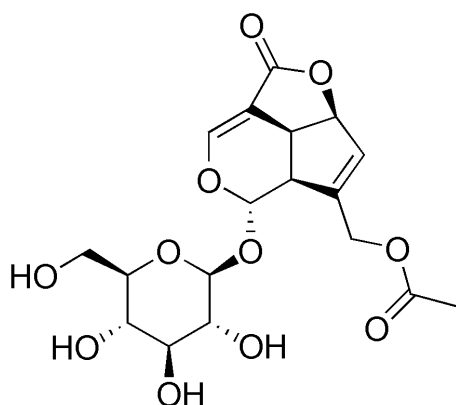


**Figure 22.** Structure of asperuloside.

Carnosic acid (Figure 23), a catecholic diterpene from the Lamiaceae family, significantly attenuated Cd-provoked nephrotoxicity by inhibiting free radicals, endorsing redox defense, suppressing apoptosis, and inhibiting fibrosis in renal cells both in vitro, in normal kidney epithelial (NKE) cells, and in vivo systems, in which twenty-four Swiss albino mice (female, ~4 weeks old, ~25 g) were treated with the compound. In docking analysis, carnosic acid established two H-bond interactions with a nonpolar amino acid (Gln73) of KEAP1 (PDB ID: 2FLU) [136].

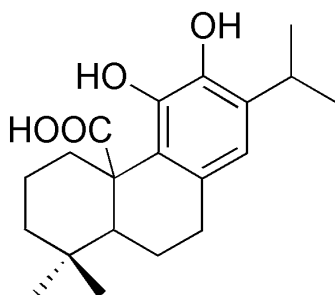


**Figure 23.** Structure of carnosic acid.

Continentalic acid (Figure 24) is a diterpene obtained from *Aralia continentalis* that showed anti-inflammatory effects and could be of interest for treating acute lung injury present in patients often joint with acute respiratory distress syndrome. Among several other effects, continentalic acid-induced NRF2 protein expression, as evaluated by immunohistochemistry analysis. Molecular docking with various protein targets (PDB IDs: 4IQK and 2FLU) gave binding energies of -9.0 and -8.4 kcal/mol, respectively, whereas the main residues involved were Val465 (KEAP1) and Phe83 (NRF2) [137]. **This is a first example of modulator in which the polar moiety is represented just by a carboxylic group, and the hydrophobic interactions seems to be more fundamental than the H-bonds.**

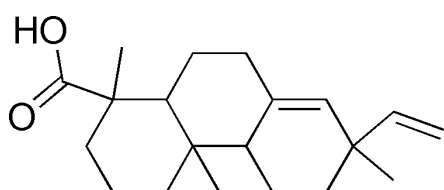


**Figure 24.** Structure of continentalic acid.

A pair of enantiomeric 15-nordolabellane diterpenoids [(-)- and (+)-caseadolabellols A (Figure 25A,B), isolated from the twigs and leaves of *Casearia kurzii*, together with several other natural products, demonstrated significant quinone reductase-inducing activity in Hepa 1c1c7 cells. It was shown by docking analysis that the compound can bind to NRF2 protein (PDB ID: 5FNQ) by H-bonds with Ser508 through the epoxide moiety, interacting also with Gln530 and Ser555 through the carbonyl group at C-14. **However, isomer 1b formed only one H-bond with Ser555. Thus, the study**

explained the different activity observed for this pair of enantiomers, which in any case might attenuate oxidative damage through the activation of the KEAP1/NRF2/ARE pathway, considering that all these amino acids are part of the protein catalytic site [138].

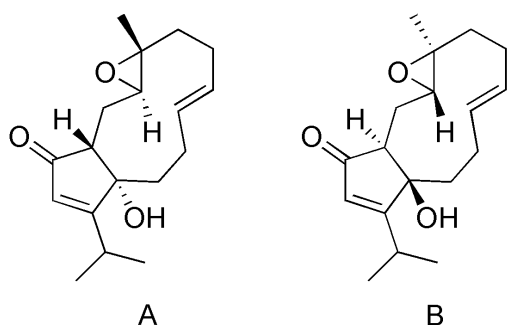


**Figure 25.** Structure of enantiomeric 15-nordolabellane diterpenoids [(-)- and (+)-caseadolabellols A (panel A, B, respectively).

Nerolidol (NER) (Figure 26), a sesquiterpene alcohol found in the essential oils of many types of plants and flowers, is a natural bioactive natural product with an interesting pharmacological profile, showing antioxidant, anti-apoptotic, and anti-inflammatory properties. NER can bind at the active site of NRF2 protein (PDB ID: 5CGJ) through two H-bonds between the hydroxyl group and the sidechain of amino acids Asn382 and Asn414, whereas further interactions involve hydrophobic and van der Waals interactions with several important amino acids (Arg380, Gly364, Ser363, Gly603, Arg415, Phe577, Ala556, Tyr572, Tyr334, and Ser602). The analysis of NER compared to continentalic acid in terms of SAR revealed that a right pattern of insaturations could be as important as H-bond interactions. An in vivo study showed a protective effect of NER against CP-induced neuroinflammation, oxidative stress, cognitive impairment, and structural abnormalities in the hippocampus and cortex regions via the NRF2 and NF- $\kappa$ B pathway [139].

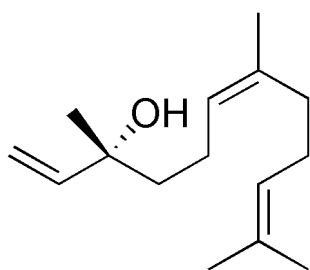


**Figure 26.** Structure of nerolidol.

In 2019, Ya-Nan Qiao and coworkers described six new labdane diterpenoids, the frullanians A–F, which were isolated from the Chinese liverwort *Frullania hamatiloba Stephani* along with five other known diterpenoids. All of them exhibited antioxidant effects mediated via NRF2 induction and thus their capability to interfere with PPI of KEAP1/NRF2 by interacting at the binding site of KEAP1

(PDB ID: 5FNQ); in particular, frullanian D (Figure 27) evidenced the key H-bond interaction with Arg483, with the carboxyl group at C-3 in the KEAP1 Kelch domain [140]. **This compound revealed to be the most active due to the loss of acetyl groups that are present in the other derivatives**

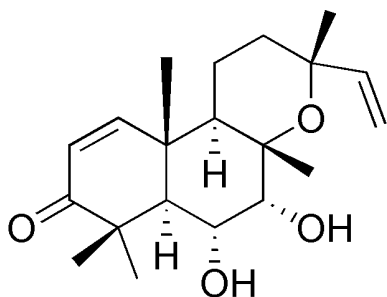


**Figure 27.** Structure of frullanian D.

Pentacyclic triterpenoids (PTs), which are produced by plants as secondary metabolites, are natural compounds possessing diverse biological activities. In an *in silico* screening of PTs and their semisynthetic as well as synthetic derivatives, reported to activate NRF2 signaling, a library of 77 derivatives was evaluated for their interaction with the 16-mer peptide-binding domain on KEAP1 (PDB ID: 2FLU). The library was analyzed using a virtual screening protocol based on the application of sequential filters to determine the NRF2 stimulatory properties of the PTs. This approach allowed the identification of specific hits, such as madecassic acid and 35siatic acid (Figure 28A, B), which represent promising starting points for the development of potent NRF2 stimulators. Furthermore, it was also possible to demonstrate the potential of natural triterpenoid as NRF2 activators with respect to the strong and persistent KEAP1 inhibition achieved by synthetic compounds. Unfortunately, no experimental validation of the computational results has been reported [141]. **For these reasons, we prefer not to try to hypothesize any SAR.**

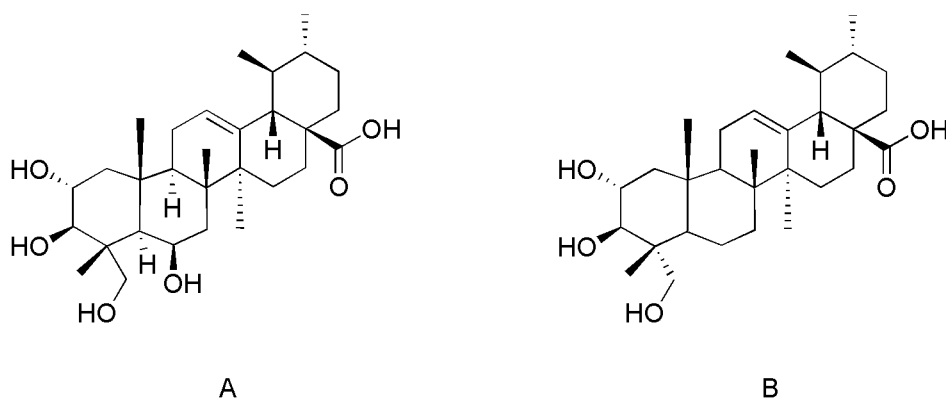


**Figure 28.** Structure of madecassic acid (A) and 35siatic acid (B).

Other natural compounds (miscellaneous)

Magnolol (Figure 29A), a lignan found in the bark of *Houpu magnolia* (*Magnolia officinalis*) or *M. grandiflora*, showed neuroprotective effects in an experimental autoimmune encephalomyelitis (EAE) model of multiple sclerosis in vitro and in vivo. It was studied by means of behavioral, biochemical, and histological analyses. Immunohistochemical detection of NRF2 expression as a marker of oxidative stress was performed. When docked in the binding site of NRF2 (PDB ID: 2FLU), high affinity with the protein was highlighted due to its interaction via H-bond (with Val604) and hydrophobic contacts with Gly364, Ala366, Ala556, and Leu557 [142].

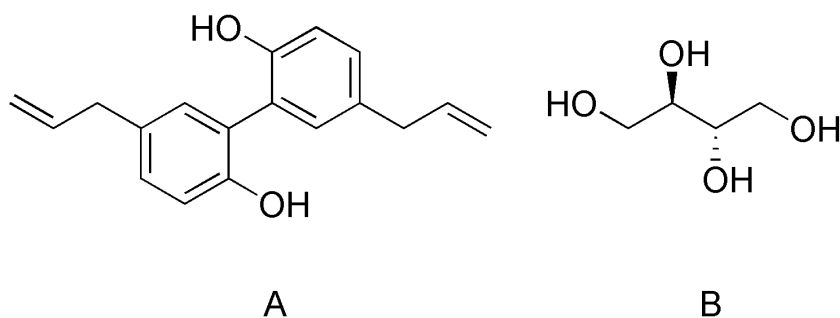


**Figure 29.** Structure of magnolol (A) and erythritol (B).

Erythritol (Figure 29B), a polyol sweetener used as a sugar substitute, effectively promoted NRF2 activation and lipid metabolism homeostasis, as evidenced by in vitro and in vivo studies, by inhibiting endoplasmic reticulum stress and lipid accumulation. In addition, molecular docking evidenced that it formed H-bonds with two key residues, Val512 and Val465 [143].

Shinorine (Figure 30), isolated from the cyanobacterium *Brasilonema* sp. present in the soil crust of some Indian places, can exert a protective role against Cr[VI]-induced toxicity in primary hepatocyte culture established from zebrafish (*Danio rerio*) liver. The estimation of free radical scavenging capacity in vitro was investigated by determining ROS production. Since it was supposed that the biological target could be the DGR domain, responsible for the KEAP1/NRF2 interaction, starting from the X-ray crystal data of *Mus musculus* KEAP1 protein (PDB ID: 5CGJ), zebrafish proteins KEAP1a and KEAP1b were prepared by homology modeling. Docking analysis evidenced that shinorine was able to interact mainly through H-bonds with key residues in the binding site, such as Arg388, Arg456, Tyr49, Gln503, and Ser528, in the case of zebrafish KEAP1a, whereas the involved amino acids resulted in Arg380, Gly427, Arg448, and Ser473, in the other case (KEAP1b). However, all these residues are important for interacting with the ETGE and DLG regions of NRF2 [144].

Shinorine is the first example of modulator we cite that bear two nitrogens as amino and imino groups, but they did not result involved in any interaction in *Mus musculus* and zebrafish KEAP1a.

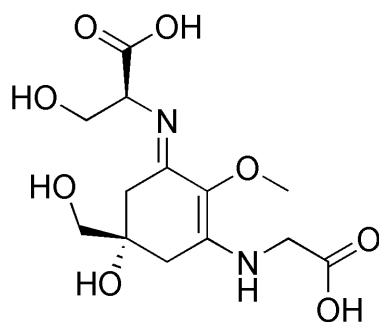


**Figure 30.** Structure of shinorine.

Schisandrol A (Figure 31A), a major bioactive lignan isolated from *Schisandrae chinensis Fructus*, a traditional Chinese medicine used as a hepatoprotective agent. An integrated study, involving UPLC-Q-TOF/MS, pharmacodynamic analysis, and histopathological data along with network pharmacology and molecular docking technology was used to clarify the therapeutic effects and mechanisms involved. Schisandrol A was docked against NRF2 after target fishing; however, no details about the potential interactions are reported in the manuscript [145].

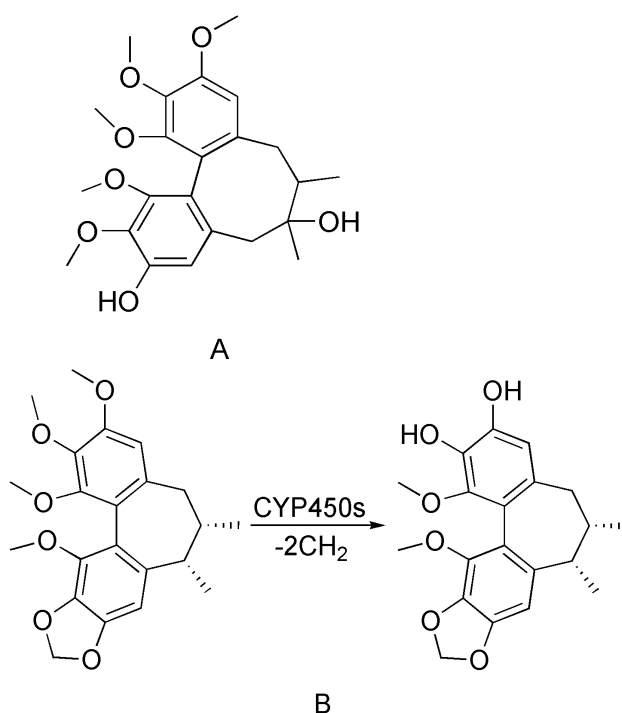


**Figure 31.** Structure of schisandrol A (A) and carbene metabolite of schisandrin B (B).

In addition, a reactive metabolite of schisandrin B (SchB), i.e., the carbene shown in Figure 31B, mainly formed by the action of CYP450, was investigated for its roles in activating the NRF2 pathway and modifying macromolecules, either *in vitro* (in human liver microsomes) and *in vivo* (in mice), where upregulation of CYP450 activity, NRF2 expression, and glutathione level was observed in SchB treatment groups. When analyzed for its interaction at the level of the binding site of KEAP1, it was possible to demonstrate that the carbene, in a compact conformation, was able to bind the hydrophobic pocket of KEAP1 and was surrounded by key residues in the BTB domain (Ile128,

Val132, Cys151 and Val155). Briefly, the 1,3-benzodioxole moiety formed  $\pi$ - $\pi$  stacking with His154, whereas the carbene was oriented toward Cys151. Carbene is characterized by electrophilicity, which activates the NRF2 signal pathway by modifying KEAP1, but it does not covalently bind the protein [146].

**Amygdalin (AMG) (Figure 32A)**, a cyanogenic glycoside derived from bitter almonds, confers protection against Ang II-induced cardiac hypertrophy, oxidative stress, and inflammatory responses. In in vitro experiments, this led to a considerable decrease in the Ang II-induced enlargement of cardiomyocytes, and attenuated the expression of hypertrophic markers (ANP, BNP and MHC-7), inflammatory markers and cytokines. In addition, oxidative stress-related proteins (NRF2, catalase, SOD-2, and GPX-4) were markedly increased following AMG treatment. In addition, AMG showed good binding affinity with the target KEAP1 when docked into the KEAP1 binding site (PDB ID: 5CGJ). The residues mainly involved in bonding were Gly267, Tyr329, Ala365, Ala376, Val397, Arg362, and Leu358 [147]. **As in the case of shinorine, the nitril group do not participate in fundamental interactions that are established by the phenyl and hydroxyls.**

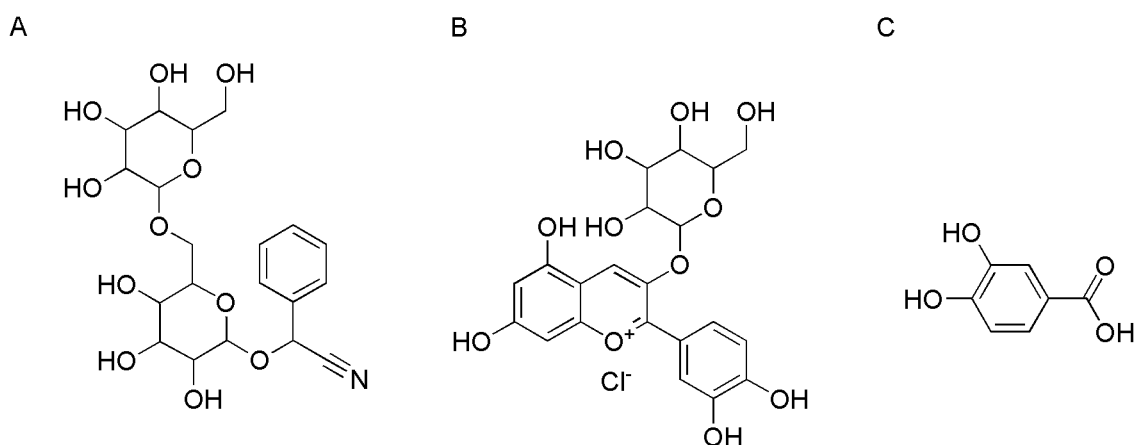


**Figure 32.** Structure of amygdalin (A), cyanidine-3-glucoside (B), protocatechuic acid (PCA) (C).

Cyanidine-3-glucoside and its major metabolite protocatechuic acid (PCA) (Figure 32B, C) showed in vitro protective activity against cytotoxicity and apoptosis in HepG2 cells induced by PhIP (2-amino-1-methyl-6-phenylimidazo[4,5-b]pyridine); thus, they interfered with NRF2 signaling and the apoptotic cascade by binding to KEAP1 and Bcl-2, as indicated by Western blot analysis. Semi-flexible molecular docking with the crystal structure of KEAP1 (PDB ID: 4L7B) showed that **Cyanidine-3-glucoside** was able to occupy the binding site of NRF2 by interacting with key residues such as serine (363, 508, 555, 602), arginine (380, 415, 483), tyrosine (334, 525, 572), and many others (Asn382, Gln530, Asn387, His436, and Phe577). The main types were H-bonds and van der Waals interactions [148]. **The activity of both compounds is mainly due to the catechol moiety**

S-methylmethionine sulfonium chloride (Figure 33), also known as vitamin U, was isolated from many vegetables (turnip, celery, cabbage, tomatoes,) and has antidepressant, antiulcer, and anti-inflammatory effects, and the capability to decrease blood lipid contents. In vivo studies have shown that vitamin U acts as a protective agent against induced oxidative stress and fibrotic alterations via the induction of NRF2 activation in valproic acid-mediated lung injury. Therefore, it was studied by molecular docking analysis to the main active sites of NRF2 and KEAP1 (PDB IDs: 2FLU and 1U6D). The interactions in the binding site involved a network of H-bonds with key residues Ile33 and Asn88 for NRF2, whereas in the case of KEAP1, Ile416 and Val463 amino acids were mainly involved, together with Asn414, Arg415, Val465, Leu557, Ile559, Val604, and Val606 [149].

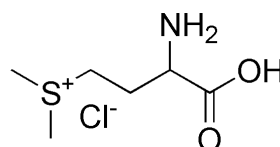
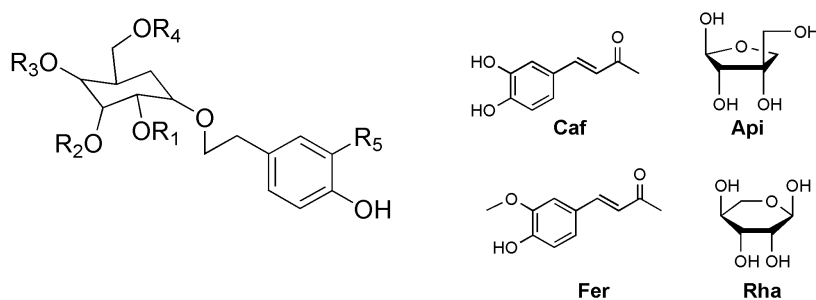


**Figure 33.** Structure of S-methylmethionine sulfonium chloride (vitamin U).

Phenylethanoid glycosides (PhGs) (Figure 34) with anti-inflammatory activity were isolated from *Callicarpa kwangtungensis*, a traditional Chinese herb. Because of their polyphenolic features, the anti-inflammatory activity of PhGs could be strongly associated with oxidative stress. Thus, in in vitro tests, pre-treatment with the main components (acteoside, forsythoside B, poliumoside, alyssonoside, parvifloroside A, and syringalide A 3'- $\alpha$ -L-rhamnopyranoside) could attenuate the intracellular ROS levels in LPS-stimulated RAW 264.7 macrophages. These results indicated that some PhGs induced NRF2 accumulation, probably by suppressing KEAP1 expression. Therefore, the components shown in Figure 34 were docked into the KEAP1 protein (PDB ID: 4L7B). More stable complexes were found in the case of alyssonoside and forsythoside B, with interactions mainly due to several H-bonds: seven between forsythoside B and Ser363, Tyr334, Arg415, Val463, Gly464, Ser508, and Ala556 and nine between alyssonoside and Arg380, Arg415, Ile416, Ser508, Gly509, Ser555, Ala556, Gly603, and Ser602 [150]. They differ just for a methyl group.



PhGs	R <sub>1</sub>	R <sub>2</sub>	R <sub>3</sub>	R <sub>4</sub>
Acteoside	H	Rha	Caf	H
Forsythoside B	H	Rha	Caf	Api
Poliumoside	H	Rha	Caf	Rha
Alyssonoside	H	Rha	Fer	Api
Parvifloroside A	Rha	H	Caf	H
Syringalide A3'-α-L-rhamnopyranoside	H	Rha	Caf	H

**Figure 34.** Structure of phenylethanoid glycosides.

Moreover, 94 inhibitors, among the natural phenylethanoid glycosides, were studied for their ability to bind with mouse KEAP1 (PDB ID: 5FNQ) or human KEAP1 (PDB ID: 4L7B) using semi-flexible docking implemented in AutoDock Vina. All PhGs exhibited high binding affinity to KEAP1 in both species. The binding pocket of KEAP1 was selected considering that three arginine residues (380, 415, 483) were considered indispensable for NRF2 binding, as demonstrated previously by alanine scanning. In fact, the capacity of KEAP1 to bind NRF2 was compromised when the residues Tyr334, Asn382, His436, Tyr525, and Tyr572 were each replaced with alanine [151]. The flexible-docking results indicated that 76 out of 94 PhGs were capable of interacting with eight important amino acids, with forsythoside-β, alyssonoside, leucosceptoside A, and teucrioside sharing similar skeletal structures by targeting Asn382, Arg380, and Arg483. **Moreover, the number of glycoside units was positively correlated with the number of these residues.** Forsythoside-β was able to suppress osteoclast differentiation in vitro in a time- and dose-dependent manner and attenuated bone loss by inhibiting osteoclastogenesis and activating NRF2 signaling in vivo. Moreover, it was also able to inhibit ROS production and induce NRF2 nuclear translocation by disrupting KEAP1/NRF2 PPI. Compared with phenylethanoid disaccharides and phenylethanoid monosaccharides, phenylethanoid trisaccharides bind to a higher number of amino acids. Thus, forsythoside-β ranked first among these promising molecules and was considered for further experiments [152].

Components of the brown alga *Sargassum serratifolium*, with antioxidant, anti-apoptotic, and neuroprotective effects, include the most abundant, sargahydroquinic acid (Figure 35). Western blotting showed that sargahydroquinic acid activated NRF2 and subsequent downstream antioxidant enzymes via a dual mechanism involving the PI3K/Akt axis and disruption of the KEAP1/NRF2 complex. In silico analysis was conducted to investigate its ability to interact with the KEAP1/NRF2

complex (PDB ID: 2FLU). It was possible to demonstrate that four H-bonds were formed with key residues at the active site (Val420, Val512, and Val463) reinforced by 19 other van der Waals interactions [153].

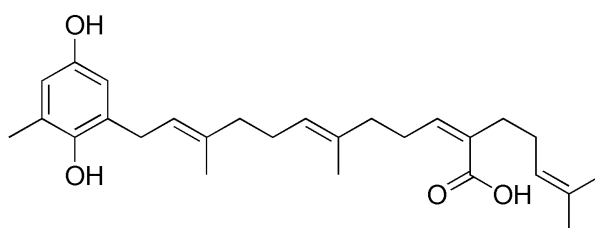


**Figure 35.** Structure of sargahydroquinoic acid.

Among naturally occurring phytohormones that have shown chemoprotective effects against chronic inflammatory diseases, strigolactones (SLs) are a class of carotenoid-derived lactones (for general structure see Figure 36A,B), produced by plant roots, which regulate many aspects of plant development. SLs have recently been proposed to have anticancer activity. Synthetic analogs, such as the two enantiomers of GR24, regulated NRF2 expression at the post-transcriptional level in Hepa1c1c7 cells and in LPS-treated RAW264.7 macrophages, as shown by evaluating mRNA levels by qRT-PCR and NRF2 knock-down by siRNA transfection. When docked within the NRF2 binding site of KEAP1 (PDB ID: 2FLU), they were able to form complexes that were more stable than the reference compound (curcumin), especially in the case of the R isomer. The interactions were mainly H-bonds with the amino acidic residues Tyr334, Arg483, Gln530, Ser555, and Tyr572 of the KEAP1 binding site in the case of compound GR24-1, whereas the other enantiomer, GR24-2, bound to diverse residues in the binding site (Arg380, Arg415 and Ala556) [154].

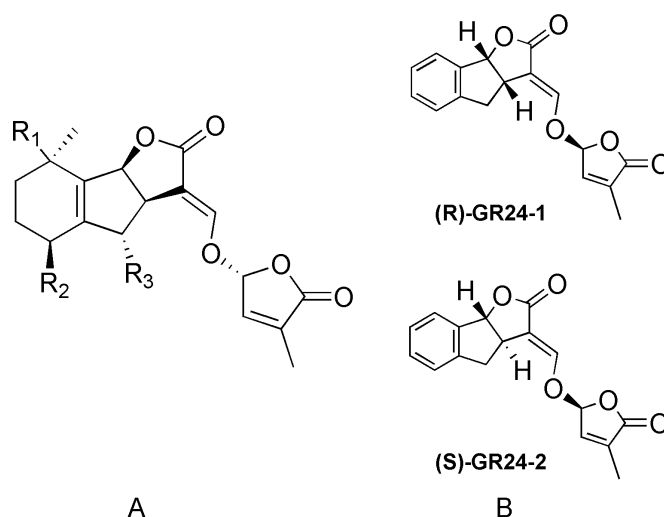


**Figure 36.** Structure of carotenoid-derived lactones (A) and two GR24 enantiomers (B).

Rutaecarpine (RUT) (Figure 37), a polycyclic heterocycle classified as a non-basic alkaloid, isolated from the Traditional Chinese Medicine of *Evodia rutaecarpa*, was reported to suppress inflammatory bowel disease, probably by binding to KEAP1, in the small ligand-binding C-terminal Kelch domain

of the protein. These results were supported by immunofluorescence and Western blot analysis in HCT116 cells, which suggested a significant increase in NRF2 nuclear translocation, and the cellular distribution of protein induced by RUT. In addition, the SPR assay suggested that RUT can interact with the KEAP1 Kelch domain, and the luciferase assay confirmed RUT as a potent NRF2 activator. Therefore, when docked into the large hydrophobic cavity (PDB ID: 4XMB), RUT established hydrophobic interactions with Tyr334, Gly364, and Ala556, whereas the H-bond interaction with Arg415 was ascribed to the amide [155].

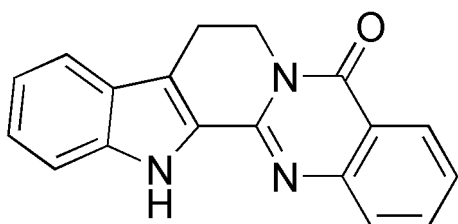


**Figure 37.** Structure of rutaecarpine.

#### Mixture of natural extracts

In some cases, a mixture of natural compounds has been isolated from natural sources, and the beneficial biological effects have been described. To better understand the probable mechanism of action and identify the suitable molecular target, the main components were studied by docking procedure to demonstrate their ability to interact with the selected protein and to rank their binding capability.

*Agastache foeniculum essential oil* (AFEO) and oil fraction (AFoil) were obtained from Lamiaceae perennial plants, which have long been used traditionally by Native American and Indian peoples and have shown anti-oxidative and anti-hyperglycemic properties. In macrophages, treatment with AFEO and AFoil reduced NF- $\kappa$ B expression while increasing NRF2, which is responsible for these effects. Molecular docking research on the main components (estragole, linoleic acid, and linolenic acid, Figure 38A-C) demonstrated that these compounds can interact with the hydrophobic pockets of the proteins. In particular, when analyzed against KEAP1 (PDB ID: 3ZGC), estragole, the olefinic compound, also found in several oils from other sources (Russian anise, anise bark oil, fennel turpentine, basil, tarragon oil), was able to form a complex stabilized at the binding site with H-bonds, van der Waals and  $\pi$ -alkyl interactions with Ala366. Linoleic and linolenic acids also bind to the same hydrophobic pocket, exhibiting analogous interactions with Gly367, Ile559, and Val606 [156].

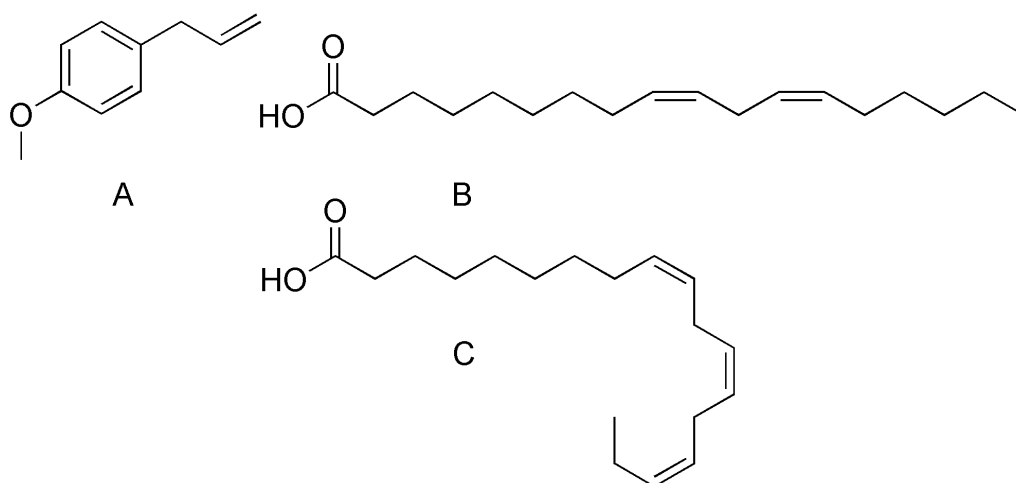


**Figure 38.** Structure of estragole (A), linoleic acid (B), and linolenic acid (C).

The phytochemical components of the butanol fraction (BUF) derived from 70% aqueous methanolic leaf extract of *Barnebydendron riedelii* were identified as three flavonoid glycosides. These derivatives: kaempferol(KAM)-3-O- $\alpha$ -L-rhamnopyranosyl-(1 $\rightarrow$ 6)- $\beta$ -D-glucopyranoside (1), QUE-3-O- $\alpha$ -L-rhamnopyranosyl-(1 $\rightarrow$ 6)- $\beta$ -D-galactopyranoside (2) and QUE-3-O- $\alpha$ -L-rhamno-yranosyl-1 $\rightarrow$ 6)- $\beta$ -D-glucopyranoside (3) (Figure 39) demonstrated significant hepato-neuroprotective effects through their modulatory effects on the NF- $\kappa$ B/IL-6 and NRF2/HO-1 signaling pathways in in vivo studies and immunohistochemical assays. They were docked into the KEAP1 protein (PDB ID: 6QMC). The compounds were found to bind in the order 2 > 3 > 1, but all of them formed more stable complexes with respect to the co-crystallized ligand (docking score = -47.91 kcal/mol). These findings were justified by the fact that the BUF phytochemicals were able to accommodate into the binding site, interacting with several H-bonds; however, the key binding sites were between galactose-OH-3'' and Ser508 (in the case of 2), glucose-OH-2'',3'' and Ser508 (in the case of 3), and glucose-OH-2'' and Arg483 (in the case of 1) [157].

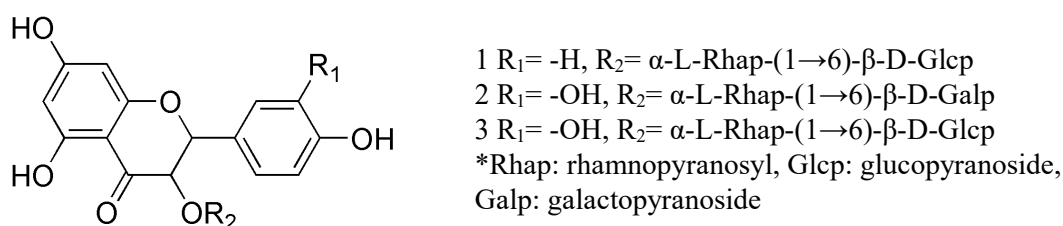


**Figure 39.** Structure of kaempferol(KAM)-3-O- $\alpha$ -L-rhamnopyranosyl-(1 $\rightarrow$ 6)- $\beta$ -D-glucopyranoside (1), QUE-3-O- $\alpha$ -L-rhamnopyranosyl-(1 $\rightarrow$ 6)- $\beta$ -D-galactopyranoside (2), and QUE-3-O- $\alpha$ -L-rhamno-yranosyl-1 $\rightarrow$ 6)- $\beta$ -D-glucopyranoside (3).

A study using MTS colorimetric methods showed that extracts of Pinot noir pomace exerted a protective effect on human endothelial cells against polycyclic aromatic hydrocarbons (PAHs) found in the polluted air of Temuco (Chile). The proposed mechanism of action was related to the release

of NRF2 from the complex with KEAP1, which was also studied by molecular docking. Thus, the main components, including derivatives of catechin, QUE, anthocyanins, and cyanidins, were demonstrated to be able to interact with the binding site of the Kelch domain (PDB ID: 6SP4). The compounds for which the best affinity values were obtained, thus suggesting strong binding, were QUE, QUE-3-rutinoside, catechin, QUE-3-glucoside, peonidin-3-glucoside, AMG, petunidin-3-glucoside, and delphinidin-3-glucoside. With regard to the residues involved in the binding, for example, in the case of catechin were Gly367, Val606, Val604, Gly462), whereas in the case of QUE resulted Val606, Gly367, Val512, Val465, Ala556, Ile416 [158].

The ethyl acetate fraction from *Veronica ciliata* (EAFVC), a traditional Tibetan medicine, used to treat hepatitis because of its hepatoprotective activity, was investigated to explore the effects of two main compounds, catalposide and verprosode. In vivo and in vitro studies showed that these compounds could act as hepatoprotective agents by activating the KEAP1/NRF2/p62 pathway. When docked into the structure of *Mus musculus* KEAP1 (PDB ID: 6QMC), the results of the simulation revealed that catalposide and verprosode strongly interact with the residues located in the active site of the protein. In particular, catalposide showed H-bonds with Arg415, Arg483, Ser508, Ser555, and Ser602, whereas verprosode formed analogous interactions with Asn382, Arg415, Arg483, Gln530, Ser555, Ser508, and Ser602 [159].

Several active compounds present in the medicinal plant *Scurrula atropurpurea*, which is known for its anticancer properties, were studied in silico for their potential ability to modulate the NRF2 signal. First, the interactions between the various active compounds and NRF2 were investigated. The strength of interaction was in the order rutin > quercitrin > aviculin > catechin > QUE > EPI > KAM > caffeine > theobromine. The main interactions were hydrophobic, but in a few cases, H-bonds were present, such as (catechin - Val478, QUE - Arg517, Cys514, quercitrin - Arg517, Leu519, rutin - Lys472, theobromine - Ile474, Leu476).

Then, the complex with active compounds from *Scurrula atropurpurea*, was analyzed, showing that these ligands cause a substantial change in the values. In this case, the energy interaction order was caffeine > catechins > KAM > QUE > quercitrine > rutin. Because the energy interactions between all the components were lower than the energy of the interaction between NRF2 and KEAP1, it was possible to conclude that various active molecules from *Scurrula atropurpurea* can positively regulate the KEAP1/NRF2 signaling pathway. Thus, inhibition facilitates the translocation of NRF2 into the nucleus, exerting its antioxidant effect [160].

An analogous in silico study was conducted to analyze the main constituents of *Si-Wu-Tang* (SWT), a popular traditional Chinese medicine for women's health, with potential for cancer prevention. This is supported by several in vitro tests that were used to evaluate the protective role of the compounds

by activating the NRF2/ARE antioxidant signaling pathway. Molecular docking was performed to investigate their ability to prevent the formation of the KEAP1/NRF2 complex using the crystallographic structure with PDB ID: 3WN7. It has been hypothesized that compounds that bind to the same region of the KEAP1 domain interfere with KEAP1/NRF2 interactions through competitive binding. Thus, it was possible to demonstrate that all compounds bind to KEAP1 at the NRF2 binding surface, except butylphthalide, which is situated deeper inside the cavity. The most promising ligands of the NRF2 binding site were GAL (Figure 20A), senkyunolide A, and Z-ligustilide (Figure 40A-C). All these derivatives showed similar binding poses, sterically blocking both NRF2 motif binding sites at the KEAP1 surface; only GAL partly blocked the binding site. Similar results were obtained when docking analysis was performed on other protein structures (PDB IDs: 2FLU and 4IQK). The three derivatives also showed the highest biological potency and clinical safety profile; therefore, they could be used in cancer preventive approaches [161]. **The aliphatic chain and saturation on benzene ring seems do not influence the binding**

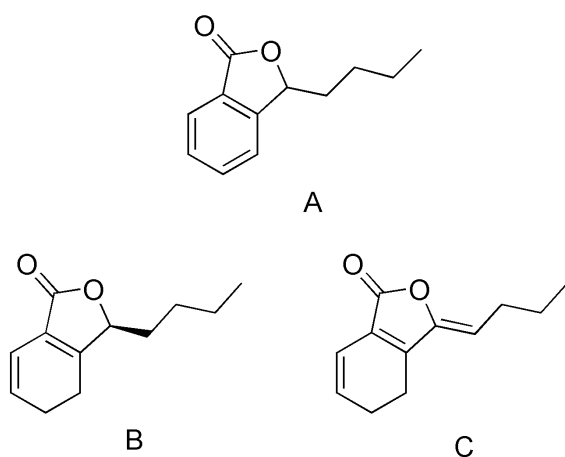


**Figure 40.** Structure of butylphthalide (A), senkyunolide A (B), and Z-ligustilide (C).

The methanolic extract of *Zanthoxylum armatum* bark (MeZb), which contains several natural compounds belonging to the classes of flavonoids, alkaloids, coumarins, lignans, amides, and terpenoid, is well known for its curative properties against many diseases, including cancer. Molecular docking analysis with the KEAP1 receptor (PDB ID: 5FNQ) was performed for several derivatives: luteolin, KAM (Figure 39), sanguinarine, isorhamnetin, myricetin, QUE (Figure 9B), hesperidin, didymin, and sweroside (Figure 41A-I). The molecules that showed potential binding capability mainly included flavonoids. Luteolin, whose polar interaction was mediated by a water molecule, has the lowest binding energy. Two additional compounds from the alkaloid (sanguinarine) and glycoside (sweroside) families were also discovered. In vitro antioxidant assays and in vivo studies involving immunofluorescence, qRT-PCR and Western blot analysis were used to evaluate the anti-breast cancer activity through the activation of the KEAP1/NRF2 pathway. The docking score indicated that the investigated compounds exhibited similar binding energies. The complex stability

in this case is also due to hydrophobic interactions with the key residues Phe214 and Ala31, which interact with aromatic  $\pi$ - $\pi$  type and methyl- $\pi$  type interactions. In the case of KAM, isorhamnetin, and QUE, the Phe214 residue is also implicated in polar contacts via backbone heavy atoms [162].

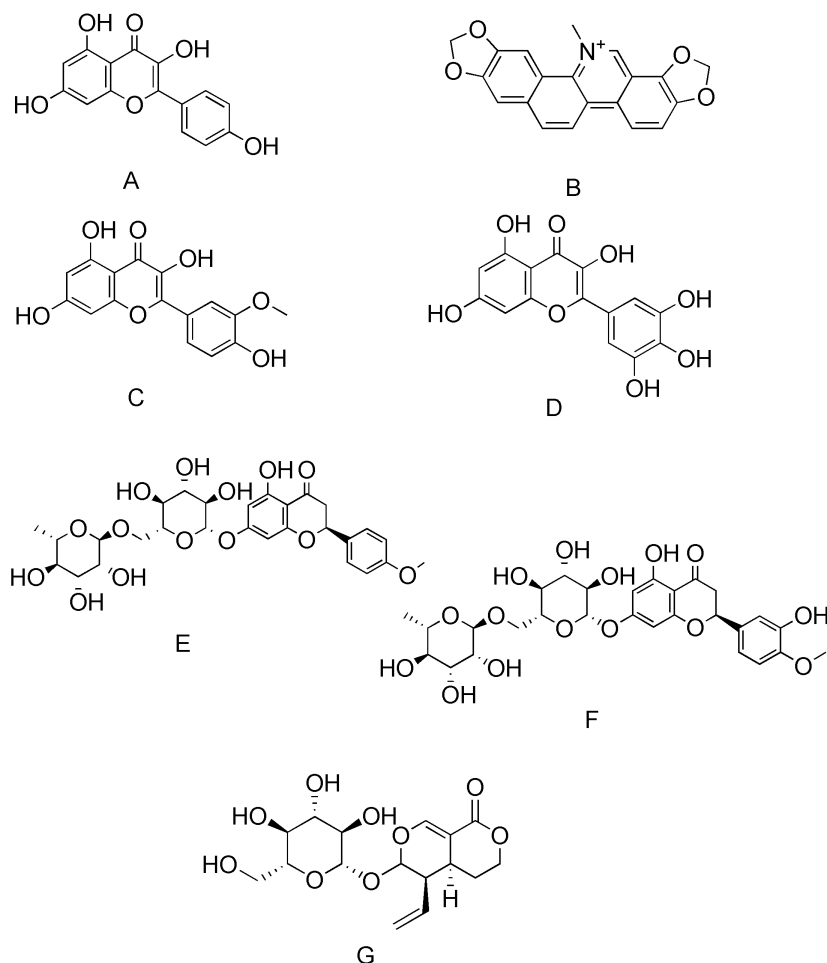


**Figure 41.** Structure of lutein (A), sangunarine (B), isorhamnetin (C), myricetin (D), hesperidin (E), didymin (F), and sweroside (G).

## Computational approaches

### *MD simulations of non-covalent natural products*

The diverse influences of the functional groups 3-OH and 7-OH in simple flavones were analyzed in depth with 18 ns time MD simulation, of course in the interaction with protein PDB ID: 2DYH. Starting from the lowest-energy conformations found by docking calculations the usual procedures in which root-mean-square deviation (RMSD), root-mean-square fluctuation (RMSF), solvent-accessible surface area (SASA), and the number of H-bonds of unbound and ligand-conjugated proteins with respect to the initial structure were employed. The results clearly indicated that the trajectories of all systems were stable and that their RMSD reached equilibrium and fluctuated around its mean value after approximately 5 ns of simulation time. In the case of the 7-OH derivative, the

average RMSD was closer to the free protein than the other complexes, whereas no significant change in SASA was observed in the presence of ligands. Analysis of RMSF highlighted the conformational adjustments of the protein in the presence of ligands at the binding sites; therefore, the residues that were in contact with the ligands were stable and suggested that the structure of the binding site remained rigid during simulation. The changes in the number of intramolecular H-bonds of proteins during the 18 ns simulation time were parallel to the variations in SASA [106].

Moreover, on the basis of the complex model attained from molecular docking (see section docking), a 100 ns MD simulation was conducted to investigate the dynamic behavior of the NRF2/UA complex. The time evolution of the weighted RMSDs for the backbone atoms of the NRF2 protein and UA from their original positions ( $t=0$ ) was obtained to calculate the structural stability during the simulation. The obtained RMSD values of the protein backbone ranged from 0.76 Å to 1.53 Å, which confirmed that the system was well-equilibrated. By the analyses of H-bonds and hydrophobic interactions, a well-defined substrate pocket was found in which there are three conserved H-bonds between UA and NRF2 in the complex, formed with residues Ser508, Arg415, and Ser602, which is consistent with the docking data [134].

In addition, the behavior of osthole with the KEAP1 protein (PDBID: 4L7B) was studied using MD simulations and MM/GBSA methodology to calculate the binding free energy ( $\Delta G_{\text{bind}}$ ). The results showed that the residues mainly contributing to the interaction were Tyr525, Ser555, Arg415, Gln530, and Ile461, whereas the RMSDs of the complex were quite small during 100 ns MD simulation. It was concluded that the stable binding of osthole to KEAP1 may occupy a portion of NRF2, which is responsible for osthole-mediated oxidative stress regulation [163].

An extended and very complete MD study has been reported in which the behavior of some compounds from natural sources toward rat and human KEAP1 binding sites was investigated. The structures of complexes with NRF2 (PDB ID: 1X2R) and Cpd16 (Figure 42) (PDB ID: 4IQK) were used, whereas the studied derivatives were 3-O- $\alpha$ -L-arabinofuranoside-7-O- $\alpha$ -L-rhamnopyranoside of KAM, GAL, ELL, and geranium acetonitrile (ACE). First, the docking results indicated that ACE and KAM could be responsible for NRF2 activation, whereas ELL and GAL could behave as free radical scavengers.

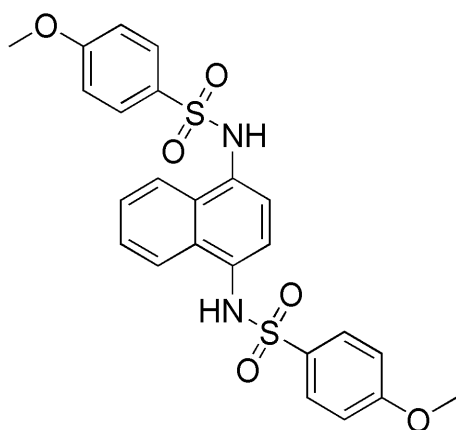


**Figure 42.** Structure of Cpd16.

Comparison of the interaction of Cpd16 in the Kelch domain of human and rat KEAP1 systems shows that the complexes are stabilized by a balanced number and type of polar, non-polar, and neutral residues in all sub-pockets (P1-P5), whereas only two amino acids of the arginine triad were involved in binding in human (Arg415 and Arg483) and rat (Arg380 and Arg415) KEAP1/Cpd16 complexes. Similar behavior was evidenced in the case of the formation of the KEAP1/ACE complex; in the KEAP1/KAM interactions, it was observed that KAM is coordinated by a similar number but dissimilar type of residues, being mostly stabilized through hydrophobic interactions in the Kelch domain of human KEAP1. In addition, similar to the KEAP1/ACE complex, binding with the triad of arginine residues is only present in rat protein and only Arg415 interacts with the human KEAP1/KAM complex. When evaluating the systems by MD simulations, by analyzing the RMSD and RG values, it was possible to prove that the free and bound systems reached stability after 20 ns. Thus, the systems were sufficiently rigid because these results indicated the lack of strong motions along the KEAP1 structure for both human and rat structures. Comparison among all the complexes showed, on average, the following tendency for binding free energies: NRF2  $\geq$  Cpd16  $\geq$  KAM  $\geq$  ACE in human and rat KEAP1 complexes. The results agreed with the experimental data [132].

Among the isomers of CGA, the ester formed between one molecule of caffeic acid and one molecule of quinic acid is called caffeoylquinic acid (CQA), which exists as multiple isomers (e.g., 3-CQA, 4-CQA, 5-CQA, 3,4-diCQA, 3,5-diCQA, and 4,5-diCQA, (Figure 43A-C). As reported by several *in vitro* studies, these six different CGA isomers were able to modify the redox biology in inflamed Caco-2 cells that involved NRF2 signaling and for this reason were also investigated using 100 ns of MD simulation using the structure of KEAP1 (PDB ID: 2FLU). It was possible to demonstrate that the interactions were mainly hydrophobic with the NH groups of valine, glycine, and isoleucine amino, and the sidechains of arginine, threonine, and serine, whereas the H-bonds were highly transient. Simulations revealed that differences between the ability of CQA and diCQA to interact with the KEAP1/NRF2 complex may be due to differences in relative orientation within the complex,

whereas these generally resulted in relatively stable interactions throughout the trajectory, with the only exception being the interaction with 3,5-diCQA, which showed one phenolic group firmly within the core of the protein and another outside the bottom. The simulation also showed that many OH groups of the caffeic acid moiety came into close proximity to the sulfur atoms, as evidenced by the distance graph for Cys368 and Cys513, with values that indicate direct atomic contact. Thus, because of the plasticity of protein structures and the potential for alternative orientations of the isomers in vivo, CGA isomers with phenolic hydroxyl groups converted to radicals at these distances could be in direct contact with the cysteine sidechains and cause oxidation of SH groups to S<sup>•</sup>, potentially leading to the dissociation of NRF2 from KEAP1 [164].

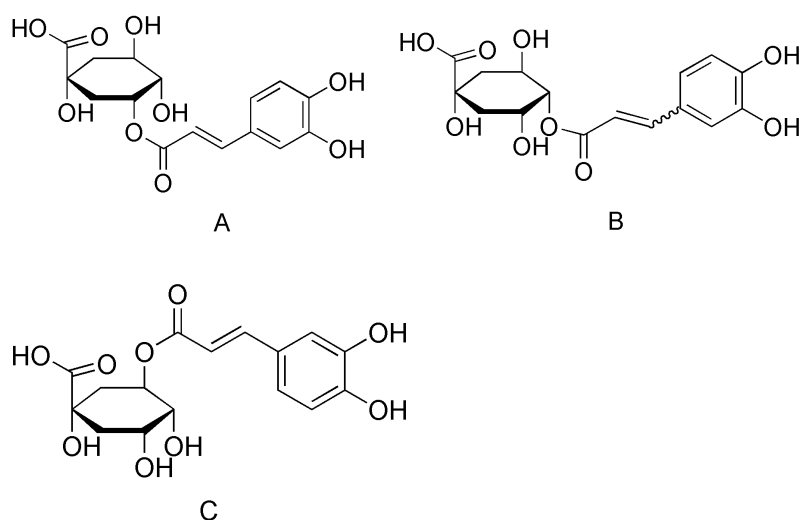


**Figure 43.** Structure of 3-CQA (A), 4-CQA (B), and 5-CQA (C).

Pterostilbene (PTS), a natural analog of resveratrol, was shown to be a potent NRF2 activator and KEAP1/NRF2 PPI inhibitor, as assessed by luciferase complementation assay. Thus, it was extensively investigated in silico for its ability to interact with the KEAP1/NRF2 complex by IFD and MD using the structure PDB ID: 2FLU. Initially, in the protein KEAP1, two main binding sites were chosen; the so-called cysteine pocket (region where the six key cysteine residues are located) and the arginine triad in the Kelch domain, named Kelch pocket, surrounded by His residues (432, 436, 553, 575), the last of which covers functional elements for the binding of NRF2. Weak binding of PTS in the cysteine pocket was evidenced, mainly through hydrophobic interactions between the aromatic ring and the backbone atoms of cysteine residues 513 and 368. In contrast, when docked to the Kelch pocket, H-bonds were observed between the carboxyl group and the sidechain NH of Arg415, Arg380, and Asn414 and several other interactions ( $\pi$ - $\pi$  stacking, charged, and polar). In addition, 6 ns MD simulation showed that the RMSD values for C- $\alpha$  and backbone atoms (KEAP1/NRF2 protein with and without ligand) remain within 2Å for the entire run, demonstrating the conformational stability of the protein structures. Moreover, the MM/GBSA calculation showed

that the binding free energies for the apoprotein are higher than those for the ligand-bound states. The observed differences also corroborate the ability of PTS to disturb PPI. Therefore, it was possible to conclude that pterostilbene formed the most favorable interaction with the arginine triad residues of the KEAP1 Kelch domain, and the binding of the ligand to the active site residues of the Kelch domain might facilitate nuclear translocation of NRF2 [165].

AST is the primary oceanic carotenoid pigment produced by marine organisms. It was demonstrated that AST could act as a strong antioxidant agent. AST was able to protect against cisplatin-induced cell death by activating the NRF2-mediated signaling pathway, acting as an NRF2 activator. A study on the interaction with KEAP1 was conducted using molecular docking and MD with this target (PDB ID: 6LRZ), hypothesizing that AST could compete with NRF2 for KEAP1 binding, leading to NRF2 dissociation, subsequent translocation to the nucleus, and promotion of downstream antioxidant factors. Preliminary docking analysis revealed that AST established interaction in two binding sites, one oriented at the bottom of the NRF2-binding site and one at the top of the loop, mainly through hydrophilic interactions with Arg319, Arg415, and Gln563. Comparison between the KEAP1/NRF2/AST complex and KEAP1/NRF2 (PDB ID: 5WFV) revealed that AST partially overlapped with the ETGE motif of the NRF2 peptide; however, NRF2 -binding sites exhibited significant changes in the orientation of several residues (Arg380, Arg415, Arg483, Ser508, and Tyr525) after AST docking to KEAP1/NRF2. In addition, 14 known small-molecule drugs (such as for example, lipoic acid, amifostine, dexamethasone, epigallocatechin, erdosteine, glutathione) known to protect against cisplatin ototoxicity were selected and compared with the docking of AST and KEAP1/NRF2. All the selected small-molecules could interact with the KEAP1/NRF2 protein, but AST had the highest binding energy score. Thus, a 10 ns MD simulation was carried out for the KEAP1/NRF2/AST and KEAP1/NRF2 complexes by analyzing, as usual, the RMSD and RMSF values. The RMSD reached equilibrium and fluctuated around the mean value after a 3 ns simulation; the stable RMSD value for the KEAP1/NRF2/AST complex was lower than that of the original KEAP1/NRF2 complex, indicating that the complex with AST may have a relatively stable conformation and that AST may exert a competitive effect on KEAP1/NRF2 peptide targets. The average RMSF value was lower than 0.1 nm, confirming the stability of the complex. In conclusion, it was suggested that AST could exert a competitive inhibition of NRF2 binding to the Kelch domain [166].

A 200 ns MD simulation to investigate its behavior at the binding site of KEAP1 (PDB ID: 5CGJ) was performed for SchB. It was suggested that SchB underwent minor adjustments compared with the docking conformation, which is consistent with the IFD theory, evidencing a reasonable binding conformation of the KEAP1/SchB complex. The ten key residues contributing the most were Tyr334, Arg415, Ile461, Phe478, Arg483, Ser508, Gly509, Tyr525, Ala556, and Tyr572, which interacted

mainly through H-bonds and hydrophobic interactions. Moreover, by analyzing the RMSD values, it was possible to demonstrate that the complex was relatively stable during simulation [167].

Schisandrin C (SchC) (Figure 44), a dibenzocyclooctadiene derivative isolated from *Schisandra chinensis*, is known for its antioxidant properties. This was demonstrated by in vivo studies and immunohistochemical assays showing that SchC targets KEAP1 and attenuates oxidative stress by activating the NRF2 pathway. In silico studies showed its ability to interact with mouse KEAP1 protein (PDB ID: 5CGJ) with 100 ns MD, MM/GBSA, and Gaussian accelerated MD (GaMD) simulation using the dual potential boost. It was possible to evidence that the interactions were with residues Gly509, Tyr525, Ala556, Tyr572, and Phe577, through H-bonds as predominant binding, but also  $\pi$ - $\pi$  stacking and hydrophobic interaction were present, explaining the inhibition of KEAP1 binding to NRF2. Analysis of the RMSD values of the backbone atoms and conformational distributions of KEAP1 by PCA revealed that no large conformational changes of KEAP1 occurred in the complex with SchC and that it exhibited excellent stability characteristics. Moreover, the GaMD simulation showed that the binding pocket of the target was neutral, accounting for the specific recognition of the uncharged ligand [168].

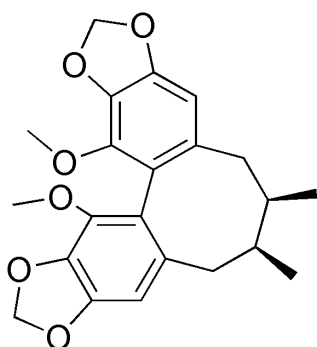


**Figure 44.** Structure of schisandrin C.

#### *Pharmacophore modeling approach*

A pharmacophore modeling study was employed to design efficient KEAP1 inhibitors starting from decussatin, loliolide, resveratrol, and scopoletin, four phytochemicals well known for their antioxidant activities and other biological properties. These were subjected to extensive structural modification to improve their chemical/biochemical profile (such as pharmacodynamic, pharmacokinetic and drug-likeness qualities). In particular, systematic isosteric substitution was performed by replacing oxygen and/or hydroxyl groups with amino or trifluoromethyl substituents. Quantum chemical descriptors, based on DFT were calculated for the geometry optimization of the novel ligands and for computing their electronic properties. The resveratrol derivative R4, which presents a bis(trifluoromethyl)benzene moiety, was demonstrated to be the most desirable candidate when the B3LYP/6-31G (d,p) level of theory was performed, especially because of its HOMO and

LUMO distribution. In fact, these properties are highly beneficial for understanding the redox chemistry of ligands during ligand-receptor interactions and their behavior in solvated micro/macroevironments.

Docking analysis was performed by choosing two targets: the BTB domain (PDB ID: 5DAD) and the Kelch domain (PDB ID: 4L7B) of the KEAP1 protein because efficient lead should have excellent binding affinities with both proteins. This study aimed to identify compounds that could prevent the homodimerization of KEAP1 and inhibit the binding and eventual ubiquitination and proteolytic degradation of NRF2. As a result, with regard to the interaction with the BTB domain, all the resveratrol-modified derivatives better interacted with the protein, whereas the scopoletin derivatives were less able to provide suitable interactions. When the Kelch domain was considered, nearly the entire set of modified resveratrol compounds could interact at the selected binding site. Thus, in each case, derivative R4 was the most interesting. In particular, the bis(trifluoromethyl)benzene moiety of R4 formed a  $\pi$  donor – H-bond and a hydrophobic bond with the Cys151 residue of the BTB active site, whereas R4 was found to interact with Tyr85, Glu86, His129, Arg135, Lys131, His154, and Val155, and with the Kelch domain. Of particular interest were the interactions with Arg415 and Ser508, residues deep present in the Kelch pore of KEAP1, suggesting thus that the R4 bis(trifluoromethyl)benzene moiety might occlude the pore, thereby rendering the KEAP1 protein incapable of forming a complex with the NRF2 protein. In addition, because of the amphoteric character of the pore, a suitable microenvironment for the charge-stabilized nucleophilic and hydrophobic  $\delta$  - (ring) systems was found with significant electronegativity of the CF<sub>3</sub> groups. Overall, this molecular docking study combined with comparative interaction analysis ranked the R4 derivative as the best multidomain antagonist of the KEAP1 protein with a binding affinity of -8 kcal/mol. The only negative issue posed by the novel derivatives could be the potential fluoride toxicity, although this type of isosteric replacement is generally well acknowledged in medicinal chemistry [169].

The antioxidant potential of a series of synthesized compounds related to natural products belonging to the classes of hydroxychalcones, hydroxyflavanones, and hydroxyflavindogenides, was evaluated, and all the derivatives, mainly chloro substituted, were subjected to *in silico* studies. Several descriptors were calculated [dipole moment, area, volume, LogP, H-bond donor (HBD), H-bond acceptor (HBA), polar surface area (PSA), solvation energy, and polarizability] together with some electronic properties, such as the distribution pattern of frontier molecular orbitals, ionization potentials (IP), and electron affinities (EA), computed using the DFT approach. Molecular docking with KEAP1 (PDB ID: 2FLU) for the activation of NRF2 was performed, using as reference compounds ascorbic acid and trolox, and analyzed considering possible correlation with experimental IC<sub>50</sub> values. The *in vitro* antioxidant activities of the compounds were evaluated by analyzing their

radical scavenging activity, which was measured through their interaction with DPPH free radicals. The compounds were also examined for their reduction ability with respect to ferric ions. Compound 1a exhibited a higher chelating power and the lowest IC<sub>50</sub> value. In addition, their reducing power in terms of IC<sub>50</sub> values was calculated: the increasing order of reducing power resulted 1a > 2a > 3a > 3b > 3c. Among the synthesized compounds (the structures of which are presented in Figure 45), 1a exhibited a lower IC<sub>50</sub> value, whereas from the computational point of view, 3c was the best ligand. Protein-ligand interactions evidenced that the complexes are stabilized mainly by van der Waals, H-bonds with key residues in the Kelch domain (Ala366, Cys368, Val465, Ala466, Val512); also, the ligands were ranked on the basis of Atomic Contact Energy (ACE) and docking score values. All the studied compounds exhibited good antioxidant potential; the QSAR analysis, paralleled by the docking results, revealed that they showed comprehensive intramolecular charge transfer from the HOMOs to the LUMOs with smaller IP and Egap values and a high docking score for NRF2 activation compared with the referenced compounds. The best ligand resulted in compound 3c substituted at position 4 of flavindogenide [170].

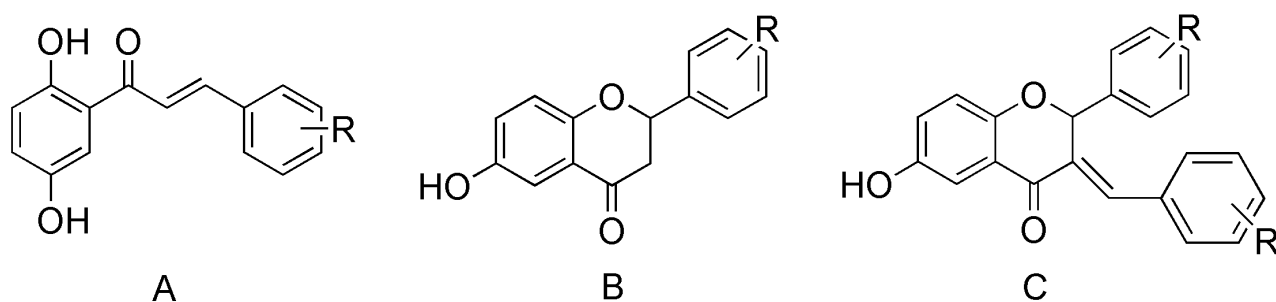


**Figure 45.** Structure of 1a (R=2-Cl) (A), 2a (R=2-Cl) (B), 3a (R=2-Cl), 3b (R=3-Cl), 3c (R=4-Cl) (C).

With semi-flexible molecular docking and 3D-QSAR method, such as Comparative Molecular Field Analysis (CoMFA), screening and classification of various natural products were achieved. Thus, the potential ability of 178 phytochemicals with antioxidant effects to target the NRF2 binding site in the KEAP1 protein was analyzed. Considering their structural features, the selected molecules were separated into the following 18 classes: alkaloids, anthocyanins, carotenoids, chalcones, coumarins, flavanols, flavanones, flavones, flavonols, isoflavonoids, organosulfurs, phenolic acids, phenylethanoid glycosides, quinones, stilbenes, terpenes, tocopherols, and others. Moreover, the classes were further separated into two sub-groups: molecules containing glycosides (i.e., anthocyanins, flavanols, flavanones, flavones, flavonols, isoflavonoids, and phenylethanoid glycosides) and molecules not containing glycosides (i.e., alkaloids, carotenoids, chalcones, coumarins, organosulfurs, phenolic acids, quinones, stilbenes, terpenes, tocopherols, and others).

According to the results of docking analysis, the investigated phytochemicals were divided into 3 groups (high, medium, and low) on the basis of the total score and hence on their binding affinity with KEAP1. Notably, the predicted binding affinity of the glycoside-containing molecules was higher than that of the derivatives not including glycosides in their structure. The best KEAP1 ligands comprised 24 derivatives containing a relevant number of oxygen atoms or glycoside groups. These molecules established relevant interactions with many pivotal residues at the KEAP1/NRF2 interface, mainly through steric, H-bond, and hydrophobic interactions. In addition, the number of oxygen atoms in the derivatives was correlated with their binding affinity for the KEAP1 protein. Consequently, 3D CoMFA was used to further investigate the link between the structural characteristics and binding affinity. The relationship between structural features and binding affinity was determined using the PLS technique, employing the usual statistical valuation of the results. As a result, 24 compounds were selected as the best binders; all of them were able to form stable interactions with several serine residues (363, 508, 555, and 602), which are important residues at the interacting KEAP1/NRF2 interface. The *in silico* data were consistent with the results of the *in vitro* assay on the H<sub>2</sub>O<sub>2</sub>-induced oxidative injury cell model. In fact, the high-total-score group (Total Score > 6) showed significant effects on the nuclear translocation of NRF2 in H<sub>2</sub>O<sub>2</sub>-induced oxidative-injured cell model. This methodology was thus proposed for discovering NRF2 activators that interfere with KEAP1/NRF2 PPI [171].

#### *In silico analysis of the mutations*

Studies of KEAP1/NRF2 pathway mutations were conducted using MD simulations to analyze the trajectory. By taking advantage of PolyPhen-2 (Polymorphism Phenotyping v2) analysis, an automatic computer-based tool for predicting the potential influence of an amino acid substitution on the structure and function of a human protein. Considering samples from pediatric patients affected by acute lymphoblastic leukemia (ALL), it was possible to demonstrate that the four changes in KEAP1 might be pathogenic because their scores were close to 1. The studied population consisted of 30 patients (19 girls and 11 boys) aged between 1 and 15 years (mean age  $\frac{1}{4}$  5.5 years), and mutation analysis was performed using somatic tissues. The detected mutations were on the BTB domain (four) and one on the IVR and DGR domains. MD analysis, according to RMSD for the protein KEAP1, after the first 990 ps on the wild-type and Ala159Tyr mutant showed a comparable deviation pattern with a slight variance of approximately 1.2 nm on average, whereas the mutation Glu121Lys was not aligned with those RMSD values relevant drift was detected in the protein trajectories, but it reached the steady state after 122.6 ns. Six novel changes have been identified using this approach, four of which are of particular interest in His129 of KEAP1. Altogether, these outcomes suggest possible important interactions in pediatric ALL at variance with an adult cell line in which only one mutation has been observed [172].

The same research group, considering that managing every mutation currently in existence in a wet lab is too difficult, further explored different computational techniques to gain suggestions to select the relevant mutations for establishing the appropriate patient population. Thus, in this case, the pathogenicity of eight detected mutations was compared by utilizing different programs with different algorithms [such as, for example, PolyPhen-2, SNAP (Screening for non-acceptable polymorphisms), CHASM (Cancer-specific High-throughput Annotation of Somatic Mutations), and VEST (Variant Effect Scoring Tool)] and MD simulation to evaluate the impact of amino acid substitutions on the structure and function of a human protein. In particular, a 10 ns time-scale molecular simulation was run for the BTB domain and its mutants, for the IVR domain with its mutant (Asn222Thr), and for the DGR domain in addition to the Neh2 domain with its mutant. Throughout the study, to analyze the MD simulation trajectories, two different parameters, RMSD and RMSF, were utilized, together with the free energy landscape (FEL) parameter. All RMSD values for the wild-type and the determined mutations of the BTB domain suggested that the native form had the most stable conformations and unfoldable structures, resulting in more flexibility and dynamic. Furthermore, from the RMSD and RMSF of the IVR domain, it was clear that the mutation at residue 222 with threonine caused an increase in RMSD, increasing the flexibility in the backbone of the IVR domain. In the DRG domain, due to mutation at residue 565, fluctuation in the region of residues 555–570 might block the binding site of the NRF2 peptide. Based on the results of FEL, all five mutants of the BTB domain showed random motion and were less energetically favored; in the case of the IVR domain, it was evidenced that the wild-type has a broader and lower free energy region compared with the Asn222Thr mutant; thus, this last has thermodynamically less stable conformations. In addition, the mutation of Asn222Thr resulted in an increase in the flexibility of IVR. Interestingly, a significant enhancement in the energetic stability of the Kelch domain of KEAP1 was also observed after the mutation of residue 565 with methionine, although RMSD and RMSF revealed that the native form was much more stable. Finally, in the Neh2 domain, there was no significant effect of mutation on the dynamic behavior of Neh2, except that wild-type Neh2 was more stable than the mutant peptide. Thus, the apathogenic effects of this mutation, as seen in the experimental results, were confirmed. The mutants were generally more rigid and altered the native protein geometry [173].

The class of KEAP1 mutations referred as ‘ANCHOR’ (Additionally NRF2-Complexed HypomORph) can be related to the high rate of mortality in lung cancer, which affects cysteine residues reactivity or promotes structural deformation of the protein, resulting in the ANCHOR phenotype. Through biochemical examination and cell biology experiments, such as transmission electron microscopy coupled with confocal fluorescent imaging, immunoprecipitation, and many others, the authors defined novel interactions between KEAP1 and valosin-containing protein (VCP), PSMD2, and PSMD4. It was also possible to determine that KEAP1 ANCHOR mutations exclusively

impact NRF2 association, appear to stabilize the KEAP1 tertiary structure, and form p62-dependent phase-separated spherical clusters containing a KEAP1-positive core surrounded by unmodified and phosphorylated p62, poly-Ub, and NRF2. Discrete MD (DMD) simulation, carried out on the X-ray crystal structures, wild-type and Arg470Cys mutation, demonstrated that in the presence of mutation, the RMSF values of several amino acid residues in the region 500-550, were significantly reduced, resulting in reduced motion, suggesting that this mutation had a stabilizing effect on these residues. Moreover, the results of the modeling also evidenced an intramolecular salt bridge between the Arg470Cys mutation and Glu493. Thus, the KEAP1 structure is stabilized by ANCHORs, which reduces flexibility at crucial residues that interact with NRF2 and affect its binding [174].

A more extensive analysis was conducted years later by the research group of Wilson and coworkers [175], who performed a 280  $\mu$ s of unbiased MD simulations on 12 different mutations in KEAP1, i.e., Gly333Cys, Gly350Ser, Gly364Cys, Gly379Asp, Arg413Leu, Arg415Gly, Ala427Val, Gly430Cys, Arg470Cys, Arg470His, Arg470Ser, and Gly476Arg, which frequently mutated in lung cancer. The study also included previously investigated ANCHOR mutant variants, and in any case, these mutants could not be experimentally analyzed for their mutagenic effects. When the behavior of H-bonds was analyzed, both destabilizing mutants (Arg413Leu and Gly333Cys) induced significant decreases in their lifetime relative to the wild-type. In contrast, the stabilizing mutants Arg415Gly and Ala427Val both resulted in increases in their lifetimes. The ANCHOR mutation Arg470Cys induced a decrease in the H-bond lifetime with Asp422. However not all the mutations directly affected the hydrogen bonding network. With regard to the observed changes in RMSF values, the mutations did not relevantly affect the protein dynamics. In the case of Arg470His and Arg470Cys mutations, the lowest fluctuation events at the binding site residues were detected. In addition, in the case of Tyr334, Ser508, and Ser555 residues, lower fluctuations were detected for the mutations compared with the wild-type. It must be demonstrated how the Arg470Cys mutation resulted in the highest fluctuation at Arg483, which is the closest binding site residue in the protein. In conclusion, MD data clearly demonstrated the different effects exerted by specific mutations on protein structure. In particular, Gly333Cys, Gly379Asp, Arg413Leu, Gly430Cys, and Gly476Arg mutants exhibited a destabilizing effect, whereas Gly350Ser, Gly364Cys, Arg415Gly, Ala427Val, Arg470Cys, Arg470His, and Arg470Ser mutants resulted neutral or stabilized the protein. Furthermore, the findings showed that the Arg470Cys ANCHOR mutant only slightly altered the protein binding site compared with the wild-type, suggesting that the frequent occurrence of the mutant in various cancers may not be fully explained by a direct allosteric effect.

*In silico discovery of new ligands - Data mining*

In addition, a computational approach can be used to screen, and therefore discover, new ligands by analyzing available databases. Data mining on whole compounds or a fragment-based approach can be very useful, and several entities that can inhibit the binding of the KEAP1a/KEAP1b Kelch DGR domain have been discovered.

A series of 472 compounds with potential pharmacological properties, selected from the PubChem structure database, were studied for their ability to interact with the DGR domains of KEAP1a and KEAP1b (two variants of the protein present in zebrafish) through docking analysis on KEAP1 of *Mus musculus* (PDB ID: 5CGJ). The ligands were ranked on the basis of the glide score. Ten top-ranked computational hits showed three possible modes of interaction with the DGR domain of KEAP1 (H-bond,  $\pi$ -cation, salt bridges). All of which targeted residues involved in PPI between the DGR region of KEAP1 and the DLG/ETGE domains of NRF2. Among the top-ranked hit compounds, salvianolic acid A, esculin, flavin-adenine-dinucleotide disodium salt hydrate (FAD-Na<sub>2</sub>), tunicamycin, and QUE-3,4'-diglucoside were selected. For example, QUE-3,4'-diglucoside formed several H-bonds with Ser49, Leu51, Arg101, Val102, Arg169, Ser194, Leu196, and Met290 with an additional  $\pi$ -cation interaction with Arg101, whereas the binding mode of FAD-Na<sub>2</sub> with KEAP1a involved the formation of both a salt bridge and H-bond with Arg169, in addition to several more H-bonds (Arg66, Asn100, Ala119 and Ser241) and a salt bridge with Arg101. Although these compounds were common hits, their interactions with KEAP1a and KEAP1b were diverse because of the relevant heterogeneity found in the KEAP1a and KEAP1b binding sites. For a detailed list of the interacting key residues, refer to the original paper. Because esculin (Figure 46) was found to be among the best hits, further experimental validation was performed. Through an in vivo experiment using 3 dpf zebrafish larvae, its lethality effect was determined: 50 mM esculin exhibited 50% lethality. Gene expression analysis showed that esculin activated NRF2, by inhibiting the interaction between KEAP1 and NRF2, and induced the expression of glutathione S-transferase pi (GSTpi), NQO1, HMOX1a, and peroxiredoxin 1 (PRDX1). The obtained results highlighted the mechanism of NRF2 activation by esculin in offering protection against harmful effects caused by oxidative stress [176].

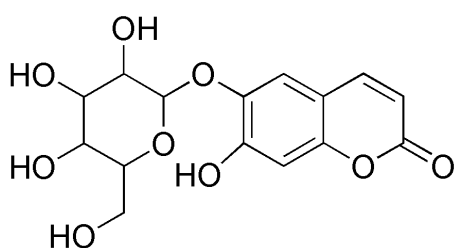


**Figure 46.** Structure of esculine.

A library of 5,000 phytochemicals was computationally screened using molecular docking technique employing the KEAP1 protein (PDB ID: 2FLU) to identify direct disruptors of the KEAP1/NRF2 interaction. All the derivatives showed the capability to strongly interact with the NRF2 binding site on the KEAP1 protein, showing a  $\Delta G_{\text{bind}}$  ranging from -18 to -26 kcal/mol, and also exhibited good calculated ADMET parameters. The results also allowed to rank the best ligands, and natural compounds such as 3-(dimethylamino)-3-imino-*N*-(4-methylphenyl)-propanamide, phlorizin, diffutin, liquiritin, and dihydrogenistin were the most promising disruptors of the KEAP1/NRF2 complex, as highlighted by their relevant predicted binding affinity and the strong network of H-bonds. Most of the selected hits (i.e. four out of top five) interacted with residues Arg415 and Ser602, and only two molecules interacted with Ser508 [177].

A chemical library, which included four parent phytochemicals with interesting pharmacological features, including antioxidant properties (decussatin, loliolide, resveratrol and scopoletin), and several modified compounds, derived via sequential replacement of the parent hydroxyl groups with isosteric  $\text{CF}_3$  and  $\text{NH}_2$  substituents, was utilized for the *in silico* studies. Preliminarily, a pharmacokinetic analysis (ADME) provided how the lead compounds should be modified to assess the maximum drug-likeness qualities such as BBB permeability and human intestinal absorption (HIA). Moreover, the geometries of the library entities and their electronic properties (simulating the water solvent system set to  $\text{pH} = 7.2$ , as in the human cerebrospinal fluid) were obtained using DFT-based quantum chemical calculations at the B3LYP/6-31G (d,p) level of theory. R4 (resveratrol in which all the OH were substituted by trifluoromethyl groups), L5 (loliolide presenting an amino substituent), and S1 (a ring isostere of scopoletin presenting the pyrimidone moiety) derivatives were the more interesting molecules with regard to their potential as antioxidant/free radical scavengers and for binding-mediated inhibition of the KEAP1 protein. In fact, these findings were supported by the findings of the molecular docking calculation of all the ligands on the two domains BTB (PDBID: 5DAD) and Kelch (PDB ID: 4L7B), which were also conducted to investigate the library for dual-site binding efficiency. This study aimed to identify the best ligand that could prevent homodimerization while inhibiting binding and eventual ubiquitination/proteolytic degradation of NRF2. The best ligand was R4, for which the calculated binding affinity was -7.3 kcal/mol (BTB domain) and -8 kcal/mol (Kelch domain). Its bis(trifluoromethyl)benzene moiety showed a  $\pi$ -donor-hydrogen bond and a hydrophobic interaction with the residue of the BTB active site Cys151, whereas it displayed some contacts with key residues in the KEAP1 active site Arg415 and Ser508, located deep in the KEAP1 Kelch domain [169].

The Dictionary of Natural Products (DNP) containing > 150,000 molecules with high structural differences was used in a molecular docking procedure to identify the cores of macrocyclic natural products that provide leads for difficult-to-drug targets. Classical molecular docking, IFD, and

MM/GBSA were used to select the best hits that modulate the KEAP1/NRF2 interaction. Because the binding site on which NRF2 is anchored on KEAP1 showed a significant degree of conformational mobility, particularly due to the sidechain of the Arg415 residue, to prevent bias toward a specific binding site conformation, four high-resolution crystal structures of KEAP1 that displayed variation were chosen. Two of them presented bound small-molecules as ligands (PDB IDs: 3VNG and 4IQK), and the other had two apo structures (PDB IDs: 1ZGK and 4IFJ). It was observed that the binding site is more open in the apo form than in the ligand-bound form. As a result, a large set of 217 cores with more complex structures and a smaller set of 41 lead-like macrocyclic nuclei were selected. A KEAP1/NRF2 uncharged macrocyclic inhibitor containing a cyclothialidine core was discovered after two iterative docking rounds with a carefully chosen group of natural product-derived cores. Suitable and systematic modification in key regions, as highlighted in Figure 47, allowed the identification of the best inhibitor. The synthesis of a small set of compounds containing 13 derivatives provided an interesting molecule, as shown in Figure 47, with significant binding affinity for KEAP1 ( $K_D = 4 \mu\text{M}$ ). However, while the potency in vitro and the activity in cellular and in vivo models were high, the oral bioavailability in rats was low (7%), possibly because of the presence of a carboxylic acid moiety [178].

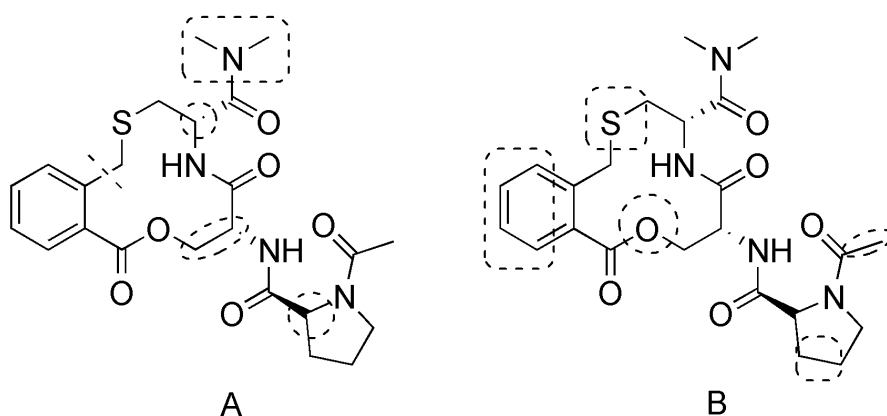


**Figure 47.** Structure of the cyclothialidine core and appropriate systematic modification in key regions (A-B) allowed the identification of the best inhibitor.

In 2022, the same research group reported how the potency of the previously identified macrocyclic natural product-based derivatives as KEAP1 inhibitors, in terms of  $K_D$  was improved from  $4.1 \mu\text{M}$  of the starting compound to  $68 \text{ nM}$  of the best newly synthesized derivative (over 100-fold), resulting in naturally-derived compounds showing activity in the nanomolar range ( $30 - 70 \text{ nM}$ ). The ability to interact with the target was studied in in vitro systems by evaluating aqueous solubility, cell permeability, and KEAP1 expression. This achievement was obtained by studying the SAR of the series at multiple positions using a dataset of 36 molecules, and MD simulation studies on the structure PDB ID: 6Z6A in which the lead compound was bound to KEAP1. Interestingly, the results

showed that further optimization should focus on the proline moiety's N-terminus and the phenylene ring's position ortho to the thiomethyl group. Thus, a virtual library was generated, and molecular docking calculations were used to prioritize the compounds to be synthesized. In particular, two sets of macrocycles comprising 46 and 20 derivatives were synthesized and computationally evaluated. The macrocyclic core of the nanomolar inhibitors was demonstrated to allocate the three pharmacophore units to produce suitable interactions with the key arginine residues of KEAP1 (Arg415, Arg483, Tyr572). However, the macrocyclic ring, an important structural feature of the lead series, is implicated in crucial interactions with KEAP1, which includes an H-bond between residue Ser602 and the carbonyl group of the lactam moiety of the selected derivatives. Moreover, the optimized ligand was able to displace the water molecule from the KEAP1 binding site, drastically modifying the thermodynamic profile, whereas reorganizations of residues Arg415 and Arg483 resulted in larger differences in affinity between ligands [179].

#### *Fragment-based approaches*

The fragment-based deconstruction–reconstruction (FBDR) method was used to investigate the ability of small-molecules to target the KEAP1 Kelch domain (Neh2-binding site), which contains many arginine residues, and it shows a large volume, thus representing an interesting cellular target for developing antioxidant drugs. This can be seen in the identified KEAP1/NRF2 PPI inhibitors, which often have high molecular weights and contain carboxylic acids, resulting in poor cell and CNS permeability. In the complete study reported by Pallesen, Bach, and coworkers [180], six classes of known small-molecule KEAP1/NRF2 PPI inhibitors were divided into 77 fragments using a FBDR approach, creating a target-biased library. The selected core heterocycles belonged to the classes 1,4-diaminonaphthalene, 1,2,3,4-tetrahydroisoquinoline, 1-phenylpyrazole, 3-phenylpropanoic acid, 1,4-diphenyl-1,2,3-triazole, and 1-(1,3,4-oxadiazol-2-yl)-urea. Initially, docking analysis was conducted employing a test set of 18 X-ray crystallized complexes including the KEAP1 Kelch domain, diverse small-molecule ligands, and the apo protein (PDB IDs: 1U6D, 4IN4, 5FNQ, 5FNU, 5FZN, 5FZJ, 5WHL, 5WHO, 5WIY). In this way, after superimposition of all of these structures, it was feasible to show that the Kelch domain's core cavity contains substantial clusters of conserved water molecules, which together create a huge H-bond network with the protein backbone. In particular, five water molecules that were close to the channel's opening appeared to act as a barrier to the protrusion of ligands. Following the self-docking of small ligands with the Kelch domain (PDB ID: 5FNU) was identified as the optimal structure, resulting in the highest success rate. Considering the subsequent FBDR computational experiments and testing in four orthogonal assays, it was possible to identify 17 fragments that could bind the KEAP1 Kelch domain. The P1, P4, and P5 sub-pockets were discovered to be hot spot areas through X-ray crystallography analysis of the docked poses of the best performing fragments bound to the KEAP1 Kelch domain and compared with the binding modes of

the reference molecules. P1 and P5 were found to be the most significant anchor points for the binding of the molecules. Finally, two promising fragment hits were recognized, and merging them into novel compounds, derivatives of the type shown in Figure 48, resulted in the proposed new inhibitors with enhanced affinity. In particular, the compound depicted in Figure 48 (where R1 = R2 = H, R3= cyclopropyl) exhibited a 220 – 380-fold stronger affinity (Ki = 16  $\mu$ M) relative to the parent fragments. Systematic optimization resulted in several novel analogs with Ki values of 0.04 –0.5  $\mu$ M, binding modes determined by X-ray crystallography, and enhanced microsomal stability.

A summary of all compounds acting as non-covalent modulators of the KAP1/NRF2 pathway is reported in Table 2, and details of the experimentally solved KEAP1 complexes cited in this study are presented in Table 3.

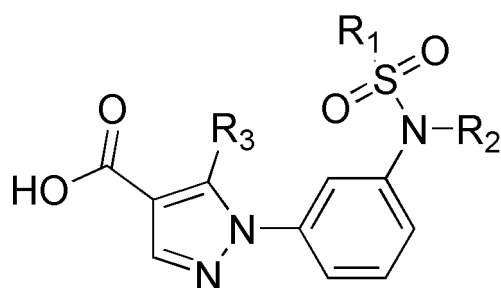


**Figure 48.** Structure of the novel compound proposed.

**Table 2.** Natural products able to act as non-covalent modulators of the KEAP1/NRF2 pathway: details on their characterization.

Compound	Chemical class	In vitro studies	In vivo studies
Umbrelliferone [99]	Coumarins	Determination of antioxidants profile, immunohistochemistry	Male and female albino BALB/c mice 5 - 7 weeks old, weighing 28 - 36 g
Osthole and O15 [100, 163]	Coumarins	Dual-luciferase, CETSA, Western blotting, qRT-PCR and siRNA-induced gene silencing	NA
Scopoletin [101]	Coumarins	Immunohistochemistry	Thirty-two male Wistar rats weighing 200 $\pm$ 20 g
Visnagin [102]	Coumarins	Assessment of ROS, LPO, and antioxidants, determination of inflammation and apoptosis markers qRT-PCR	Thirty-six male Wistar rats weighing 180–200 g
Esculetin [103]	Coumarins	Cell cycle analysis, detection of apoptosis, Western blotting, measurement of intracellular ROS level, co-immunoprecipitation, confocal microscopy, and qRT-PCR	NA
Coumarin Derivative [104]	Coumarins	Western blotting, ELISA	NA
Polypodiside [105]	Coumarins	Immunofluorescence, Western blotting, densitometric analysis and ARE-luciferase	NA
3-OH and 7-OH flavone derivatives [106]	Flavones	Measurement of intracellular ROS production, Manipulation of NRF2 or MnSOD expression as well as ERK or CREB activation and luciferase assay	NA
Morin [107]	Flavones	ELISA, Western blotting, qRT-PCR, and immunohistochemistry	Male Sprague-Dawley rats (200 – 250 g)

Dihydrokaempferol [108]	Flavones	ELISA, RT-PCR and Western blotting	C57BL/6 mice (20 ± 2 g)
Myricitrin [109]	Flavones	NA	NA
Liquiritigenin and liquiritin [110]	Flavones	Western blotting and qRT-PCR	Specific pathogen free male Sprague Dawley rats (weight: 200 – 220 g). NRF2 knock-out C57BL/6 mice were generated by using TALEN
Apigenin [111]	Flavones	Western blotting	Male KM mice at 20 – 22 g of weight
Quercetin [112, 113]	Flavones	Luciferase assay, NRF2 nuclear translocation, immunofluorescence, and qRT-PCR	NA
Taxifolin [114]	Flavones	Immunohistochemistry and Western blotting	Male Swiss albino mice (25 – 30 g)
Oxidized products of Quercetin [115]	Flavones	NA	NA
Tricetin [116]	Flavones	Western blotting, qRT-PCR	NA
Rhoifolin [117]	Flavones	Western blotting, qRT-PCR, ELISA	ACLT rat model
Isovitexin [118]	Flavones	Western blotting, qRT-PCR, ELISA	NA
Glyceollins [119]	Flavones	Western blotting, EMSA, qRT-PCR	NA
Biochanin A [120]	Flavones	Western blotting	NA
Japoflavone D [121]	Flavones	MTT assay, Annexin V, qPCR, Western blotting	NA
(-)-Epicatechin [122, 123]	Catechins	Western blotting, qRT-PCR	Specific pathogen free male Sprague-Dawley rats (200 – 240 g) and C57BL/6 male mice (16 – 20 g). NRF2 knock-out (NRF2 <sup>-/-</sup> ) C57BL/6 mice were generated by TALEN
Epigallocatechin gallate [124]	Catechins	Western blotting	Healthy adult male albino rats of Wistar strain
Resveratrol [125]	Polyphenols	Western blotting	C57BL/6 mice (18 – 22 g, male)
Caffeic acid [126]	Polyphenols	Biochemical assays	<i>Drosophila melanogaster</i>
Chlorogenic acid [127]	Polyphenols	Western blotting, luciferase assay, siRNA, qRT-PCR	Specific pathogen-free ICR and C57BL/6 mice (16 – 20 g body weight). NRF2 knock-out (NRF2 <sup>-/-</sup> ) C57BL/6 mice were generated by TALEN
Phlorizin [128]	Polyphenols	mRNA expression assay on KEAP1	<i>Drosophila melanogaster</i>
Astaxanthin [129, 166]	Polyphenols	Biochemical and histopathological assessment on liver samples	Male Wistar albino rats weighing 130 – 150 g
Gallic acid [130]	Polyphenols	Immunofluorescence assay, siRNA transfection, Western blotting, and CETSA	NA
Ginnalin A [131]	Polyphenols	qRT-PCR measurements, Western blotting, and immunofluorescence assay	NA
Ellagic acid [132] [132, 133]	Polyphenols	Liver and blood analysis	NA
Urolithins [134]	Polyphenols	Adeno-associated virus serotype 8 (AAV8)-based liver-specific knockdown of NRF2, siRNA transfection and Western blotting	Male C57BL/6J (6 to 8 weeks old)
Asperuloside [135]	Terpenes	Immunofluorescence, transfection of siRNA, and Western blotting.	6–8 weeks old male KM mice
Carnosic acid [136]	Terpenes	Immunohistochemistry and co-immunoprecipitation	Twenty-four Swiss albino mice (female, ~4 weeks old, ~25 g)
Continentalic acid [137]	Terpenes	Immunohistochemistry	Male albino mice (BALB/c) (22 – 26 g)

(-)- and (+)- caseadolabellols A [138]	Terpenes	Cell cycle and Annexin V	NA
Nerolidol [139]	Terpenes	Immunohistochemistry	Male Swiss albino mice (35 – 40 g)
Frullanian D [140]	Terpenes	Immunohistochemistry and immunofluorescence in MOVAS cells	NA
Madecassic acid (A) and asiatic acid [141]	Terpenes	NA	NA
Magnolol [142]	Lignan	Flow cytometry assay, immunohistochemistry	Female Swiss mice of age (8 - 12 weeks)
Erythritol [143]	Polyol	ROS assays, Western blotting, immunohistochemistry, and immunofluorescence	Male C57BL/6 mice aged 6 – 8 weeks. NRF2 knock-out C57BL/6 mice
Shinorine [144]	Mycosporine-like amino acid	MTT, ROS determination, qRT-PCR	NA
Schisandrol A [145]	Lignan	PCR	Male ICR mice (20 ± 2 g)
Schisandrin B [146]	Lignan	Identification of modified peptides and corresponding microsomal proteins in human liver microsomes treated with schisandrin B, Western blotting, immunofluorescence and microsomal CYP450 activity detection	KM male mice (18 – 22 g)
Schisandrin B [167]	Lignan	TUNEL staining, Determination of MMP, Determination of ROS, qRT-PCR, Western blotting, and co-immunoprecipitation	NA
Amygdalin [147]	Cyanogenic glycoside	Western blotting and immunofluorescence	NA
Cyanidin-3-O-glucoside (C3G) and protocatechuic acid (PCA) [148]	Cyanogenic glycoside	Antimutagenicity, cytotoxicity, apoptosis assay and Western blotting	NA
Vitamin U [149]	Vitamin	Microscopic assays and Western blotting	Female Sprague-Dawley rats (aged: 6.0 - 6.5 months, weighing: 150 – 190 g)
Phenylethanoid glycosides [150]	Phenylethanoid glycosides	NO detection, determination of TNF- $\alpha$ and IL-6, measurement of intracellular ROS and Western blotting	NA
Forsythoside- $\beta$ [152]	Phenylethanoid glycosides	qRT-PCR, immunofluorescence, cell transfection and inflammatory osteoporosis model, micro-CT scanning, and histological analysis	Primary mouse bone marrow-derived macrophages were isolated from the 6 – 8-week-old C57BL/6 mice
Sargahydroquinoic acid [153]	plastoquinone	ROS determination, cellular apoptosis analysis, measurement of mitochondrial membrane potential, and Western blotting	NA
GR24 [154]	Carotenoid-derived	MTT, NO assay, IL-1 $\beta$ secretion, Western blotting, qRT-PCR and NRF2 knock-down by siRNA transfection	NA
Rutaecarpine [155]	Alkaloid	Western blotting, immunofluorescence, SPR and luciferase assay	Male 6- to 8-week-old C57BL/6J wild-type (NRF2 <sup>+/+</sup> ) and NRF2-null (NRF2 <sup>-/-</sup> ) mice
AFOE and AFOil [156]	Mixture	Determination of H <sub>2</sub> O <sub>2</sub> , NOX activity, SOD activity, CAT activity and qRT-PCR	NA
Kaempferol(KAM)-3-O- $\alpha$ -L-rhamnopyranosyl-(1 $\rightarrow$ 6)- $\beta$ -D-glucopyranoside, QUE-3-O- $\alpha$ -L-rhamnopyranosyl-(1 $\rightarrow$ 6)- $\beta$ -D-	Mixture	qRT-PCR and immunohistochemistry	Adult male Wistar rats, weighing 150 – 250 g

galactopyranoside, QUE-3-O- $\alpha$ -L-rhamno-yranosyl-1 $\rightarrow$ 6)- $\beta$ -D-glucopyranoside [157]				
Extract of Pinot noir pomace [158]	Mixture	Cell viability and MTS colorimetric assay		NA
Catalposide and verproside [159]	Mixture	MTT, detection of AST and ALT activity, ELISA, detection of intracellular ROS, qRT-PCR and Western blotting	Group of mice (normal, model, positive, EAFVC)	
Scurrula atropurpurea extract [160]	Mixture		NA	NA
Butylphthalide, senkyunolide A, and Z-ligustilide [161]	Mixture	qRT-PCR and luciferase assay		NA
Lutein, sanguinarine, isorhamnetin, myricetin, hesperidin, didymin, and sweroside [162]	Mixture	Antioxidant assay, MTT, immunofluorescence, qRT-PCR, and Western blotting	Fifty-five days old female Sprague Dawley rats	
Isomers of Chlorogenic acid sch [164]	Polyphenolic	MTT, ORAC assays, NO assays, Western blotting, NRF2 nuclear translocation immunocytochemistry and qRT-PCR		NA
Pterostilbene [165]	Stilbenes	Nuclear and cytosolic fractionation, Western blotting, and ARE-luciferase		NA
Schisandrin C [168]	Lignan	MTT, ROS determination, MDA level, SOD activity, qRT-PCR, Western blotting, and co-immunoprecipitation	Four-week-old male C57BL/6 mice weighing 18 – 22 g	
Phytochemicals [169]	Mixture		NA	NA
Chloro-derivatives of flavonoids [170]	Flavones	DPPH free radical scavenging activity, ABTS activity, iron chelating activity, FeCl <sub>3</sub> reducing power activity, and phosphomolybdenum activity		NA
Mixture [171]	Phytochemicals	MTT and Western blotting		NA
Mixture [172]	Mixture	MTT, ROS generation, EMSA, apoptosis assay, Western blotting, qRT-PCR, immunofluorescence, luciferase assay, flow cytometry	NOD/SCID immunodeficient mice (aged 5 – 6 weeks), fertile chicken eggs	
Esculin [176]	Coumarins	qRT-PCR		Zebrafish
Cyclothialidine core [178]	Cyclothialidine	SPR inhibition in solution assay, SPR direct binding assay, cell permeability, cell assay and KEAP1 expression, purification, and crystallization with macrocycle		NA
Macrocyclic compounds [179]	Macrocycle	SPR inhibition in solution assay, SPR direct binding assay, cell permeability, cell assay and KEAP1 expression, purification, and crystallization with macrocycle		NA
Fragments [180]	Mixture	Fluorescence polarization assay and SPR		NA

**Table 3.** PDB details considering the KEAP1 complexes cited in this article.

PDB ID	Biological assembly	Resolution	Organism
1ZGK	Kelch domain of KEAP1	1.35 Å	<i>Homo sapiens</i>

2FLU	KEAP1/NRF2	1.50 Å	<i>Homo sapiens</i>
6LRZ	KEAP1/DMF	1.54 Å	<i>Mus musculus</i>
3WN7	KEAP1/NRF2 (N-terminal region)	1.57 Å	<i>Mus musculus</i>
1X2R	KEAP1/NRF2	1.70 Å	<i>Mus musculus</i>
6QMC	KEAP1/NRF2/J6H	1.77 Å	<i>Mus musculus</i>
4ZY3	KEAP1/K67	1.80 Å	<i>Mus musculus</i>
1U6D	Kelch domain of KEAP1	1.85 Å	<i>Homo sapiens</i>
2DYH	KEAP1/NRF2	1.90 Å	<i>Mus musculus</i>
5WVW	Kelch domain of KEAP1/NRF2 ETGE peptide	1.91 Å	<i>Homo sapiens</i>
5FNQ	KEAP1/S0W (Kelch domain)	1.91 Å	<i>Mus musculus</i>
4IQK	KEAP1/IQG (Cmpd16) (Kelch domain)	1.97 Å	<i>Homo sapiens</i>
3VNG	KEAP1/FUU	2.10 Å	<i>Homo sapiens</i>
3ZGC	KEAP1/Nrf2	2.20 Å	<i>Homo sapiens</i>
4IFN	KEAP1/12O	2.40 Å	<i>Homo sapiens</i>
4L7B	KEAP1/1VV	2.41 Å	<i>Homo sapiens</i>
4XMB	KEAP1/41P	2.43 Å	<i>Homo sapiens</i>
6SP4	KEAP1/Cmpd23	2.59 Å	<i>Homo sapiens</i>
3I3N	KEAP1 BTB-BACK domain	2.60 Å	<i>Homo sapiens</i>
5DAD	KEAP1/TX6 (BTB Domain)	2.61 Å	<i>Homo sapiens</i>
4CXT	KEAP1 BTB domain/SXJ	2.66 Å	<i>Homo sapiens</i>
4CXJ	KEAP1 BTB domain (C151W mutant)	2.80 Å	<i>Homo sapiens</i>
5CGJ	KEAP1/RA839	3.36 Å	<i>Mus musculus</i>
2LZ1	NRF2	NMR	<i>Homo sapiens</i>

## Conclusions

In summary, in this review article, we have presented an updated perspective on natural products as antioxidant agents. In particular, we have presented an analysis of how these classes of compounds exert their antioxidant ability by targeting the KEAP1/NRF2 pathway. During the last decades, several natural compounds have been investigated as possible antioxidant agents that can provide beneficial features to human cells, preventing and/or slowing several diseases, including cancer and neurodegenerative disorders. This class of compounds can target the pathway by targeting KEAP1 in a reversible or irreversible manner. In terms of structure-activity relationships, these classes of inhibitors are easily recognizable. Covalent modulators bear Michael acceptor moieties in the structure as  $\alpha,\beta$ -unsaturated carbonyl. Just a few examples of inhibitors do not bear an  $\alpha,\beta$ -unsaturated carbonyl such as Sulphorafane and Andrografolide characterized by an isocyanate moiety and an exocyclic double bond, respectively. Challenging is the case of the carnosic acid in which the involvement of Cys151 is highly probable. The potential mechanism of action could be due to the oxidation of the catechol moiety in a quinone moiety transforming it into the activated form of the drug that reacts with the critical thiol of Cys151. Non-covalent modulators are able to establish several H-Bonds and  $\pi$ -stacking interactions with different residues and in many cases the presence of a glycoside moiety seems to improve the activity. A major part of the natural products identified are coumarins, flavones, catechines, polyphenols, and terpenes. It is worthy noting the low presence

of nitrogenous modulators, such as shinorine, amigdaline and rutaecarpine and cpd. 16. The identification of new modulators should pay attention to the right balance of aromatic moieties and hydroxyl or isosteric groups by means of a ligand-based pharmacophore approach followed by docking exploiting the plenty of experimental structure available. Accordingly, in this survey, we have discussed the mechanism of action and how natural products can interact with KEAP1 at the molecular level. Furthermore, we analyzed the antioxidant profile and possible therapeutic applications of the most promising compounds. Considering the improved knowledge about KEAP1/NRF2 and the huge progress in computer-aided drug discovery as well as experimental methods, we expect further clinical studies in the future to highlight the possible therapeutic profile of some natural products by producing strong antioxidant effects for treating diseases in which oxidative stress plays a crucial role in the development and progression of the disorders.

## Acknowledgments

This article is facilitated by the collaboration through COST Action CA20121, supported by the European Cooperation in Science and Technology ([www.cost.eu](http://www.cost.eu); <https://benbedphar.org/about-benbedphar/> accessed on 16 October 2023).

## Author Contributions

All authors have read and agreed to the published version of the manuscript.

## Conflicts of Interest

The authors declare no conflict of interest.

## References

- [1] D.C. Moreira, M.F. Oliveira, L. Liz-Guimaraes, N. Diniz-Rojas, E.G. Campos, M. Hermes-Lima, Current Trends and Research Challenges Regarding "Preparation for Oxidative Stress", *Front Physiol*, 8 (2017) 702.
- [2] A. Cuadrado, G. Manda, A. Hassan, M.J. Alcaraz, C. Barbas, A. Daiber, P. Ghezzi, R. Leon, M.G. Lopez, B. Oliva, M. Pajares, A.I. Rojo, N. Robledinos-Anton, A.M. Valverde, E. Guney, H. Schmidt, Transcription Factor NRF2 as a Therapeutic Target for Chronic Diseases: A Systems Medicine Approach, *Pharmacol Rev*, 70 (2018) 348-383.
- [3] A. Cuadrado, A.I. Rojo, G. Wells, J.D. Hayes, S.P. Cousin, W.L. Rumsey, O.C. Attucks, S. Franklin, A.L. Levonen, T.W. Kensler, A.T. Dinkova-Kostova, Therapeutic targeting of the NRF2 and KEAP1 partnership in chronic diseases, *Nat Rev Drug Discov*, 18 (2019) 295-317.
- [4] F. He, X. Ru, T. Wen, NRF2, a Transcription Factor for Stress Response and Beyond, *Int J Mol Sci*, 21 (2020).
- [5] P. Moi, K. Chan, I. Asunis, A. Cao, Y.W. Kan, Isolation of NF-E2-related factor 2 (Nrf2), a NF-E2-like basic leucine zipper transcriptional activator that binds to the tandem NF-E2/AP1 repeat of the beta-globin locus control region, *Proc Natl Acad Sci U S A*, 91 (1994) 9926-9930.
- [6] J.Z. Wu, C.C. Cheng, L.L. Shen, Z.K. Wang, S.B. Wu, W.L. Li, S.H. Chen, R.P. Zhou, P.H. Qiu, Synthetic chalcones with potent antioxidant ability on H(2)O(2)-induced apoptosis in PC12 cells, *Int J Mol Sci*, 15 (2014) 18525-18539.
- [7] C. Tonelli, I.I.C. Chio, D.A. Tuveson, Transcriptional Regulation by Nrf2, *Antioxid Redox Signal*, 29 (2018) 1727-1745.
- [8] M. Ashrafizadeh, Z. Ahmadi, T. Farkhondeh, S. Samarghandian, Back to Nucleus: Combating with Cadmium Toxicity Using Nrf2 Signaling Pathway as a Promising Therapeutic Target, *Biol Trace Elem Res*, 197 (2020) 52-62.
- [9] M.X. Wang, J. Zhao, H. Zhang, K. Li, L.Z. Niu, Y.P. Wang, Y.J. Zheng, Potential Protective and Therapeutic Roles of the Nrf2 Pathway in Ocular Diseases: An Update, *Oxid Med Cell Longev*, 2020 (2020) 9410952.
- [10] A.T. Dinkova-Kostova, A.Y. Abramov, The emerging role of Nrf2 in mitochondrial function, *Free Radic Biol Med*, 88 (2015) 179-188.
- [11] S. Saha, B. Buttari, E. Panieri, E. Profumo, L. Saso, An Overview of Nrf2 Signaling Pathway and Its Role in Inflammation, *Molecules*, 25 (2020).
- [12] I. Perez-Torres, V. Guarner-Lans, M.E. Rubio-Ruiz, Reductive Stress in Inflammation-Associated Diseases and the Pro-Oxidant Effect of Antioxidant Agents, *Int J Mol Sci*, 18 (2017).
- [13] I. Bellezza, I. Giambanco, A. Minelli, R. Donato, Nrf2-Keap1 signaling in oxidative and reductive stress, *Biochim Biophys Acta Mol Cell Res*, 1865 (2018) 721-733.
- [14] M.B. Sporn, K.T. Liby, NRF2 and cancer: the good, the bad and the importance of context, *Nat Rev Cancer*, 12 (2012) 564-571.
- [15] L. Saso, O. Firuzi, Pharmacological applications of antioxidants: lights and shadows, *Curr Drug Targets*, 15 (2014) 1177-1199.
- [16] F. Katsuoka, M. Yamamoto, Small Maf proteins (MafF, MafG, MafK): History, structure and function, *Gene*, 586 (2016) 197-205.

- [17] M. Theodore, Y. Kawai, J. Yang, Y. Kleshchenko, S.P. Reddy, F. Villalta, I.J. Arinze, Multiple nuclear localization signals function in the nuclear import of the transcription factor Nrf2, *J Biol Chem*, 283 (2008) 8984-8994.
- [18] P. Rada, A.I. Rojo, S. Chowdhry, M. McMahon, J.D. Hayes, A. Cuadrado, SCF/beta-TrCP promotes glycogen synthase kinase 3-dependent degradation of the Nrf2 transcription factor in a Keap1-independent manner, *Mol Cell Biol*, 31 (2011) 1121-1133.
- [19] M. Lin, X. Zhai, G. Wang, X. Tian, D. Gao, L. Shi, H. Wu, Q. Fan, J. Peng, K. Liu, J. Yao, Salvianolic acid B protects against acetaminophen hepatotoxicity by inducing Nrf2 and phase II detoxification gene expression via activation of the PI3K and PKC signaling pathways, *J Pharmacol Sci*, 127 (2015) 203-210.
- [20] Y. Katoh, K. Itoh, E. Yoshida, M. Miyagishi, A. Fukamizu, M. Yamamoto, Two domains of Nrf2 cooperatively bind CBP, a CREB binding protein, and synergistically activate transcription, *Genes Cells*, 6 (2001) 857-868.
- [21] P. Nioi, T. Nguyen, P.J. Sherratt, C.B. Pickett, The carboxy-terminal Neh3 domain of Nrf2 is required for transcriptional activation, *Mol Cell Biol*, 25 (2005) 10895-10906.
- [22] V. Krajka-Kuzniak, J. Paluszczak, W. Baer-Dubowska, The Nrf2-ARE signaling pathway: An update on its regulation and possible role in cancer prevention and treatment, *Pharmacol Rep*, 69 (2017) 393-402.
- [23] P. Rada, A.I. Rojo, N. Evrard-Todeschi, N.G. Innamorato, A. Cotte, T. Jaworski, J.C. Tobon-Velasco, H. Devijver, M.F. Garcia-Mayoral, F. Van Leuven, J.D. Hayes, G. Bertho, A. Cuadrado, Structural and functional characterization of Nrf2 degradation by the glycogen synthase kinase 3/beta-TrCP axis, *Mol Cell Biol*, 32 (2012) 3486-3499.
- [24] H. Wang, K. Liu, M. Geng, P. Gao, X. Wu, Y. Hai, Y. Li, Y. Li, L. Luo, J.D. Hayes, X.J. Wang, X. Tang, RXRalpha inhibits the NRF2-ARE signaling pathway through a direct interaction with the Neh7 domain of NRF2, *Cancer Res*, 73 (2013) 3097-3108.
- [25] E.H. Heiss, D. Schachner, K. Zimmermann, V.M. Dirsch, Glucose availability is a decisive factor for Nrf2-mediated gene expression, *Redox Biol*, 1 (2013) 359-365.
- [26] S.S. Chambel, A. Santos-Goncalves, T.L. Duarte, The Dual Role of Nrf2 in Nonalcoholic Fatty Liver Disease: Regulation of Antioxidant Defenses and Hepatic Lipid Metabolism, *Biomed Res Int*, 2015 (2015) 597134.
- [27] L.J. Cao, H.D. Li, M. Yan, Z.H. Li, H. Gong, P. Jiang, Y. Deng, P.F. Fang, B.K. Zhang, The Protective Effects of Isoliquiritigenin and Glycyrrhetic Acid against Triptolide-Induced Oxidative Stress in HepG2 Cells Involve Nrf2 Activation, *Evid Based Complement Alternat Med*, 2016 (2016) 8912184.
- [28] K. Itoh, M. Mochizuki, Y. Ishii, T. Ishii, T. Shibata, Y. Kawamoto, V. Kelly, K. Sekizawa, K. Uchida, M. Yamamoto, Transcription factor Nrf2 regulates inflammation by mediating the effect of 15-deoxy-Delta(12,14)-prostaglandin j(2), *Mol Cell Biol*, 24 (2004) 36-45.
- [29] D. Stewart, E. Killeen, R. Naquin, S. Alam, J. Alam, Degradation of transcription factor Nrf2 via the ubiquitin-proteasome pathway and stabilization by cadmium, *J Biol Chem*, 278 (2003) 2396-2402.
- [30] T. Ogura, K.I. Tong, K. Mio, Y. Maruyama, H. Kurokawa, C. Sato, M. Yamamoto, Keap1 is a forked-stem dimer structure with two large spheres enclosing the intervening, double glycine repeat, and C-terminal domains, *Proc Natl Acad Sci U S A*, 107 (2010) 2842-2847.
- [31] E. Panieri, L. Saso, Potential Applications of NRF2 Inhibitors in Cancer Therapy, *Oxid Med Cell Longev*, 2019 (2019) 8592348.
- [32] S. Tao, P. Liu, G. Luo, M. Rojo de la Vega, H. Chen, T. Wu, J. Tillotson, E. Chapman, D.D. Zhang, p97 Negatively Regulates NRF2 by Extracting Ubiquitylated NRF2 from the KEAP1-CUL3 E3 Complex, *Mol Cell Biol*, 37 (2017).
- [33] L. Cheng, H. Zhang, F. Wu, Z. Liu, Y. Cheng, C. Wang, Role of Nrf2 and Its Activators in Cardiocerebral Vascular Disease, *Oxid Med Cell Longev*, 2020 (2020) 4683943.
- [34] M. Komatsu, H. Kurokawa, S. Waguri, K. Taguchi, A. Kobayashi, Y. Ichimura, Y.S. Sou, I. Ueno, A. Sakamoto, K.I. Tong, M. Kim, Y. Nishito, S. Iemura, T. Natsume, T. Ueno, E. Kominami, H. Motohashi, K. Tanaka, M. Yamamoto, The selective autophagy substrate p62 activates the stress responsive transcription factor Nrf2 through inactivation of Keap1, *Nat Cell Biol*, 12 (2010) 213-223.
- [35] A. Lau, X.J. Wang, F. Zhao, N.F. Villeneuve, T. Wu, T. Jiang, Z. Sun, E. White, D.D. Zhang, A noncanonical mechanism of Nrf2 activation by autophagy deficiency: direct interaction between Keap1 and p62, *Mol Cell Biol*, 30 (2010) 3275-3285.
- [36] A. Jain, T. Lamark, E. Sjøttem, K.B. Larsen, J.A. Awuh, A. Overvatn, M. McMahon, J.D. Hayes, T. Johansen, p62/SQSTM1 is a target gene for transcription factor NRF2 and creates a positive feedback loop by inducing antioxidant response element-driven gene transcription, *J Biol Chem*, 285 (2010) 22576-22591.
- [37] J.W. Kaspar, S.K. Niture, A.K. Jaiswal, Nrf2: Nrf2 (Keap1) signaling in oxidative stress, *Free Radic Biol Med*, 47 (2009) 1304-1309.

- [38] P. Shaw, A. Chattopadhyay, Nrf2-ARE signaling in cellular protection: Mechanism of action and the regulatory mechanisms, *J Cell Physiol*, 235 (2020) 3119-3130.
- [39] A.L. Stefanson, M. Bakovic, Dietary regulation of Keap1/Nrf2/ARE pathway: focus on plant-derived compounds and trace minerals, *Nutrients*, 6 (2014) 3777-3801.
- [40] D.D. Zhang, M. Hannink, Distinct cysteine residues in Keap1 are required for Keap1-dependent ubiquitination of Nrf2 and for stabilization of Nrf2 by chemopreventive agents and oxidative stress, *Mol Cell Biol*, 23 (2003) 8137-8151.
- [41] A.M. Choi, J. Alam, Heme oxygenase-1: function, regulation, and implication of a novel stress-inducible protein in oxidant-induced lung injury, *Am J Respir Cell Mol Biol*, 15 (1996) 9-19.
- [42] E. Kansanen, H.K. Jyrkkanen, A.L. Levonen, Activation of stress signaling pathways by electrophilic oxidized and nitrated lipids, *Free Radic Biol Med*, 52 (2012) 973-982.
- [43] E. Kansanen, S.M. Kuosmanen, H. Leinonen, A.L. Levonen, The Keap1-Nrf2 pathway: Mechanisms of activation and dysregulation in cancer, *Redox Biol*, 1 (2013) 45-49.
- [44] N. Cancer Genome Atlas Research, Comprehensive genomic characterization of squamous cell lung cancers, *Nature*, 489 (2012) 519-525.
- [45] T. Shibata, T. Ohta, K.I. Tong, A. Kokubu, R. Odogawa, K. Tsuta, H. Asamura, M. Yamamoto, S. Hirohashi, Cancer related mutations in NRF2 impair its recognition by Keap1-Cul3 E3 ligase and promote malignancy, *Proc Natl Acad Sci U S A*, 105 (2008) 13568-13573.
- [46] K. Taguchi, M. Yamamoto, The KEAP1-NRF2 System in Cancer, *Front Oncol*, 7 (2017) 85.
- [47] Y. Horie, T. Suzuki, J. Inoue, T. Iso, G. Wells, T.W. Moore, T. Mizushima, A.T. Dinkova-Kostova, T. Kasai, T. Kamei, S. Koshihara, M. Yamamoto, Molecular basis for the disruption of Keap1-Nrf2 interaction via Hinge & Latch mechanism, *Commun Biol*, 4 (2021) 576.
- [48] K. Taguchi, H. Motohashi, M. Yamamoto, Molecular mechanisms of the Keap1-Nrf2 pathway in stress response and cancer evolution, *Genes Cells*, 16 (2011) 123-140.
- [49] S.A. Courtneidge, S. Fumagalli, M. Koegl, G. Superti-Furga, G.M. Twamley-Stein, The Src family of protein tyrosine kinases: regulation and functions, *Dev Suppl*, (1993) 57-64.
- [50] M. Salazar, A.I. Rojo, D. Velasco, R.M. de Sagarra, A. Cuadrado, Glycogen synthase kinase-3beta inhibits the xenobiotic and antioxidant cell response by direct phosphorylation and nuclear exclusion of the transcription factor Nrf2, *J Biol Chem*, 281 (2006) 14841-14851.
- [51] S. Dhakshinamoorthy, A.K. Jain, D.A. Bloom, A.K. Jaiswal, Bach1 competes with Nrf2 leading to negative regulation of the antioxidant response element (ARE)-mediated NAD(P)H:quinone oxidoreductase 1 gene expression and induction in response to antioxidants, *J Biol Chem*, 280 (2005) 16891-16900.
- [52] K. Igarashi, H. Hoshino, A. Muto, N. Suwabe, S. Nishikawa, H. Nakauchi, M. Yamamoto, Multivalent DNA binding complex generated by small Maf and Bach1 as a possible biochemical basis for beta-globin locus control region complex, *J Biol Chem*, 273 (1998) 11783-11790.
- [53] T. Oyake, K. Itoh, H. Motohashi, N. Hayashi, H. Hoshino, M. Nishizawa, M. Yamamoto, K. Igarashi, Bach proteins belong to a novel family of BTB-basic leucine zipper transcription factors that interact with MafK and regulate transcription through the NF-E2 site, *Mol Cell Biol*, 16 (1996) 6083-6095.
- [54] J. Sun, H. Hoshino, K. Takaku, O. Nakajima, A. Muto, H. Suzuki, S. Tashiro, S. Takahashi, S. Shibahara, J. Alam, M.M. Taketo, M. Yamamoto, K. Igarashi, Hemoprotein Bach1 regulates enhancer availability of heme oxygenase-1 gene, *EMBO J*, 21 (2002) 5216-5224.
- [55] J.W. Kaspar, A.K. Jaiswal, Antioxidant-induced phosphorylation of tyrosine 486 leads to rapid nuclear export of Bach1 that allows Nrf2 to bind to the antioxidant response element and activate defensive gene expression, *J Biol Chem*, 285 (2010) 153-162.
- [56] Y. Zenke-Kawasaki, Y. Dohi, Y. Katoh, T. Ikura, M. Ikura, T. Asahara, F. Tokunaga, K. Iwai, K. Igarashi, Heme induces ubiquitination and degradation of the transcription factor Bach1, *Mol Cell Biol*, 27 (2007) 6962-6971.
- [57] R. Holland, A.E. Hawkins, A.L. Eggler, A.D. Mesecar, D. Fabris, J.C. Fishbein, Prospective type 1 and type 2 disulfides of Keap1 protein, *Chem Res Toxicol*, 21 (2008) 2051-2060.
- [58] D.D. Zhang, Mechanistic studies of the Nrf2-Keap1 signaling pathway, *Drug Metab Rev*, 38 (2006) 769-789.
- [59] K.I. Tong, B. Padmanabhan, A. Kobayashi, C. Shang, Y. Hirotsu, S. Yokoyama, M. Yamamoto, Different electrostatic potentials define ETGE and DLG motifs as hinge and latch in oxidative stress response, *Mol Cell Biol*, 27 (2007) 7511-7521.
- [60] J.D. Hayes, A.T. Dinkova-Kostova, The Nrf2 regulatory network provides an interface between redox and intermediary metabolism, *Trends Biochem Sci*, 39 (2014) 199-218.
- [61] T. Suzuki, H. Motohashi, M. Yamamoto, Toward clinical application of the Keap1-Nrf2 pathway, *Trends Pharmacol Sci*, 34 (2013) 340-346.

- [62] K. Itoh, N. Wakabayashi, Y. Katoh, T. Ishii, K. Igarashi, J.D. Engel, M. Yamamoto, Keap1 represses nuclear activation of antioxidant responsive elements by Nrf2 through binding to the amino-terminal Neh2 domain, *Genes Dev*, 13 (1999) 76-86.
- [63] N. Wakabayashi, A.T. Dinkova-Kostova, W.D. Holtzclaw, M.I. Kang, A. Kobayashi, M. Yamamoto, T.W. Kensler, P. Talalay, Protection against electrophile and oxidant stress by induction of the phase 2 response: fate of cysteines of the Keap1 sensor modified by inducers, *Proc Natl Acad Sci U S A*, 101 (2004) 2040-2045.
- [64] M.H. Wong, H.K. Bryan, I.M. Copple, R.E. Jenkins, P.H. Chiu, J. Bibby, N.G. Berry, N.R. Kitteringham, C.E. Goldring, P.M. O'Neill, B.K. Park, Design and Synthesis of Irreversible Analogues of Bardoxolone Methyl for the Identification of Pharmacologically Relevant Targets and Interaction Sites, *J Med Chem*, 59 (2016) 2396-2409.
- [65] A.L. Levonen, A. Landar, A. Ramachandran, E.K. Ceaser, D.A. Dickinson, G. Zanoni, J.D. Morrow, V.M. Darley-Usmar, Cellular mechanisms of redox cell signalling: role of cysteine modification in controlling antioxidant defences in response to electrophilic lipid oxidation products, *Biochem J*, 378 (2004) 373-382.
- [66] H. Zhou, Y. Wang, Q. You, Z. Jiang, Recent progress in the development of small molecule Nrf2 activators: a patent review (2017-present), *Expert Opin Ther Pat*, 30 (2020) 209-225.
- [67] W. Hur, Z. Sun, T. Jiang, D.E. Mason, E.C. Peters, D.D. Zhang, H. Luesch, P.G. Schultz, N.S. Gray, A small-molecule inducer of the antioxidant response element, *Chem Biol*, 17 (2010) 537-547.
- [68] S. Unni, P. Deshmukh, G. Krishnappa, P. Kommu, B. Padmanabhan, Structural insights into the multiple binding modes of Dimethyl Fumarate (DMF) and its analogs to the Kelch domain of Keap1, *FEBS J*, 288 (2021) 1599-1613.
- [69] S. Magesh, Y. Chen, L. Hu, Small molecule modulators of Keap1-Nrf2-ARE pathway as potential preventive and therapeutic agents, *Med Res Rev*, 32 (2012) 687-726.
- [70] D.D. Zhang, E. Chapman, The role of natural products in revealing NRF2 function, *Nat Prod Rep*, 37 (2020) 797-826.
- [71] H. Zhou, C.S. Beevers, S. Huang, The targets of curcumin, *Curr Drug Targets*, 12 (2011) 332-347.
- [72] J.K. Lin, Molecular targets of curcumin, *Adv Exp Med Biol*, 595 (2007) 227-243.
- [73] A.B. Kunnumakkara, D. Bordoloi, G. Padmavathi, J. Monisha, N.K. Roy, S. Prasad, B.B. Aggarwal, Curcumin, the golden nutraceutical: multitargeting for multiple chronic diseases, *Br J Pharmacol*, 174 (2017) 1325-1348.
- [74] J.W. Shin, K.S. Chun, D.H. Kim, S.J. Kim, S.H. Kim, N.C. Cho, H.K. Na, Y.J. Surh, Curcumin induces stabilization of Nrf2 protein through Keap1 cysteine modification, *Biochem Pharmacol*, 173 (2020) 113820.
- [75] E. Hee Jo, J. Eun Moon, M. Han Chang, Y. Jin Lim, J. Hyun Park, S. Hee Lee, Y. Rae Cho, A.E. Cho, S. Pil Pack, H.W. Kim, L. Crowley, B. Le, A.B. Nukhet, Y. Chen, Y. Zhong, J. Zhao, Y. Li, H. Cha, J. Hoon Pan, J. Kyeom Kim, J. Hyup Lee, Sensitization of GSH synthesis by curcumin curtails acrolein-induced alveolar epithelial apoptosis via Keap1 cysteine conjugation: A randomized controlled trial and experimental animal model of pneumonitis, *J Adv Res*, 46 (2023) 17-29.
- [76] Y. Cheng, L. Cheng, X. Gao, S. Chen, P. Wu, C. Wang, Z. Liu, Covalent modification of Keap1 at Cys77 and Cys434 by pubescenoside suppresses oxidative stress-induced NLRP3 inflammasome activation in myocardial ischemia-reperfusion injury, *Theranostics*, 11 (2021) 861-877.
- [77] C. Hu, A.L. Eggler, A.D. Mesecar, R.B. van Breemen, Modification of keap1 cysteine residues by sulforaphane, *Chem Res Toxicol*, 24 (2011) 515-521.
- [78] F. Hong, M.L. Freeman, D.C. Liebler, Identification of sensor cysteines in human Keap1 modified by the cancer chemopreventive agent sulforaphane, *Chem Res Toxicol*, 18 (2005) 1917-1926.
- [79] Y.H. Ahn, Y. Hwang, H. Liu, X.J. Wang, Y. Zhang, K.K. Stephenson, T.N. Boronina, R.N. Cole, A.T. Dinkova-Kostova, P. Talalay, P.A. Cole, Electrophilic tuning of the chemoprotective natural product sulforaphane, *Proc Natl Acad Sci U S A*, 107 (2010) 9590-9595.
- [80] K. Heyninck, L. Sabbe, C.S. Chirumamilla, K. Szarc Vel Szic, P. Vander Veken, K.J.A. Lemmens, M. Lahtela-Kakkonen, S. Naulaerts, K. Op de Beeck, K. Laukens, G. Van Camp, A.R. Weseler, A. Bast, G. Haenen, G. Haegeman, W. Vanden Berghe, Withaferin A induces heme oxygenase (HO-1) expression in endothelial cells via activation of the Keap1/Nrf2 pathway, *Biochem Pharmacol*, 109 (2016) 48-61.
- [81] D.L. Palliyaguru, D.V. Chartoumpekis, N. Wakabayashi, J.J. Skoko, Y. Yagishita, S.V. Singh, T.W. Kensler, Withaferin A induces Nrf2-dependent protection against liver injury: Role of Keap1-independent mechanisms, *Free Radic Biol Med*, 101 (2016) 116-128.
- [82] S. Tao, S.L. Park, M. Rojo de la Vega, D.D. Zhang, G.T. Wondrak, Systemic administration of the apocarotenoid bixin protects skin against solar UV-induced damage through activation of NRF2, *Free Radic Biol Med*, 89 (2015) 690-700.

- [83] S. Tao, M. Rojo de la Vega, H. Quijada, G.T. Wondrak, T. Wang, J.G. Garcia, D.D. Zhang, Bixin protects mice against ventilation-induced lung injury in an NRF2-dependent manner, *Sci Rep*, 6 (2016) 18760.
- [84] Z. Xu, X.Q. Kong, Bixin ameliorates high fat diet-induced cardiac injury in mice through inflammation and oxidative stress suppression, *Biomed Pharmacother*, 89 (2017) 991-1004.
- [85] L. Xue, H. Zhang, J. Zhang, B. Li, Z. Zhang, S. Tao, Bixin protects against particle-induced long-term lung injury in an NRF2-dependent manner, *Toxicol Res (Camb)*, 7 (2018) 258-270.
- [86] H. Zhang, L. Xue, B. Li, H. Tian, Z. Zhang, S. Tao, Therapeutic potential of bixin in PM2.5 particles-induced lung injury in an Nrf2-dependent manner, *Free Radic Biol Med*, 126 (2018) 166-176.
- [87] M. Sthijns, P.M. Schiffers, G.M. Janssen, K.J.A. Lemmens, B. Ides, P. Vangrieken, F.G. Bouwman, E.C. Mariman, I. Pader, E.S.J. Arner, K. Johansson, A. Bast, G. Haenen, Rutin protects against H<sub>2</sub>O<sub>2</sub>-triggered impaired relaxation of placental arterioles and induces Nrf2-mediated adaptation in Human Umbilical Vein Endothelial Cells exposed to oxidative stress, *Biochim Biophys Acta Gen Subj*, 1861 (2017) 1177-1189.
- [88] B.K. Ooi, K.G. Chan, B.H. Goh, W.H. Yap, The Role of Natural Products in Targeting Cardiovascular Diseases via Nrf2 Pathway: Novel Molecular Mechanisms and Therapeutic Approaches, *Front Pharmacol*, 9 (2018) 1308.
- [89] S.J. Mascuch, P.D. Boudreau, T.M. Carland, N.T. Pierce, J. Olson, M.E. Hensler, H. Choi, J. Campanale, A. Hamdoun, V. Nizet, W.H. Gerwick, T. Gaasterland, L. Gerwick, Marine Natural Product Honaucin A Attenuates Inflammation by Activating the Nrf2-ARE Pathway, *J Nat Prod*, 81 (2018) 506-514.
- [90] Y. Luo, A.L. Egger, D. Liu, G. Liu, A.D. Mesecar, R.B. van Breemen, Sites of alkylation of human Keap1 by natural chemoprevention agents, *J Am Soc Mass Spectrom*, 18 (2007) 2226-2232.
- [91] J. Yao, B. Zhang, C. Ge, S. Peng, J. Fang, Xanthohumol, a polyphenol chalcone present in hops, activating Nrf2 enzymes to confer protection against oxidative damage in PC12 cells, *J Agric Food Chem*, 63 (2015) 1521-1531.
- [92] H. Chen, J. Fu, H. Chen, Y. Hu, D.N. Soroka, J.R. Prigge, E.E. Schmidt, F. Yan, M.B. Major, X. Chen, S. Sang, Ginger compound [6]-shogaol and its cysteine-conjugated metabolite (M2) activate Nrf2 in colon epithelial cells in vitro and in vivo, *Chem Res Toxicol*, 27 (2014) 1575-1585.
- [93] Y. Yuan, L. Ji, L. Luo, J. Lu, X. Ma, Z. Ma, Z. Chen, Quinone reductase (QR) inducers from *Andrographis paniculata* and identification of molecular target of andrographolide, *Fitoterapia*, 83 (2012) 1506-1513.
- [94] D.P.W. Wong, M.Y. Ng, J.Y. Leung, B.K. Boh, E.C. Lim, S.H. Tan, S. Lim, W.H. Seah, C.Z. Hu, B.C. Ho, D.H.P. Ng, T. Hagen, Regulation of the NRF2 transcription factor by andrographolide and organic extracts from plant endophytes, *PLoS One*, 13 (2018) e0204853.
- [95] B. Schulte, M. Konig, B.I. Escher, S. Wittenburg, M. Proj, V. Wolf, C. Lemke, G. Schnakenburg, I. Sobic, H. Streeck, C.E. Muller, M. Gutschow, C. Steinebach, Andrographolide Derivatives Target the KEAP1/NRF2 Axis and Possess Potent Anti-SARS-CoV-2 Activity, *ChemMedChem*, 17 (2022) e202100732.
- [96] T. Satoh, K. Kosaka, K. Itoh, A. Kobayashi, M. Yamamoto, Y. Shimojo, C. Kitajima, J. Cui, J. Kamins, S. Okamoto, M. Izumi, T. Shirasawa, S.A. Lipton, Carnosic acid, a catechol-type electrophilic compound, protects neurons both in vitro and in vivo through activation of the Keap1/Nrf2 pathway via S-alkylation of targeted cysteines on Keap1, *J Neurochem*, 104 (2008) 1116-1131.
- [97] T. Ohnuma, S. Nakayama, E. Anan, T. Nishiyama, K. Ogura, A. Hiratsuka, Activation of the Nrf2/ARE pathway via S-alkylation of cysteine 151 in the chemopreventive agent-sensor Keap1 protein by faltarindiol, a conjugated diacetylene compound, *Toxicol Appl Pharmacol*, 244 (2010) 27-36.
- [98] T. Ohnuma, T. Komatsu, S. Nakayama, T. Nishiyama, K. Ogura, A. Hiratsuka, Induction of antioxidant and phase 2 drug-metabolizing enzymes by faltarindiol isolated from *Notopterygium incisum* extract, which activates the Nrf2/ARE pathway, leads to cytoprotection against oxidative and electrophilic stress, *Arch Biochem Biophys*, 488 (2009) 34-41.
- [99] Younas, A. Khan, O. Shehzad, E.K. Seo, A. Onder, S. Khan, Anti-allergic activities of Umbelliferone against histamine- and Picryl chloride-induced ear edema by targeting Nrf2/iNOS signaling in mice, *BMC Complement Med Ther*, 21 (2021) 215.
- [100] W. Huang, Y. Huang, J. Cui, Y. Wu, F. Zhu, J. Huang, L. Ma, Design and synthesis of Osthole-based compounds as potential Nrf2 agonists, *Bioorg Med Chem Lett*, 61 (2022) 128547.
- [101] M.M. Khalaf, S.M. Hassan, A.M. Sayed, A.M. Abo-Youssef, Ameliorate impacts of scopoletin against vancomycin-induced intoxication in rat model through modulation of Keap1-Nrf2/HO-1 and I $\kappa$ B/ $\alpha$ -P65 NF- $\kappa$ B/P38 MAPK signaling pathways: Molecular study, molecular docking evidence and network pharmacology analysis, *Int Immunopharmacol*, 102 (2022) 108382.

- [102] M.H. Abukhalil, O.E. Hussein, S.H. Aladaileh, O.Y. Althunibat, W. Al-Amarat, S.A. Saghir, M.A. Alfuwaires, A.I. Algefare, K.M. Alanazi, F.K. Al-Swailmi, E.M. Kamel, A.M. Mahmoud, Visnagin prevents isoproterenol-induced myocardial injury by attenuating oxidative stress and inflammation and upregulating Nrf2 signaling in rats, *J Biochem Mol Toxicol*, 35 (2021) e22906.
- [103] R. Arora, S. Sawney, V. Saini, C. Steffi, M. Tiwari, D. Saluja, Esculetin induces antiproliferative and apoptotic response in pancreatic cancer cells by directly binding to KEAP1, *Mol Cancer*, 15 (2016) 64.
- [104] H. Yao, N. Zhang, W. Zhang, J. Li, H. Hua, Y. Li, Discovery of a coumarin derivative as Nrf2 activator mitigating oxidative stress and fibrosis in mesangial cells under high glucose, *Bioorg Med Chem Lett*, 30 (2020) 127490.
- [105] H. Yao, N. Zhang, W. Zhang, J. Li, H. Hua, Y. Li, Discovery of polypodiside as a Keap1-dependent Nrf2 activator attenuating oxidative stress and accumulation of extracellular matrix in glomerular mesangial cells under high glucose, *Bioorg Med Chem*, 28 (2020) 115833.
- [106] B. Sengupta, M. Sahihi, M. Dehkhodaei, D. Kelly, I. Arany, Differential roles of 3-Hydroxyflavone and 7-Hydroxyflavone against nicotine-induced oxidative stress in rat renal proximal tubule cells, *PLoS One*, 12 (2017) e0179777.
- [107] A. Gendy, M.R. Elnagar, A. Soubh, A. Al-Mokaddem, A. El-Haddad, M.K. El-Sayed, Morin alleviates hepatic ischemia/reperfusion-induced mischief: In vivo and in silico contribution of Nrf2, TLR4, and NLRP3, *Biomed Pharmacother*, 138 (2021) 111539.
- [108] X. Liang, C. Hu, C. Liu, K. Yu, J. Zhang, Y. Jia, Dihydrokaempferol (DHK) ameliorates severe acute pancreatitis (SAP) via Keap1/Nrf2 pathway, *Life Sci*, 261 (2020) 118340.
- [109] T.K.Q. Ha, T.P. Doan, H.T.T. Pham, N.H. Nguyen, T.T. Nguyen, T.B.H. Bui, Molecular networking-based chemical profiling and anti-influenza viral and neuroprotective effects of *Elaeocarpus hygrophilus* Kurz, *Chem Pap*, 75 (2021) 5323-5337.
- [110] Z. Huang, Y. Sheng, M. Chen, Z. Hao, F. Hu, L. Ji, Liquiritigenin and liquiritin alleviated MCT-induced HSOS by activating Nrf2 antioxidative defense system, *Toxicol Appl Pharmacol*, 355 (2018) 18-27.
- [111] M. Yang, Z.H. Jiang, C.G. Li, Y.J. Zhu, Z. Li, Y.Z. Tang, C.L. Ni, Apigenin prevents metabolic syndrome in high-fructose diet-fed mice by Keap1-Nrf2 pathway, *Biomed Pharmacother*, 105 (2018) 1283-1290.
- [112] L.L. Ji, Y.C. Sheng, Z.Y. Zheng, L. Shi, Z.T. Wang, The involvement of p62-Keap1-Nrf2 antioxidative signaling pathway and JNK in the protection of natural flavonoid quercetin against hepatotoxicity, *Free Radic Biol Med*, 85 (2015) 12-23.
- [113] Z. Shao, B. Wang, Y. Shi, C. Xie, C. Huang, B. Chen, H. Zhang, G. Zeng, H. Liang, Y. Wu, Y. Zhou, N. Tian, A. Wu, W. Gao, X. Wang, X. Zhang, Senolytic agent Quercetin ameliorates intervertebral disc degeneration via the Nrf2/NF-kappaB axis, *Osteoarthritis Cartilage*, 29 (2021) 413-422.
- [114] K. Manigandan, D. Manimaran, R.L. Jayaraj, N. Elangovan, V. Dhivya, A. Kaphle, Taxifolin curbs NF-kappaB-mediated Wnt/beta-catenin signaling via up-regulating Nrf2 pathway in experimental colon carcinogenesis, *Biochimie*, 119 (2015) 103-112.
- [115] A. Vasquez-Espinal, O. Yanez, E. Osorio, C. Areche, O. Garcia-Beltran, L.M. Ruiz, B.K. Cassels, W. Tiznado, Theoretical Study of the Antioxidant Activity of Quercetin Oxidation Products, *Front Chem*, 7 (2019) 818.
- [116] J. Ren, L. Yuan, W. Wang, M. Zhang, Q. Wang, S. Li, L. Zhang, K. Hu, Tricetin protects against 6-OHDA-induced neurotoxicity in Parkinson's disease model by activating Nrf2/HO-1 signaling pathway and preventing mitochondria-dependent apoptosis pathway, *Toxicol Appl Pharmacol*, 378 (2019) 114617.
- [117] H. Chen, J. Qin, H. Shi, Q. Li, S. Zhou, L. Chen, Rhoifolin ameliorates osteoarthritis via the Nrf2/NF-kappaB axis: in vitro and in vivo experiments, *Osteoarthr Cartil*, 30 (2022) 735-745.
- [118] X. Hu, R. Li, M. Sun, Y. Kong, H. Zhu, F. Wang, Q. Wan, Isovitexin Depresses Osteoarthritis Progression via the Nrf2/NF-kappaB Pathway: An in vitro Study, *J Inflamm Res*, 14 (2021) 1403-1414.
- [119] H.J. Kim, E. di Luccio, A.N. Kong, J.S. Kim, Nrf2-mediated induction of phase 2 detoxifying enzymes by glyceollins derived from soybean exposed to *Aspergillus sojae*, *Biotechnol J*, 6 (2011) 525-536.
- [120] F. Liang, W. Cao, Y. Huang, Y. Fang, Y. Cheng, S. Pan, X. Xu, Isoflavone biochanin A, a novel nuclear factor erythroid 2-related factor 2 (Nrf2)-antioxidant response element activator, protects against oxidative damage in HepG2 cells, *Biofactors*, 45 (2019) 563-574.
- [121] H. Wan, L. Ge, J. Li, K. Zhang, W. Wu, S. Peng, X. Zou, H. Zhou, B. Zhou, X. Zeng, Effects of a novel biflavonoid of *Lonicera japonica* flower buds on modulating apoptosis under different oxidative conditions in hepatoma cells, *Phytomedicine*, 57 (2019) 282-291.
- [122] Z. Huang, X. Jing, Y. Sheng, J. Zhang, Z. Hao, Z. Wang, L. Ji, (-)-Epicatechin attenuates hepatic sinusoidal obstruction syndrome by inhibiting liver oxidative and inflammatory injury, *Redox Biol*, 22 (2019) 101117.

- [123] X. Jing, J. Zhang, Z. Huang, Y. Sheng, L. Ji, The involvement of Nrf2 antioxidant signalling pathway in the protection of monocrotaline-induced hepatic sinusoidal obstruction syndrome in rats by (+)-catechin hydrate, *Free Radic Res*, 52 (2018) 402-414.
- [124] T. Shanmugam, M. Selvaraj, S. Poomalai, Epigallocatechin gallate potentially abrogates fluoride induced lung oxidative stress, inflammation via Nrf2/Keap1 signaling pathway in rats: An in-vivo and in-silico study, *Int Immunopharmacol*, 39 (2016) 128-139.
- [125] Q. Zeng, Q. Xiong, M. Zhou, X. Tian, K. Yue, Y. Li, X. Shu, Q. Ru, Resveratrol attenuates methamphetamine-induced memory impairment via inhibition of oxidative stress and apoptosis in mice, *J Food Biochem*, 45 (2021) e13622.
- [126] R.G. Dos Santos Nunes, P.S. Pereira, O.O. Elekofehinti, K.R. Fidelis, C.S. da Silva, M. Ibrahim, L.M. Barros, F.A.B. da Cunha, K.E. Lukong, I.R.A. de Menezes, A. Tsopmo, A.E. Duarte, J.P. Kamdem, Possible involvement of transcriptional activation of nuclear factor erythroid 2-related factor 2 (Nrf2) in the protective effect of caffeic acid on paraquat-induced oxidative damage in *Drosophila melanogaster*, *Pestic Biochem Physiol*, 157 (2019) 161-168.
- [127] M. Wei, Z. Zheng, L. Shi, Y. Jin, L. Ji, Natural Polyphenol Chlorogenic Acid Protects Against Acetaminophen-Induced Hepatotoxicity by Activating ERK/Nrf2 Antioxidative Pathway, *Toxicol Sci*, 162 (2018) 99-112.
- [128] H. Wang, Z. Sun, D. Liu, X. Li, R.U. Rehman, H. Wang, Z. Wu, Apple phlorizin attenuates oxidative stress in *Drosophila melanogaster*, *J Food Biochem*, 43 (2019) e12744.
- [129] F.K. El-Baz, R.A. Hussein, G.A.R. Abdel Jaleel, D.O. Saleh, Astaxanthin-Rich *Haematococcus pluvialis* Algal Hepatic Modulation in D-Galactose-Induced Aging in Rats: Role of Nrf2, *Adv Pharm Bull*, 8 (2018) 523-528.
- [130] R.B. Feng, Y. Wang, C. He, Y. Yang, J.B. Wan, Gallic acid, a natural polyphenol, protects against tert-butyl hydroperoxide- induced hepatotoxicity by activating ERK-Nrf2-Keap1-mediated antioxidative response, *Food Chem Toxicol*, 119 (2018) 479-488.
- [131] Z. Zhang, L. Peng, Y. Fu, W. Wang, P. Wang, F. Zhou, Ginnalin A Binds to the Subpockets of Keap1 Kelch Domain To Activate the Nrf2-Regulated Antioxidant Defense System in SH-SY5Y Cells, *ACS Chem Neurosci*, 12 (2021) 872-882.
- [132] M. Bello, J.A. Morales-Gonzalez, Molecular recognition between potential natural inhibitors of the Keap1-Nrf2 complex, *Int J Biol Macromol*, 105 (2017) 981-992.
- [133] M. Bautista, J.A.G. de Lcio, N.V. Mendoza, C. Velzquez, M.D. la O Arciniega, G. Almaguer, Geranium Species as Antioxidants, *InTech*, (2013).
- [134] Z. Gao, W. Yi, J. Tang, Y. Sun, J. Huang, T. Lan, X. Dai, S. Xu, Z.G. Jin, X. Wu, Urolithin A protects against acetaminophen-induced liver injury in mice via sustained activation of Nrf2, *Int J Biol Sci*, 18 (2022) 2146-2162.
- [135] Y.E. Chen, S.J. Xu, Y.Y. Lu, S.X. Chen, X.H. Du, S.Z. Hou, H.Y. Huang, J. Liang, Asperuloside suppressing oxidative stress and inflammation in DSS-induced chronic colitis and RAW 264.7 macrophages via Nrf2/HO-1 and NF-kappaB pathways, *Chem Biol Interact*, 344 (2021) 109512.
- [136] S. Das, S. Dewanjee, T.K. Dua, S. Joardar, P. Chakraborty, S. Bhowmick, A. Saha, S. Bhattacharjee, V. De Feo, Carnosic Acid Attenuates Cadmium Induced Nephrotoxicity by Inhibiting Oxidative Stress, Promoting Nrf2/HO-1 Signalling and Impairing TGF-beta1/Smad/Collagen IV Signalling, *Molecules*, 24 (2019).
- [137] H. Ali, A. Khan, J. Ali, H. Ullah, A. Khan, H. Ali, N. Irshad, S. Khan, Attenuation of LPS-induced acute lung injury by continentalic acid in rodents through inhibition of inflammatory mediators correlates with increased Nrf2 protein expression, *BMC Pharmacol Toxicol*, 21 (2020) 81.
- [138] L.T. Zhang, X.L. Wang, T. Wang, J.S. Zhang, Z.Q. Huang, T. Shen, H.X. Lou, D.M. Ren, X.N. Wang, Dolabellane and Clerodane Diterpenoids from the Twigs and Leaves of *Casearia kurzii*, *J Nat Prod*, 83 (2020) 2817-2830.
- [139] A. Iqbal, S. Sharma, A.K. Najmi, M.A. Syed, J. Ali, M.M. Alam, S.E. Haque, Nerolidol ameliorates cyclophosphamide-induced oxidative stress, neuroinflammation and cognitive dysfunction: Plausible role of Nrf2 and NF- kappaB, *Life Sci*, 236 (2019) 116867.
- [140] Y.N. Qiao, Y. Sun, T. Shen, J.Z. Zhang, J.C. Zhou, Y. Li, W. Chen, Z.J. Ren, Y.L. Li, X. Wang, H.X. Lou, Diterpenoids from the Chinese liverwort *Frullania hamatiloba* and their Nrf2 inducing activities, *Phytochemistry*, 158 (2019) 77-85.
- [141] S.M. Kamble, H.M. Patel, S.N. Goyal, M.N. Noolvi, U.B. Mahajan, S. Ojha, C.R. Patil, In silico Evidence for Binding of Pentacyclic Triterpenoids to Keap1-Nrf2 Protein-Protein Binding Site, *Comb Chem High Throughput Screen*, 20 (2017) 215-234.

- [142] T. Bibi, A. Khan, A.U. Khan, B. Shal, H. Ali, E.K. Seo, S. Khan, Magnolol prevented brain injury through the modulation of Nrf2-dependent oxidative stress and apoptosis in PLP-induced mouse model of multiple sclerosis, *Naunyn Schmiedeberg's Arch Pharmacol*, 395 (2022) 717-733.
- [143] M. Jin, Y. Wei, H. Yu, X. Ma, S. Yan, L. Zhao, L. Ding, J. Cheng, H. Feng, Erythritol Improves Nonalcoholic Fatty Liver Disease by Activating Nrf2 Antioxidant Capacity, *J Agric Food Chem*, 69 (2021) 13080-13092.
- [144] P. Shaw, A. Sen, P. Mondal, A. Dey Bhowmik, J. Rath, A. Chattopadhyay, Shinorine ameliorates chromium induced toxicity in zebrafish hepatocytes through the facultative activation of Nrf2-Keap1-ARE pathway, *Aquat Toxicol*, 228 (2020) 105622.
- [145] X. Li, J. Ge, M. Li, S. Deng, J. Li, Y. Ma, J. Zhang, Y. Zheng, L. Ma, Network pharmacology, molecular docking technology integrated with pharmacodynamic study to reveal the potential targets of Schisandrol A in drug-induced liver injury by acetaminophen, *Bioorg Chem*, 118 (2022) 105476.
- [146] S. Feng, B. Qiu, L. Zou, K. Liu, X. Xu, H. Zhu, Schisandrin B elicits the Keap1-Nrf2 defense system via carbene reactive metabolite which is less harmful to mice liver, *Drug Des Devel Ther*, 12 (2018) 4033-4046.
- [147] Y.L. Kung, C.Y. Lu, K.F. Badrealam, W.W. Kuo, M.A. Shibu, C.H. Day, R.J. Chen, S.Y. Lu, V.V. Padma, C.Y. Huang, Cardioprotective potential of amygdalin against angiotensin II induced cardiac hypertrophy, oxidative stress and inflammatory responses through modulation of Nrf2 and NF-kappaB activation, *Environ Toxicol*, 36 (2021) 926-934.
- [148] L. Zhao, N. Zhou, H. Zhang, F. Pan, X. Ai, Y. Wang, S. Hao, C. Wang, Cyanidin-3-O-glucoside and its metabolite protocatechuic acid ameliorate 2-amino-1-methyl-6-phenylimidazo[4,5-b]pyridine (PhIP) induced cytotoxicity in HepG2 cells by regulating apoptotic and Nrf2/p62 pathways, *Food Chem Toxicol*, 157 (2021) 112582.
- [149] F. Oztay, S. Tunali, O. Kayalar, R. Yanardag, The protective effect of vitamin U on valproic acid-induced lung toxicity in rats via amelioration of oxidative stress, *J Biochem Mol Toxicol*, 34 (2020) e22602.
- [150] A. Wu, Z. Yang, Y. Huang, H. Yuan, C. Lin, T. Wang, Z. Zhao, Y. Zhou, C. Zhu, Natural phenylethanoid glycosides isolated from *Callicarpa kwangtungensis* suppressed lipopolysaccharide-mediated inflammatory response via activating Keap1/Nrf2/HO-1 pathway in RAW 264.7 macrophages cell, *J Ethnopharmacol*, 258 (2020) 112857.
- [151] S.C. Lo, X. Li, M.T. Henzl, L.J. Beamer, M. Hannink, Structure of the Keap1:Nrf2 interface provides mechanistic insight into Nrf2 signaling, *EMBO J*, 25 (2006) 3605-3617.
- [152] J. Hong, Z. Shi, C. Li, X. Ji, S. Li, Y. Chen, G. Jiang, M. Shi, W. Wang, Y. Zhang, B. Hu, S. Yan, Virtual screening identified natural Keap1-Nrf2 PPI inhibitor alleviates inflammatory osteoporosis through Nrf2-mir214-Traf3 axis, *Free Radic Biol Med*, 171 (2021) 365-378.
- [153] J.H. Yoon, K. Youn, M. Jun, Protective effect of sargahydroquinone acid against Abeta(25-35)-evoked damage via PI3K/Akt mediated Nrf2 antioxidant defense system, *Biomed Pharmacother*, 144 (2021) 112271.
- [154] T.B. Tumer, B. Yilmaz, A. Ozleyen, B. Kurt, T.T. Tok, K.M. Taskin, S.S. Kulabas, GR24, a synthetic analog of Strigolactones, alleviates inflammation and promotes Nrf2 cytoprotective response: In vitro and in silico evidences, *Comput Biol Chem*, 76 (2018) 179-190.
- [155] Y. Zhang, T. Yan, D. Sun, C. Xie, T. Wang, X. Liu, J. Wang, Q. Wang, Y. Luo, P. Wang, T. Yagai, K.W. Krausz, X. Yang, F.J. Gonzalez, Rutaecarpine inhibits KEAP1-NRF2 interaction to activate NRF2 and ameliorate dextran sulfate sodium-induced colitis, *Free Radic Biol Med*, 148 (2020) 33-41.
- [156] F. Najafi, G. Kavooosi, R. Siahbalei, A. Kariminia, Anti-oxidative and anti-hyperglycemic properties of *Agastache foeniculum* essential oil and oily fraction in hyperglycemia-stimulated and lipopolysaccharide-stimulated macrophage cells: In vitro and in silico studies, *J Ethnopharmacol*, 284 (2022) 114814.
- [157] S.M. Baraka, D.O. Saleh, N.S. Ghaly, F.R. Melek, A.A. Gamal El Din, W.K.B. Khalil, M.M. Said, A.M. Medhat, Flavonoids from *Barnebydendron riedelii* leaf extract mitigate thioacetamide-induced hepatic encephalopathy in rats: The interplay of NF-kappaB/IL-6 and Nrf2/HO-1 signaling pathways, *Bioorg Chem*, 105 (2020) 104444.
- [158] J. Herrera-Bravo, J.F. Beltran-Lissabet, K. Saavedra, N. Saavedra, M. Hevia, M. Alvear, F. Lanas, L.A. Salazar, Protective effect of Pinot noir pomace extract against the cytotoxicity induced by polycyclic aromatic hydrocarbons on endothelial cells, *Food Chem Toxicol*, 148 (2021) 111947.
- [159] Q. Lu, S. Tan, W. Gu, F. Li, W. Hua, S. Zhang, F. Chen, L. Tang, Phytochemical composition, isolation and hepatoprotective activity of active fraction from *Veronica ciliata* against acetaminophen-induced acute liver injury via p62-Keap1-Nrf2 signaling pathway, *J Ethnopharmacol*, 243 (2019) 112089.
- [160] H. Prasetya, F.R.P. Dewi, B. Setiawan, Urological cancer: molecular docking of the active compound *Scurrula atropurpurea* against nuclear factor erythroid2-related factor2 (Nrf2), *J Phys Conf Ser*, 1374 (2019) 012055.

- [161] M.M. Liu, K.M. Huang, L. Qian, P. Chatterjee, S. Zhang, R. Li, S. Zhou, Z. Wang, Y. Luo, Y. Huang, Effects of bioactive constituents in the Traditional Chinese Medicinal formula Si-Wu-Tang on Nrf2 signaling and neoplastic cellular transformation, *Phytomedicine*, 40 (2018) 1-9.
- [162] R. Sahu, R.K. Kar, P. Sunita, P. Bose, P. Kumari, S. Bharti, S. Srivastava, S.P. Pattanayak, LC-MS characterized methanolic extract of *Zanthoxylum armatum* possess anti-breast cancer activity through Nrf2-Keap1 pathway: An in-silico, in-vitro and in-vivo evaluation, *J Ethnopharmacol*, 269 (2021) 113758.
- [163] L. Tao, X. Gu, E. Xu, S. Ren, L. Zhang, W. Liu, X. Lin, J. Yang, C. Chen, Osthole protects against Ang II-induced endotheliocyte death by targeting NF-kappaB pathway and Keap-1/Nrf2 pathway, *Am J Transl Res*, 11 (2019) 142-159.
- [164] N. Liang, J.H. Dupuis, R.Y. Yada, D.D. Kitts, Chlorogenic acid isomers directly interact with Keap 1-Nrf2 signaling in Caco-2 cells, *Mol Cell Biochem*, 457 (2019) 105-118.
- [165] E. Bhakkiyalakshmi, K. Dineshkumar, S. Karthik, D. Sireesh, W. Hopper, R. Paulmurugan, K.M. Ramkumar, Pterostilbene-mediated Nrf2 activation: Mechanistic insights on Keap1:Nrf2 interface, *Bioorg Med Chem*, 24 (2016) 3378-3386.
- [166] B. Nan, Z. Zhao, K. Jiang, X. Gu, H. Li, X. Huang, Astaxanthine attenuates cisplatin ototoxicity in vitro and protects against cisplatin-induced hearing loss in vivo, *Acta Pharm Sin B*, 12 (2022) 167-181.
- [167] J. Han, X. Shi, Z. Zheng, B. Zhang, F. Shi, L. Jiang, J. Xu, Schisandrin B protects against angiotensin II-induced endotheliocyte deficits by targeting Keap1 and activating Nrf2 pathway, *Drug Des Devel Ther*, 12 (2018) 3985-3997.
- [168] J. Han, X. Shi, Y. Du, F. Shi, B. Zhang, Z. Zheng, J. Xu, L. Jiang, Schisandrin C targets Keap1 and attenuates oxidative stress by activating Nrf2 pathway in Ang II-challenged vascular endothelium, *Phytother Res*, 33 (2019) 779-790.
- [169] Srinidhi, Quantum chemical studies and pharmacophore modeling for designing novel keap1 antagonists that enhance nrf2 mediated neuroprotection, *African J Biol Sci*, 3 (2021) 130.
- [170] A. Siddiqa, A. Tajammal, A. Irfan, M.A. Munawar, M. Azam, M.A.R. Basra, Synthesis, antioxidant, in silico and computational investigation of 2,5-dihydroxyacetophenone derived chloro-substituted hydroxychalcones, hydroxyflavanones and hydroxyflavindogenides, *J Biomol Struct Dyn*, 40 (2022) 10265-10277.
- [171] M. Li, W. Huang, F. Jie, M. Wang, Y. Zhong, Q. Chen, B. Lu, Discovery of Keap1-Nrf2 small-molecule inhibitors from phytochemicals based on molecular docking, *Food Chem Toxicol*, 133 (2019) 110758.
- [172] D.F. Akin-Bali, S.H. Aktas, M.A. Unal, T. Kankilic, Identification of novel Nrf2/Keap1 pathway mutations in pediatric acute lymphoblastic leukemia, *Pediatr Hematol Oncol*, 37 (2020) 58-75.
- [173] D.F. Akin-Bali, K. Al-Khafaji, S.H. Aktas, T. Taskin-Tok, Bioinformatic and computational analysis for predominant mutations of the Nrf2/Keap1 complex in pediatric leukemia, *J Biomol Struct Dyn*, 39 (2021) 4290-4303.
- [174] E.W. Cloer, P.F. Siesser, E.M. Cousins, D. Goldfarb, D.D. Mowrey, J.S. Harrison, S.J. Weir, N.V. Dokholyan, M.B. Major, p62-Dependent Phase Separation of Patient-Derived KEAP1 Mutations and NRF2, *Mol Cell Biol*, 38 (2018).
- [175] C.J. Wilson, M. Chang, M. Karttunen, W.Y. Choy, KEAP1 Cancer Mutants: A Large-Scale Molecular Dynamics Study of Protein Stability, *Int J Mol Sci*, 22 (2021).
- [176] A. Raghunath, R. Nagarajan, K. Sundarraj, K. Palanisamy, E. Perumal, Identification of compounds that inhibit the binding of Keap1a/Keap1b Kelch DGR domain with Nrf2 ETGE/DLG motifs in zebrafish, *Basic Clin Pharmacol Toxicol*, 125 (2019) 259-270.
- [177] A. Akmal, A. Javaid, R. Hussain, A. Kanwal, M. Zubair, U.A. Ashfaq, Screening of phytochemicals against Keap1-NRF2 interaction to reactivate NRF2 Functioning: Pharmacoinformatics based approach, *Pak J Pharm Sci*, 32 (2019) 2823-2828.
- [178] F. Begnini, V. Poongavanam, B. Over, M. Castaldo, S. Geschwindner, P. Johansson, M. Tyagi, C. Tyrchan, L. Wissler, P. Sjo, S. Schiesser, J. Kihlberg, Mining Natural Products for Macrocycles to Drug Difficult Targets, *J Med Chem*, 64 (2021) 1054-1072.
- [179] F. Begnini, S. Geschwindner, P. Johansson, L. Wissler, R.J. Lewis, E. Danelius, A. Luttens, P. Matricon, J. Carlsson, S. Lenders, B. Konig, A. Friedel, P. Sjo, S. Schiesser, J. Kihlberg, Importance of Binding Site Hydration and Flexibility Revealed When Optimizing a Macrocyclic Inhibitor of the Keap1-Nrf2 Protein-Protein Interaction, *J Med Chem*, 65 (2022) 3473-3517.
- [180] J.S. Pallesen, D. Narayanan, K.T. Tran, S.M.O. Solbak, G. Marseglia, L.M.E. Sorensen, L.J. Hoj, F. Munafo, R.M.C. Carmona, A.D. Garcia, H.L. Desu, R. Brambilla, T.N. Johansen, G.M. Popowicz, M. Sattler, M. Gajhede, A. Bach, Deconstructing Noncovalent Kelch-like ECH-Associated Protein 1 (Keap1) Inhibitors into Fragments to Reconstruct New Potent Compounds, *J Med Chem*, 64 (2021) 4623-4661.

